The Pennsylvania State University

The Graduate School

College of Engineering

TRACE/PARCS ASSESSMENT BASED ON PEACH BOTTOM TURBINE TRIP AND LOW FLOW STABILITY TESTS

A Thesis in

Nuclear Engineering

by

Boyan S. Neykov

Submitted in Partial Fulfillment
of the Requirements
for the Degree of

Master of Science

December 2008

The thesis of Boyan S. Neykov was reviewed and approved* by the following:

Kostadin N. Ivanov
Distinguished Professor of Nuclear Engineering
Thesis Advisor

John Mahaffy
Associate Professor of Nuclear Engineering

Jack S. Brenizer
J. 'Lee' Everett Professor of Mechanical and Nuclear Engineering
Chair, Nuclear Engineering Program

*Signatures are on file in the Graduate School

ABSTRACT

The simulation of the nuclear reactor core behavior and plant dynamics as well as their mutual interactions has a significant impact on the design and operation, safety and economics of nuclear power plants.

The U. S. NRC uses computer models to study the phenomena associated with reactor safety issues. The reactor system analysis code TRACE (TRAC RELAP5 Advanced Computational Engine) is used to study the reactor coolant system under a wide variety of flow conditions including multi-phase thermal hydraulics. Multidimensional time dependent power distributions are required for accurate simulation and the PARCS (Purdue Advanced Reactor Core Simulator) multi-dimensional reactor kinetics code has been coupled to TRACE to provide accurate simulation capabilities of some reactor transient or accident scenarios. TRACE/PARCS has been previously validated for Pressurized Water Reactor (PWR) transient analysis using the OECD/NEA Main Steam Line Break (MSLB) Benchmark.

During the last decade the OECD/NEA has sponsored the Boiling Water Reactor (BWR) Turbine Trip (TT) Benchmark, designed to provide a validation basis for the new generation best estimate codes - coupled three-dimensional (3D) kinetics system thermal-hydraulic codes.

The objectives of this thesis are focused on the assessment of TRACE/PARCS for BWR transient analysis. In this case the BWR TT benchmark problem and Low Flow Stability Tests are appropriate to assess the accuracy of TRACE/PARCS for BWR analysis. The problems exhibit significant space/time flux variations and are based on the measurement of plant data during the transients. These are the Peach Bottom 2 (PB2) Turbine Trip (TT) experiment and Low Flow Stability tests performed in 1977. The analyses of both the Peach Bottom Turbine Trip 2 experiment and the Low Flow Stability tests using TRACE/PARCS showed that calculation results agree reasonably well with both initial steady-state and transient measured data for each

test. The thesis provides a detailed description of the developed methods and the obtained results of the analyses for both PB2 TT and Low Flow Stability Tests with TRACE/PARCS.

TABLE OF CONTENTS

LIST OF FIGURES

LIST OF TABLES

ACKNOWLEDGEMENTS

I would like to express my profound appreciation to a list of people who gave me support and help for the completion of this work.

I thank my thesis advisor, Dr. Kostadin Ivanov for the guidance in my research and accurate decisions concerning my academic requirements, in easy and troubled times. I would like to thank, Dr. John Mahaffy for his scientific direction and guidance towards the application TRACE thermal hydraulic code and his feedback prior the submission of the final thesis draft.

I thank Dr. Brenizer for spending time on reading my thesis.

I would like to thank Dr. Bedirhan Akdeniz who worked with me to obtain the results presented in this dissertation, for his help and discussions concerning the Peach Bottom Turbine Trip Benchmark and TRACE input deck.

Thanks to the late Dr. Tom Downar , Dr. Yunlin Xu for their guidance and discussions during our weekly phone conferences on the subject.

I want to express my gratitude to the faculty and staff of the Mechanical and Nuclear Engineering department.

Thanks to all the ones who believe in me in the adversity, my friends, my family and wife who never doubted that I was able to reach the goal.

.

Chapter 1

Introduction

1 Background

The simulation of the nuclear reactor core behavior and plant dynamics as well as their mutual interactions has a significant impact on the design and operation, safety and economics of nuclear power plants. Three dimensional (3D) models of the reactor core incorporated into system transient codes allows for a "best-estimate" calculation of interactions between the core behavior and plant dynamics. Such models are used for simulating transients that involve core spatial asymmetric phenomena and strong feedback effects between core neutronics and reactor thermal-hydraulics.

The U. S. NRC uses computer models to study the phenomena associated with reactor safety issues. The reactor system analysis code TRACE (TRAC RELAP5 Advanced Computational Engine) is used to study the reactor coolant system under a wide variety of flow conditions including multi-phase thermal hydraulics. Multidimensional time dependent power distributions are required for accurate simulation and the PARCS (Purdue Advanced Reactor Core Simulator) multi-dimensional reactor kinetics code has been coupled to TRACE to provide accurate simulation capabilities of some reactor transient or accident scenarios. TRACE/PARCS has been previously validated for Pressurized Water Reactor transient analysis using the OECD/NEA Main Steam Line Break (MSLB) Benchmark [1].

The objectives of this thesis are focused on the assessment of TRACE/PARCS for BWR transient analysis. In this case Boiling Water Reactor (BWR) Turbine Trip (TT) and Low Flow Stability (LFS) tests are appropriate to assess the accuracy of TRACE/PARCS for BWR analysis.

Such tests exhibit significant space/time flux variations and utilize measurement of plant data during the simulated transients. The selected experiments are the Peach Bottom 2 (PB2) TT and LFS tests performed in 1977 [2]. After the completion of the turbine trip tests, several stability tests were performed at PB2 and all of the tests are documented in EPRI reports [2], [3].

The OECD/NRC BWR TT Benchmark is designed to provide a validation basis for the new generation best estimate codes – coupled 3D kinetics system thermal-hydraulic codes, and is based on the second of the PB2 TT tests [4]. The codes were tested for simulation of the PB2 (a General Electric designed BWR/4) TT transient with a sudden closure of the turbine stop valve.

Three turbine trip transients at different power levels were performed at the PB2 Nuclear Power Plant (NPP) prior to shutdown for refuelling at the end of Cycle 2 in April 1977 [5, 6]. The second test (TT2) was selected for the benchmark problem to investigate the effect of the pressurisation transient (following the sudden closure of the turbine stop valve) on the neutron flux in the reactor core. In a best-estimate manner the test conditions approached the design basis conditions as closely as possible.

The transient selected for this benchmark is a dynamically complex event and it constitutes a good problem to test the coupled codes on both levels: neutronics/thermal-hydraulics coupling, and core/plant system coupling. In the TT2 test, the thermal-hydraulic feedback alone limited the power peak and initiated the power reduction. The void feedback plays the major role while the Doppler feedback plays a subordinate role. The reactor scram then inserted additional negative reactivity and completed the power reduction and eventual core shutdown.

Three exercises were performed in the BWR TT Benchmark. These exercises include the evaluation of different steady-states, and simulation of different transient scenarios.

The purpose of the first exercise is to test the thermal-hydraulic system response and to initialize the participants' system models for use of the second and third exercises on coupled 3-D kinetics/system thermal-hydraulics simulations.

The second exercise consists of performing coupled-core boundary conditions calculations. The purpose of the second exercise is to test and initiate the participants' core models. The thermal-hydraulic core boundary conditions provided are the core inlet pressure, core exit pressure, core inlet temperature and core inlet flow.

The last exercise, Exercise 3, primarily comprises the best estimate of coupled 3D core/thermal-hydraulic system modeling. This exercise combines elements of the first two exercises of this benchmark and is an analysis of the transient in its entirety.

1.1 Peach Bottom Turbine Trip Tests

Both the Peach Bottom turbine trip transient and stability tests were performed at the End of Cycle (EOC) 2. The Peach Bottom turbine trip experiments were pressurization events in which the coupling between core phenomena and system dynamics plays an important role in predicting the plant response.

The PB2 TT tests start with a sudden closure of the turbine stop valve (TSV) and then the turbine by-pass valve begins to open. From a fluid phenomena point of view, pressure and flow waves play an important role during the early phase of the transient (of about 1.5 seconds) because rapid valve actions cause sonic waves, which propagate through the main steam piping to the reactor core with relatively little attenuation. The induced core pressure oscillations results in changes of the core void distribution and fluid flow. The magnitude of the neutron flux transient taking place in the BWR core is affected by the initial rate of pressure rise caused by the pressure oscillation and has a spatial variation. The simulation of the power response to the pressure pulse and subsequent void collapse requires a 3D core modeling supplemented by 1D simulation of the remainder of the reactor coolant system.

There have been several previous efforts to perform analysis of the OECD/NRC BWR TT benchmark Peach Bottom turbine trip transients to include an analysis with the TRAC-M/PARCS coupled code [7]. This previous effort with TRAC-M differs from the work here since it used a TRAC-B model of Peach Bottom and specially modified version of the TRAC-M computer code. For the current thesis, a Peach Bottom model was developed using TRACE components and the information provided by the OECD/NRC BWR TT benchmark specification [17]. Subsequently the TT and LFS test simulations were performed with a standard version of the TRACE code v5.0rc3. The details of the TRACE Peach Bottom model and the steady state and transient results are provided in Chapter 4. The work described in this thesis provides modeling and results not only for TT2 test (within the framework of the OECD/NRC BWR TT benchmark) but also for TT1, TT2 and four LFS tests.

1.2 Peach Bottom Low Flow Stability Tests

The Low Flow Stability Tests were intended to measure the reactor core stability margins at the limiting conditions used in design and safety analysis, providing a one-to-one comparison to design calculations. These tests were performed in the right boundary of the instability region in the Power/Flow Map, i.e. in the area of low flow from 38 % to 51.3 % of total nominal core flow rate and corresponding power of 43.5% to 60.6% of rated power

The stability tests were initiated from steady-state conditions after obtaining P1 edits from the process computer for nuclear and thermal-hydraulic conditions of the core. The Peach Bottom stability tests were conducted along the low-flow end of the rated power-flow line, and along the power-flow line corresponding to minimum recirculation pump speed. The reactor core stability margin was determined from an empirical model fitted to the experimentally derived transfer function measurement between core pressure and the APRM, average neutron flux

signals. The low flow stability tests consisted of periodic pressure step recording and pseudorandom pressure step recording.

Chapter 2 of this thesis gives detailed description about the PB2 TT tests and OECD/NRC BWR TT benchmark as well as the LFS tests.

Chapter 3 describes the TRACE/PARCS codes and coupling methodology.

Chapter 4 provides comparative analysis of the TRACE/PARCS PB2 TT tests results

Chapter 5 provides comparative analysis of the TRACE/PARCS PB2 LFS tests results.

Chapter 6 provides a summary of the conclusions drawn from the analysis of TRACE/PARCS.

Chapter 2

PB TT2 Benchmark and Low Flow Stability Tests Description

2.1 OECD/NRC BWR TT Benchmark Description

A TT transient in a BWR type reactor is considered one of the most complex events to be analyzed because it involves the reactor core, the high pressure coolant boundary, associated valves and piping in highly complex interactions with variables changing very rapidly. The reference design for the BWR is derived from real reactor, plant and operation data for the PB2 NPP and it is based on the information provided in EPRI reports [2 - 5] and some additional sources such as the PECo Energy Topical report [7].

The OECD/NRC BWR TT benchmark consists of three exercises. Exercise 1 and Exercise 2 provided with the opportunity to initialize system and core models and to test code capabilities for coupling of thermal hydraulic and neutronics phenomena. Measured core power has been used as a boundary condition in the first exercise, and only core calculations have been performed using specified boundary conditions in the second exercise. The successes of Exercise 1 and 2 lead to the third exercise which combines elements of the first two exercises of this benchmark and is an analysis of the transient and its entirety.

Exercise 3 is composed of base case (so-called Best Estimate Case) and hypothetical cases (so-called Extreme Scenarios) The purpose of the Exercise 3 Best Estimate Case is to provide comprehensive assessment of the code in analyzing complex transients with 3D coupled core and system calculations. In order to validate such assessments, available measured plant data are utilized for this case during the comparative analyses presented in this thesis. In addition to

the base case, the analysis of the Extreme scenarios provide a further understanding of the reactor behavior, which is the result of the dynamic coupling of the whole system, i.e. the interaction between steam line and vessel flows, the pressure, the Doppler, void and control reactivity and power. The best estimate case as well as extreme scenario 2 were analyzed by the TRACE/PARCS code in the course of this thesis.

Extreme scenario 1: Turbine trip (TT) with steam bypass relief system failure

Extreme scenario 2: TT without reactor scram

Extreme scenario 3: TT with steam bypass relief system failure without scram

Extreme scenario 4: Combined Scenario – Turbine trip with steam bypass system failure, without scram and without Safety Relief Valves (SRV) opening.

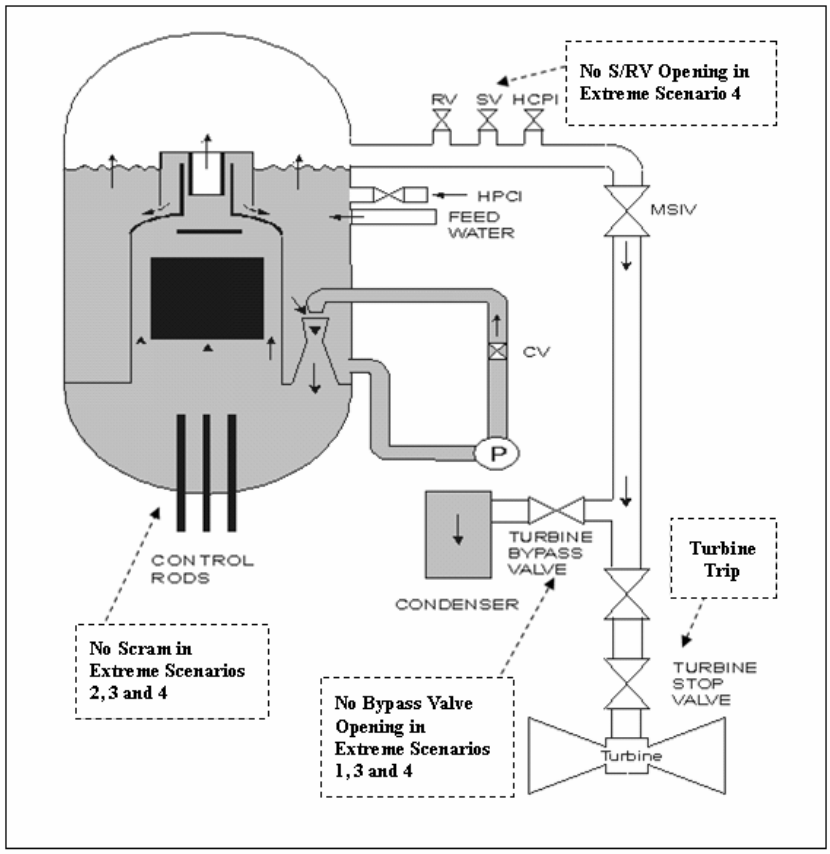

Figure **2-1**: Key Elements of Exercise 3 *Best Estimate Case* and *Extreme Scenarios*

The key elements of Exercise 3 are illustrated in the simple BWR schematic given above. Extreme Scenario 2 (TT without scram) can be considered as single failure and therefore provides information from the perspective of the safety of the plant. Extreme Scenario 3 (combination of 1 and 2) considers the coincidence of two independent failures. Extreme Scenario 4 (in addition to 3 no opening of safety relief valves) considers the coincidence of three independent failures, which are extremely unlikely from a safety perspective and therefore not considered in the current work. In the base case, SRVs are not opening during the transient while this happens in the extreme scenario 2. In the hypothetical case, the dynamical response of the system due to the interaction of the flow in the steam line with the dynamics of the SRVs happens to be more challenging for the coupled codes. It should be noted that no comparison with measured data is possible for the extreme cases since they are hypothetical scenarios. Therefore, submitted extreme scenario results are compared with an "average" of the results of the OECD/NRC BWR TT benchmark participants.

The PB2 neutronics and thermal-hydraulic data as well as initial TT2 conditions for steady state and transient calculations are given in the following subsections of this chapter.

2.1.1 Core and Neutronics Data

The reference design for the BWR is derived from real reactor, plant and operation data for the PB2 BWR/4 NPP and it is based on the information provided in EPRI reports and some additional sources such as the PECO Energy Topical Report. This section specifies the core and neutronics data to be used in the calculation of Exercise 3

The radial geometry of the reactor core is shown in Figure 2-2. At radial plane the core is divided into cells 15.24 cm wide, each corresponding to one fuel assembly (FA), plus a radial

reflector (shaded area of Figure 2-2) of the same width. There are total of 888 assemblies, 764 FA and 124 reflector assemblies. Axially, the reactor core is divided into 26 layers (24 core layers plus top and bottom reflectors) with a constant height of 15.24 cm (including reflector nodes). The total active core height is 365.76 cm. The axial nodalization accounts for material changes in the fuel design and for exposure and history variations. Geometric data for the FA and fuel rod is provided in Table 2-1. Data for different assembly designs is given in Tables 2-2 through 2-8. Fuel assembly lattice drawings, including detailed dimensions, for initial fuel, reload fuel with 100 and 120 mil channels and the lead test assemblies (LTA) are shown in Figures 2-3 through 2-6. The numbers 100 and 120 refer to the wall thickness of the channel (1mil = 0.001 inches). The core loading during the test was as follows: 576 fuel assemblies were the original 7x7 type from Cycle 1 (C1) and the remaining 188 were a reload of 8x8 fuel assemblies. One hundred eighty five control rods provided reactivity control. To build the participant's given neutronics model, these control rods can be grouped according to their initial insertion position. The control rod grouping used for TRACE/PARCS to perform calculations is presented in Figure 2-7.

Two neutron energy groups and six delayed neutron precursor families are modeled. The energy released per fission for the two prompt neutron groups is 0.3213×10^{-10} and 0.3206×10^{-10} W-s/fission, and this energy release is considered to be independent of time and space. It is assumed that 2 % of fission power is released as direct gamma heating for the in-channel coolant flow and 1.7 % for the bypass flow. Table 2-9 shows global core-wide decay time constants and fractions of delayed neutrons. In addition delayed parameters are provided in the cross-section library for each of the compositions. The prompt neutron lifetime is 0.45085E-04.

The ANS-79 is used as a decay heat standard model. 71 decay heat groups are used: 69 groups are used for the three isotopes ^{235}U, ^{239}Pu and ^{238}U with the decay heat constants defined in the 1979 ANS standard; plus, the heavy-element decay heat groups for ^{239}U and ^{239}Np are used

with constants given in Table 2-10. The assumption of an infinite operation at a power of 3 293 MWt is used.

Nineteen assembly types are contained within the core geometry with 435 compositions. The corresponding sets of cross-sections are provided. Each composition is defined by material properties (due to changes in the fuel design) and burn-up. The burn-up dependence is a three-component vector of variables: exposure (GWd/t), spectral history (void fraction) and control rod history. Assembly designs are defined in Tables 2-11 through 2-15. Control rod geometry data is provided in Table 2-16. The definition of assembly type is shown in Table 2-17. The radial distribution of these assembly types within the reactor geometry is shown in Figure 2-8. The axial locations of compositions of each assembly type are shown in Table 2-18.

A complete set of diffusion coefficients, macroscopic cross-sections for scattering, absorption, and fission, assembly discontinuity factors (ADFs), as a function of the moderator density and fuel temperature is defined for each composition. The group inverse neutron velocities are also provided for each composition. Dependence of the cross-sections of the above variables is specified through a two-dimensional table lookup. Each composition is assigned to a cross-section set containing separate tables for the diffusion coefficients and cross-sections, with each point in the table representing a possible core state. The expected range of the transient is covered by the selection of an adequate range for the independent variables shown in Table 2-19. Specifically, Exercise 1 was used for selecting the range of thermal-hydraulic variables. A steady state calculation was run using the TRAC-BF1 code and initial conditions of the second turbine trip for choosing discrete values of the thermal hydraulic variables (pressure, void fraction and coolant/moderator temperature). A transient calculation was performed to determine the expected range of change of the above variables.

A modified linear interpolation scheme (which includes extrapolation outside the thermal-hydraulic range) is used to obtain the appropriate total cross-sections from the tabulated

ones based on the reactor conditions being modeled. Table 2-20 shows the definition of a cross-section table associated with a composition. Table 2-21 shows the macroscopic cross-section table structure for one cross-section set. All cross section sets are assembled into a cross-section library. The cross-sections are provided in a separate libraries for rodded (nemtabr) and un-rodded compositions (nemtab).

Lattice physics calculations are performed by homogenizing the fuel lattice and the bypass flow associated with it. When obtaining the average coolant density, a correction that accounts for the bypass channel conditions should be included since this is going to influence the feedback effect on the cross-section calculation through the average coolant density. The following approach should be applied:

$$\rho_{act}^{\ eff} = \frac{A_{act}\rho_{act} + A_{byp}\left(\rho_{byp} - \rho_{sat}\right)}{A_{act}} \qquad 2.1$$

where $\rho_{act}^{\ eff}$ is the effective average coolant density for cross-section calculation, ρ_{byp} is the average moderator coolant density of the bypass channel, ρ_{sat} is the saturated moderator coolant density of the bypass channel, A_{act} is flow cross-sectional area of the active heated channel and A_{byp} is the flow cross-sectional area of the bypass channel.

Bypass conditions should be obtained by adding a bypass channel to represent the core bypass region in the thermal-hydraulic model

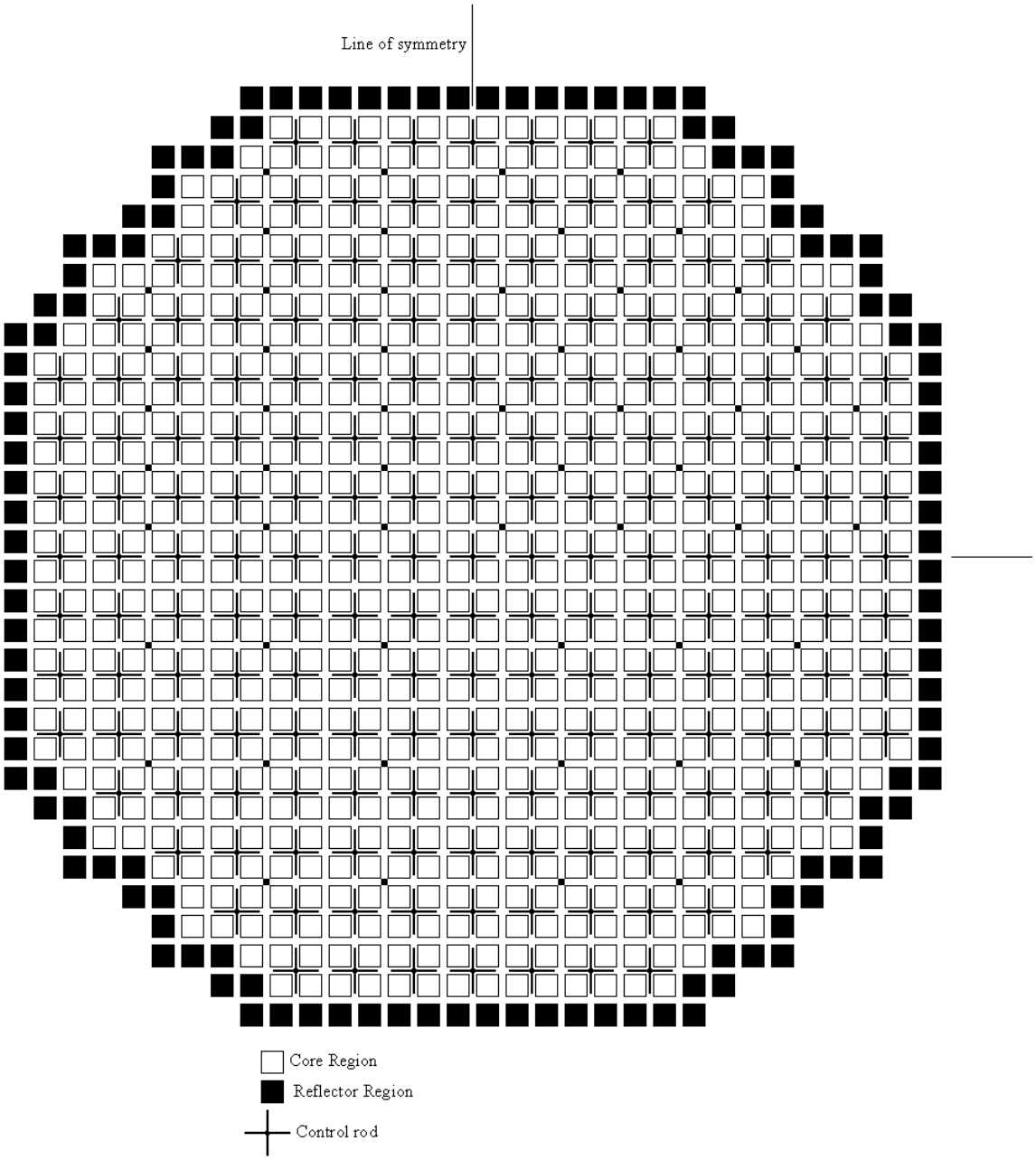

Figure **2-2**: Reactor Core Cross-sectional View

Table **2-1**: PB2 Fuel Assembly Data.

	Initial load			Reload	Reload	LTA special
Assembly type	1	2	3	4	5	6
No. of assemblies, initial core	168	263	333	0	0	0
No. of assemblies, Cycle 2	0	261	315	68	116	4
Geometry	7 × 7	7 × 7	7 × 7	8 × 8	8 × 8	8 × 8
Assembly pitch, in	6.0	6.0	6.0	6.0	6.0	6.0
Fuel rod pitch	0.738	0.738	0.738	0.640	0.640	0.640
Fuel rods per assembly	49	49	49	63	63	62
Water rods per assembly	0	0	0	1	1	2
Burnable poison positions	0	4	5	5	5	5
No. of spacer grids	7	7	7	7	7	7
Inconel per grid, lb	0.102	0.102	0.102	0.102	0.102	0.102
Zr-4 per grid, lb	0.537	0.537	0.537	0.614	0.614	0.614
Spacer width, in	1.625	1.625	1.625	1.625	1.625	1.625
Assembly average fuel composition:						
Gd_2O_3, g	0	441	547	490	328	313
UO_2, kg	222.44	212.21	212.06	207.78	208.0	207.14
Total fuel, kg	222.44	212.65	212.61	208.27	208.33	207.45

Table **2-2**: Assembly Design 1

Rod type	Number of rods	Pellet density		Stack density (g/cm^3)	Gd_2O_3 (g)	UO_2 (g)	Stack length (cm)
		UO_2 (g/cm^3)	UO_2+Gd_2O_3 (g/cm^3)				
1	31	10.42	-	10.34	0	4 548	365.76
2	17	10.42	-	10.34	0	4 548	365.76
2s	01	10.42	-	10.34	0	4 140	330.2

Pellet outer diameter = 1.23698 cm.

Cladding = Zircaloy-2, 1.43002 cm outer diameter × .08128 cm wall thickness, all rods.

Gas plenum length = 40.64 cm.

Table **2-3**: Assembly Design 1

Rod type	Number of rods	Pellet density		Stack density (g/cm^3)	Gd_2O_3 (g)	UO_2 (g)	Stack length (cm)
		UO_2 (g/cm^3)	$UO_2+Gd_2O_3$ (g/cm^3)				
1	31	10.42	-	10.34	0	4 548	365.76
2	17	10.42	-	10.34	0	4 548	365.76
2s	01	10.42	-	10.34	0	4 140	330.2

Pellet outer diameter = 1.23698 cm.

Cladding = Zircaloy-2, 1.43002 cm outer diameter × .08128 cm wall thickness, all rods.

Gas plenum length = 40.64 cm.

Table **2-4**: Assembly Design 2

Rod type	Number of rods	Pellet density		Stack density (g/cm^3)	Gd_2O_3 (g)	UO_2 (g)	Stack length (cm)
		UO_2 (g/cm^3)	$UO_2+Gd_2O_3$ (g/cm^3)				
1	25	10.42	–	10.32	0	4 352	365.76
1s	1	10.42	–	10.32	0	3 935	330.20
2	12	10.42	–	10.32	0	4 352	365.76
3	6	10.42	–	10.32	0	4 352	365.76
4	1	10.42	–	10.32	0	4 352	365.76
5A	3	–	10.29	10.19	129	4 171	365.76
6B	1	10.42	10.29	10.27	54	4 277	365.76

Pellet outer diameter = 1.21158 cm.

Cladding = Zircaloy-2, 1.43002 cm outer diameter × .09398 cm wall thickness, all rods.

Gas plenum length = 40.132 cm.

Table **2-5**: Assembly Design 3

Rod type	Number of rods	Pellet density		Stack density (g/cm^3)	Gd_2O_3 (g)	UO_2 (g)	Stack length (cm)
		UO_2 (g/cm^3)	$UO_2+Gd_2O_3$ (g/cm^3)				
1	26	10.42	–	10.32	0	4 352	365.76
2	11	10.42	–	10.32	0	4 352	365.76
3	6	10.42	–	10.32	0	4 352	365.76
4	1	10.42	–	10.32	0	4 352	365.76
5A	2	–	10.29	10.19	129	4 171	365.76
6C	1	–	10.29	10.19	117	3 771	330.20
7E	1	10.42	10.25	10.28	43	4 292	365.76
8D	1	10.42	10.25	10.19	129	4 172	365.76

Pellet outer diameter = 1.21158 cm.

Cladding = Zircaloy-2, 1.43002 cm outer diameter × .09398 cm wall thickness, all rods.

Gas plenum length = 40.132 cm.

Table **2-6**: Assembly Design 4

Rod type	Number of rods	Pellet density		Stack density (g/cm^3)	Gd_2O_3 (g)	UO_2 (g)	Stack length (cm)
		UO_2 (g/cm^3)	$UO_2+Gd_2O_3$ (g/cm^3)				
1	39	10.42	–	10.32	0	3 309	365.76
2	14	10.42	–	10.32	0	3 309	365.76
3	4	10.42	–	10.32	0	3 309	365.76
4	1	10.42	–	10.32	0	3 309	365.76
5	5	–	10.29	10.19	98	3 172	365.76
WS	1	–	–	–	0	0	–

Pellet outer diameter = 1.05664 cm.

Cladding = Zircaloy-2, 1.25222 cm outer diameter × .08636 cm wall thickness, all rods.

Gas plenum length = 40.64 cm except water rod.

Gd_2O_3 in rod type 5 runs full 365.76 cm.

Water rod (WS) has holes drilled top and bottom to provide water flow and little or no boiling.

Water rod is also a spacer positioning rod.

Table **2-7**: Assembly Design 5

Rod type	Number of rods	Pellet density		Stack density (g/cm^3)	Gd_2O_3 (g)	UO_2 (g)	Stack length (cm)
		UO_2 (g/cm^3)	UO_2+Gd_2O_3 (g/cm^3)				
1	39	10.42	–	10.32	0	3 309	365.76
2	14	10.42	–	10.32	0	3 309	365.76
3	4	10.42	–	10.32	0	3 309	365.76
4	1	10.42	–	10.32	0	3 309	365.76
5	5	–	10.33	10.23	66	3 216	365.76
WS	1	–	–	–	0	0	–

Pellet outer diameter = 1.05664 cm.

Cladding = Zircaloy-2, 1.25222 cm outer diameter × .08636 cm wall thickness, all rods.

Gas plenum length = 40.64 cm, except water rod.

Gd_2O_3 in rod type 5 runs full 365.76 cm.

Water rod (WS) has holes drilled top and bottom to provide water flow and little or no boiling.

Water rod is also a spacer positioning rod.

Table **2-8**: Assembly Design 6

Rod type	Number of rods	Pellet density		Stack density (g/cm^3)	Gd_2O_3 (g)	UO_2 (g)	Stack length (cm)
		UO_2 (g/cm^3)	UO_2+Gd_2O_3 (g/cm^3)				
1	38	10.42	–	10.32	0	3 125	355.6
2	14	10.42	–	10.32	0	3 125	355.6
3	4	10.42	–	10.32	0	3 125	355.6
4	1	10.42	–	10.32	0	3 125	355.6
5	5	–	10.33	10.23	63	3 037	355.6
WR,WS	2	–	–	–	0	0	–
ENDS	62	10.42	–	10.32	0	223	25.4

Pellet outer diameter = 1.0414 cm.

Cladding = Zircaloy-2, 1.22682 cm outer diameter × .08128 cm wall thickness, all fuelled rods

= Zircaloy-2, 1.50114 cm outer diameter × .07620 cm wall thickness, water rods.

Gas plenum length = 24.0792 cm.

Gd_2O_3 in rod type 5 runs full 355.6 cm.

Water rod (WS) has holes drilled top and bottom to provide water flow and little or no boiling.

Table **2-9**: Decay Constant and Fractions of Delayed neutrons

Group	Decay constant (s^{-1})	Relative fraction of delayed neutrons in %
1	0.012813	0.0167
2	0.031536	0.1134
3	0.124703	0.1022
4	0.328273	0.2152
5	1.405280	0.0837
6	3.844728	0.0214

Total fraction of delayed neutrons: 0.5526%.

Table **2-10**: Heavy-element Decay Heat Constants

Group no. (isotope)	Decay constant (s^{-1})	Available energy from a single atom (MeV)
70 (^{239}U)	4.91×10^{-4}	0.474
71 (^{239}Np)	3.41×10^{-6}	0.419

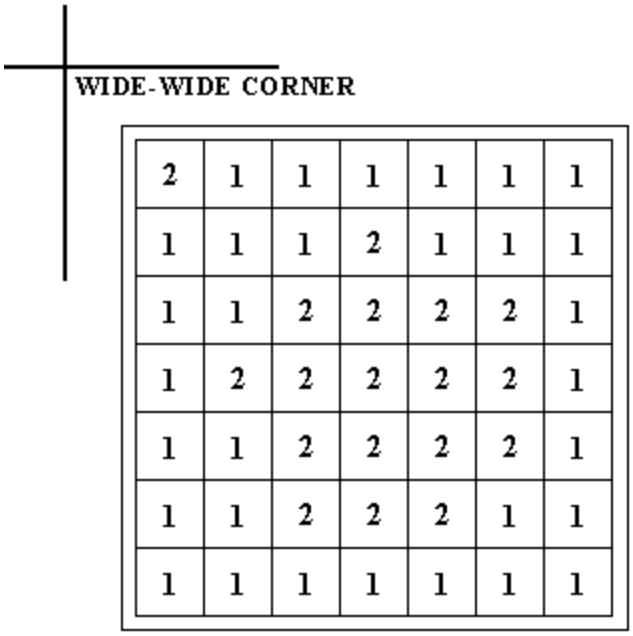

Table **2-11**: Assembly Design for Type 1 Initial Fuel

Rod type	^{23}U (wt.%)	Gd_2O_3 (wt.%)	No. of rods
1	1.33	0	31
2	0.71	0	18

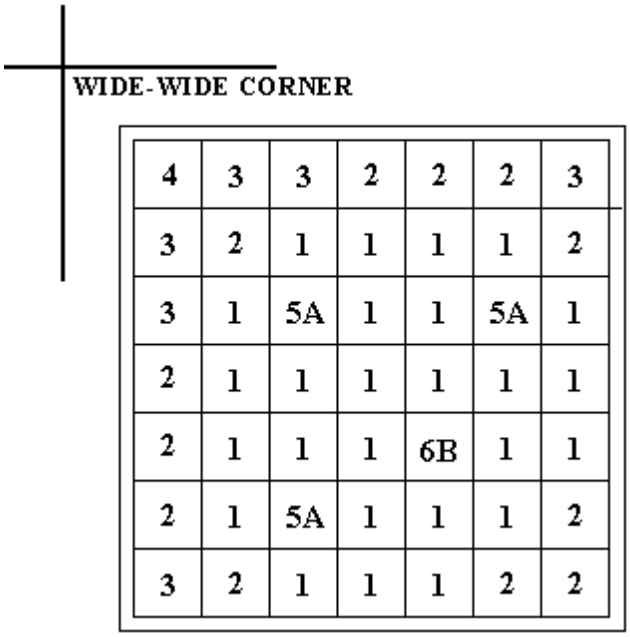

Table **2-12**: Assembly Design for Type 2 Initial Fuel

Rod type	^{235}U (wt.%)	Gd_2O_3 (wt.%)	No. of rods
1	2.93	0	26
2	1.94	0	12
3	1.69	0	6
4	1.33	0	1
5A	2.93	3.0	3
6B	2.93	3.0	1

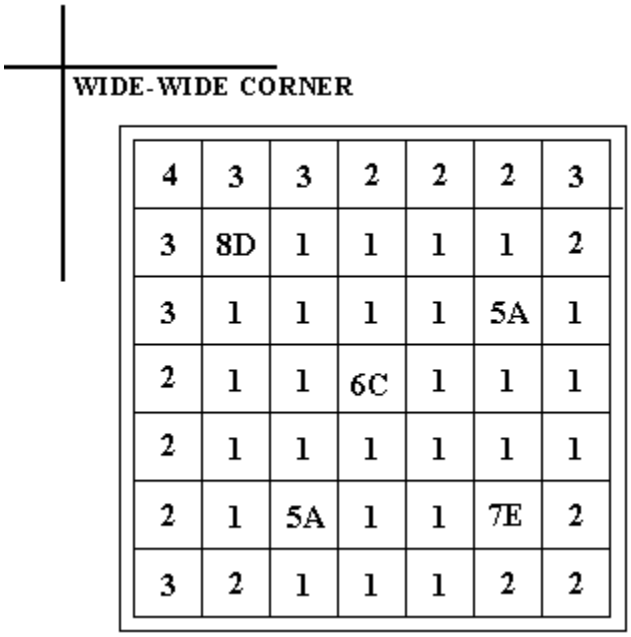

Table **2-13** Assembly Design for Type 3 Initial Fuel

Rod type	^{235}U (wt.%)	Gd_2O_3 (wt.%)	No. of rods
1	2.93	0	26
2	1.94	0	11
3	1.69	0	6
4	1.33	0	1
5A	2.93	3.0	2
6C	2.93	3.0	1
7E	2.93	4.0	1
8D	1.94	4.0	1

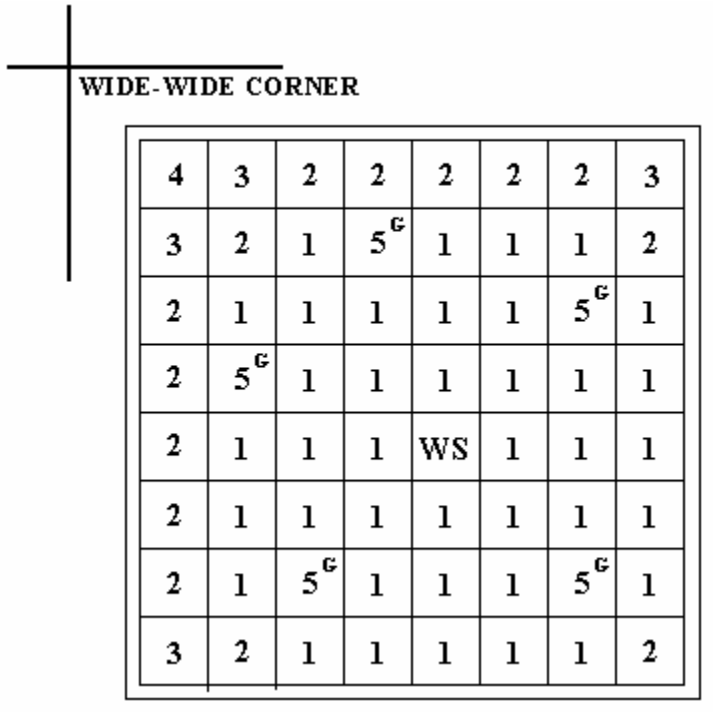

Table **2-14**: Assembly Design for Type 4 8 × 8 UO_2 Reload

Rod type	^{235}U (wt.%)	Gd_2O_3 (wt.%)	No. of rods
1	3.01	0	39
2	2.22	0	14
3	1.87	0	4
4	1.45	0	1
5	3.01	3.0	5
WS	–	0	1

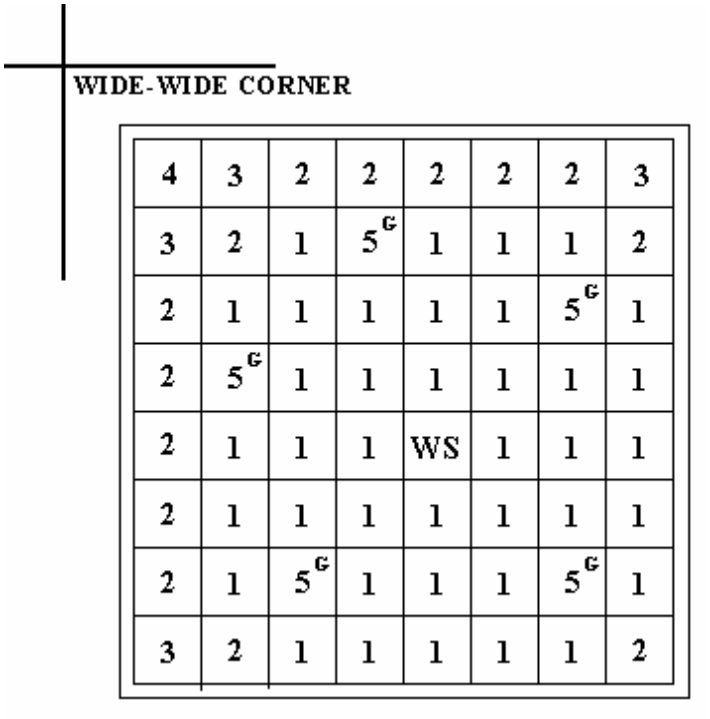

Table **2-15**: Assembly Design for Type 5 8 × 8 UO_2 Reload

Rod type	^{235}U (wt.%)	Gd_2O_3 (wt.%)	No. of rods
1	3.01	0	39
2	2.22	0	14
3	1.87	0	4
4	1.45	0	1
5	3.01	2.0	5
WS	–	0	1

WS – Spacer positioning water rod.

G – Gadolinium rods.

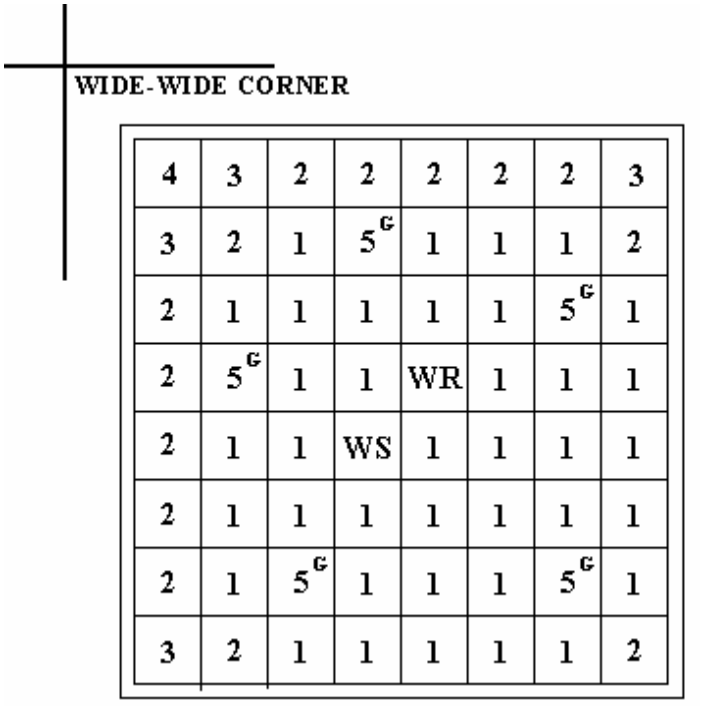

Table **2-16**: Assembly Design for Type 6 8 × 8 UO_2 Reload, LTA

Rod type	^{235}U (wt.%)	Gd_2O_3 (wt.%)	No. of rods
1	3.01	0	38
2	2.22	0	14
3	1.87	0	4
4	1.45	0	1
5	3.01	2.0	5
WS	–	0	1
WR	–	0	1

WS – Spacer positioning water rod.

WR – Water rod.

G – Gadolinium rods.

Table **2-17**: Control Rod Data (*Movable Control Rods*)

Shape	Cruciform
Pitch, cm	30.48
Stroke, cm	365.76
Control length, cm	363.22
Control material	B_4C granules in Type-304, stainless steel tubes and sheath
Material density	70% of theoretical
Number of control material tubes per rod	84
Tube dimensions	.47752 cm outer diameter by .0635 cm wall
Control blade half span, cm	12.3825
Control blade full thickness, cm	.79248
Control blade tip radius, cm	.39624
Sheath thickness, cm	.14224
Central structure wing length, cm	1.98501
Blank tubes per wing	None

Table **2-18**: Definition of Assembly Types

Assembly type	Assembly design (see Tables 2.10 through 2.15)
1	5
2	4
3	5
4	6
5	2
6	2
7	2
8	2
9	2
10	2
11	3
12	2
13	3
14	2
15	3
16	2
17	3
18	2
19	Reflector

Table **2-19**: Composition Numbers in Axial Layer for Each Assembly Type

	1	2	3	4	5	6	7	8	9	10	11	12	13	14	15	16	17	18	19
1	433	433	433	433	433	433	433	433	433	433	433	433	433	433	433	433	433	433	433
2	1	25	49	73	97	121	145	169	193	217	241	265	289	313	337	361	385	409	435
3	2	26	50	74	98	122	146	170	194	218	242	266	290	314	338	362	386	410	435
4	3	27	51	75	99	123	147	171	195	219	243	267	291	315	339	363	387	411	435
5	4	28	52	76	100	124	148	172	196	220	244	268	292	316	340	364	388	412	435
6	5	29	53	77	101	125	149	173	197	221	245	269	293	317	341	365	389	413	435
7	6	30	54	78	102	126	150	174	198	222	246	270	294	318	342	366	390	414	435
8	7	31	55	79	103	127	151	175	199	223	247	271	295	319	343	367	391	415	435
9	8	32	56	80	104	128	152	176	200	224	248	272	296	320	344	368	392	416	435
10	9	33	57	81	105	129	153	177	201	225	249	273	297	321	345	369	393	417	435
11	10	34	58	82	106	130	154	178	202	226	250	274	298	322	346	370	394	418	435
12	11	35	59	83	107	131	155	179	203	227	251	275	299	323	347	371	395	419	435
13	12	36	60	84	108	132	156	180	204	228	252	276	300	324	348	372	396	420	435
14	13	37	61	85	109	133	157	181	205	229	253	277	301	325	349	373	397	421	435
15	14	38	62	86	110	134	158	182	206	230	254	278	302	326	350	374	398	422	435
16	15	39	63	87	111	135	159	183	207	231	255	279	303	327	351	375	399	423	435
17	16	40	64	88	112	136	160	184	208	232	256	280	304	328	352	376	400	424	435
18	17	41	65	89	113	137	161	185	209	233	257	281	305	329	353	377	401	425	435
19	18	42	66	90	114	138	162	186	210	234	258	282	306	330	354	378	402	426	435
20	19	43	67	91	115	139	163	187	211	235	259	283	307	331	355	379	403	427	435
21	20	44	68	92	116	140	164	188	212	236	260	284	308	332	356	380	404	428	435
22	21	45	69	93	117	141	165	189	213	237	261	285	309	333	357	381	405	429	435
23	22	46	70	94	118	142	166	190	214	238	262	286	310	334	358	382	406	430	435
24	23	47	71	95	119	143	167	191	215	239	263	287	311	335	359	383	407	431	435
25	24	48	72	96	120	144	168	192	216	240	264	288	312	336	360	384	408	432	435
26	434	434	434	434	434	434	434	434	434	434	434	434	434	434	434	434	434	434	434

Table **2-20**: Range of Variables

T Fuel (°K)	Rho M. (kg/m^3)
400.0	141.595
800.0	141.595
1 200.0	141.595
1 600.0	141.595
2 000.0	141.595
2 400.0	141.595
400.0	226.154
800.0	226.154
1 200.0	226.154
1 600.0	226.154
2 000.0	226.154
2 400.0	226.154
400.0	299.645
800.0	299.645
1 200.0	299.645
1 600.0	299.645
2 000.0	299.645
2 400.0	299.645
400.0	435.045
800.0	435.045
1 200.0	435.045
1 600.0	435.045
2 000.0	435.045
2 400.0	435.045
400.0	599.172
800.0	599.172
1 200.0	599.172
1 600.0	599.172
2 000.0	599.172
2 400.0	599.172
400.0	779.405
800.0	779.405
1 200.0	779.405
1 600.0	779.405
2 000.0	779.405
2 400.0	779.405

Table **2-21**: Key to Macroscopic Cross-section Tables

T_{f1}	T_{f2}	T_{f3}	T_{f4}	T_{f5}	T_{f6}
ρ_{m1}	ρ_{m2}	ρ_{m3}	ρ_{m4}	ρ_{m5}	ρ_{m6}
Σ_1	Σ_2	...			
		...	Σ_{34}	Σ_{35}	Σ_{36}

Where:
– T_f is the Doppler (fuel) temperature (°K)
– ρ_m is the moderator density (kg/m^3)
Macroscopic cross-sections are in units of cm^{-1}

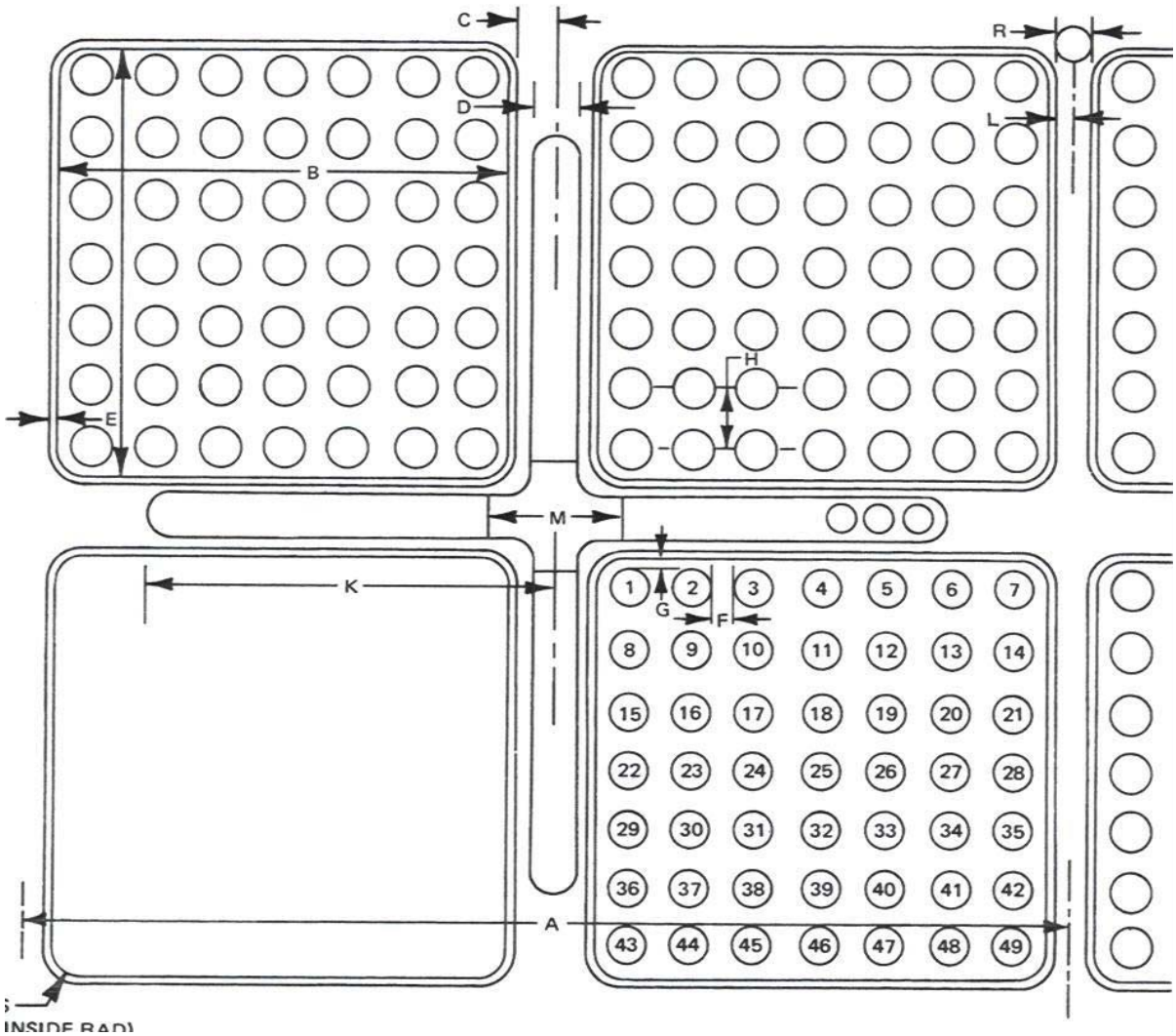

Dim. ID	A	B	C	D	E	F	G	H	I	J
Dim. (in)	12.0	5.278	0.375		0.080	0.175	0.1435	0.738		
Dim. (cm)	30.48	13.40612	.9525		.2032	.4445	.36449	1.87452		

Dim. ID	K	L	M	N	O	P	Q	R	S
Dim. (in)		0.187							0.38
Dim. (cm)		.47498							.9652

Figure **2-3**: PB2 Initial Fuel Assembly Lattice

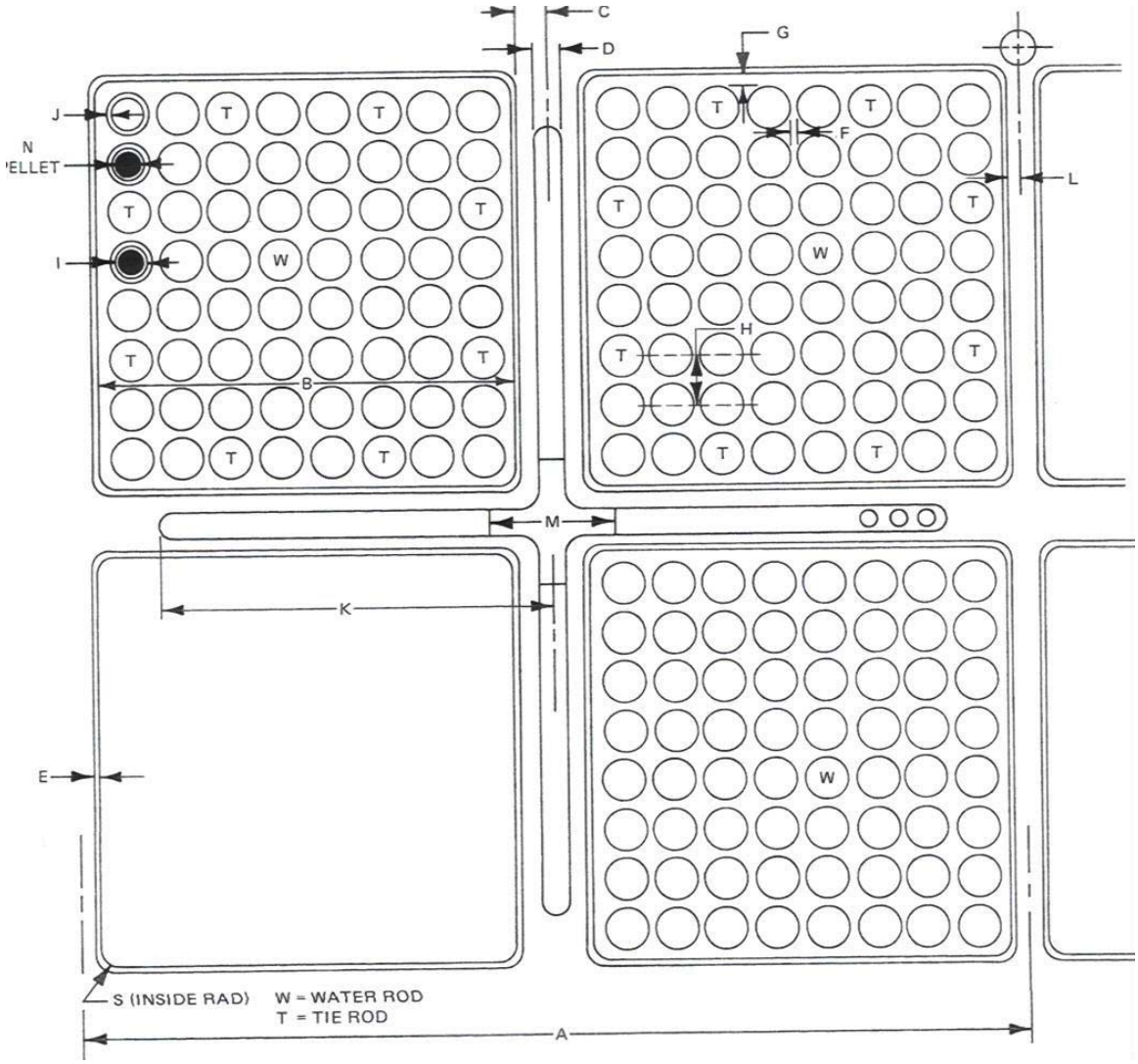

Dim. ID	A	B	C	D	E	F	G	H	I	J
Dim. (in)	12.0	5.278	0.355		0.100	0.147	0.153	0.64		
Dim. (cm)	30.48	13.40612	.9017		.254	.37338	.38862	1.6256		

Dim. ID	K	L	M	N	O	P	Q	R	S
Dim. (in)		0.167							0.38
Dim. (cm)		.42418							.9652

Figure **2-4**: PB2 Reload Fuel Assembly Lattice for 100 mil Channels

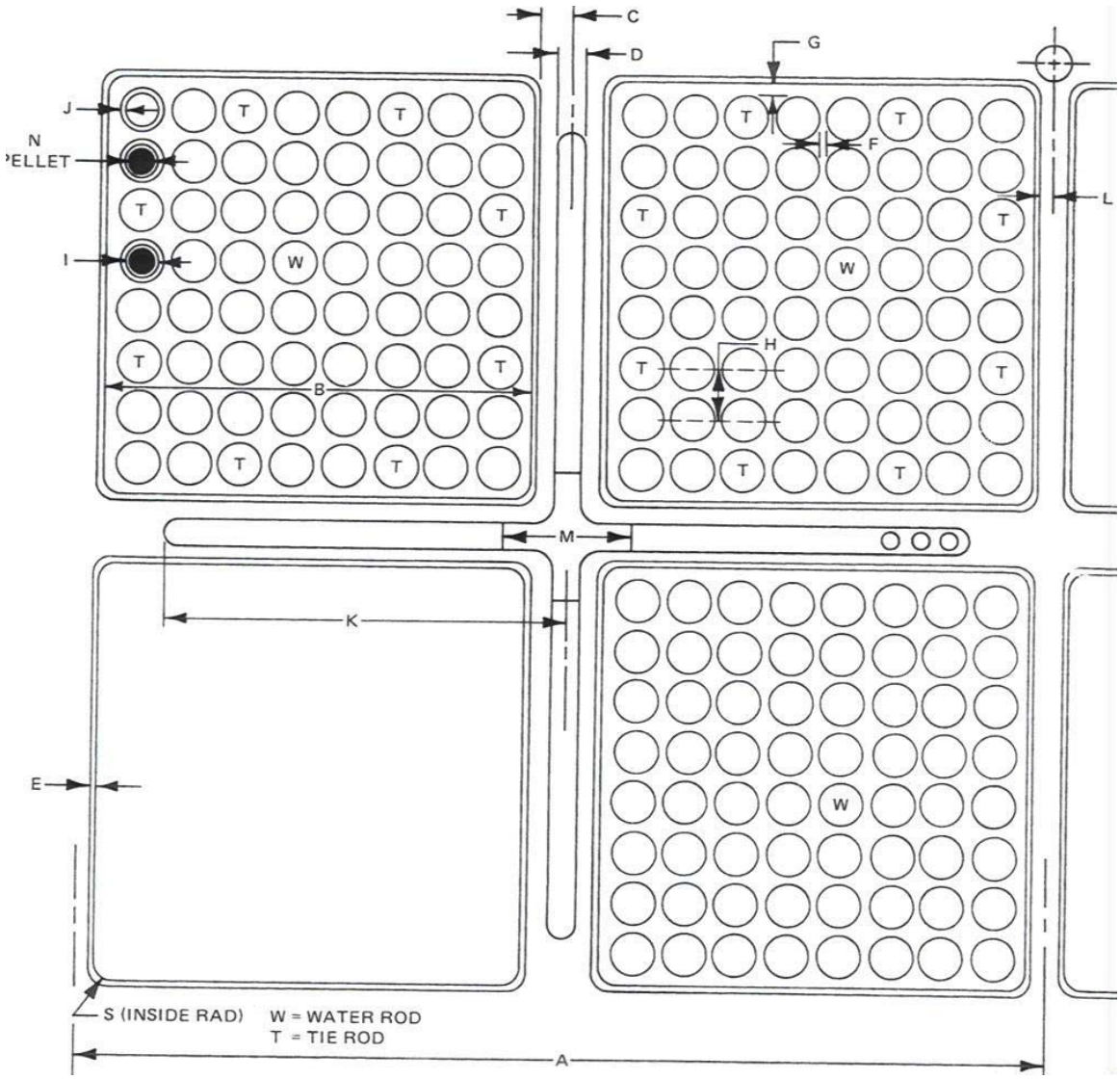

Dim. ID	A	B	C	D	E	F	G	H	I	J
Dim. (in)	12.0	5.278	0.355		0.120	0.147	0.153	0.64		
Dim. (cm)	30.48	13.40612	.8509		.3048	.37338	.38862	1.6256		

Dim. ID	K	L	M	N	O	P	Q	R	S
Dim. (in)		0.147							0.38
Dim. (cm)		.42418							.9652

Figure **2-5**: PB2 Reload Fuel Assembly Lattice for 120 mil Channels

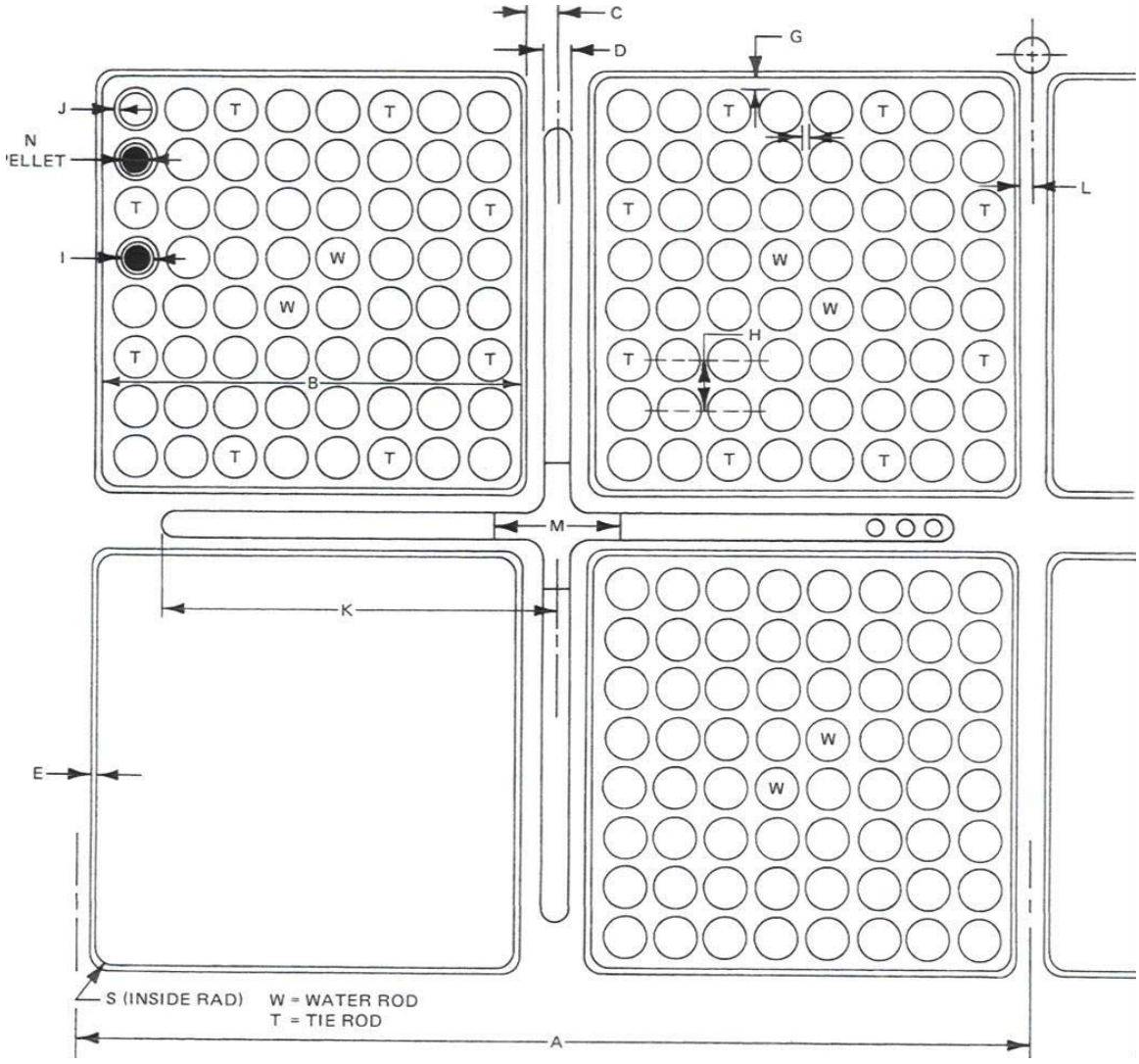

Dim. ID	A	B	C	D	E	F	G	H	I	J
Dim. (in)	12.0	5.278	0.355		0.100	0.157	0.158	0.64		
Dim. (cm)	30.48	13.40612	.9017		.254	.39878	.40132	1.6256		

Dim. ID	K	L	M	N	O	P	Q	R	S
Dim. (in)		0.167							0.38
Dim. (cm)		.42418							.9652

Figure **2-6**: PB2 Reload Fuel Assembly Lattice for LTA Assemblies

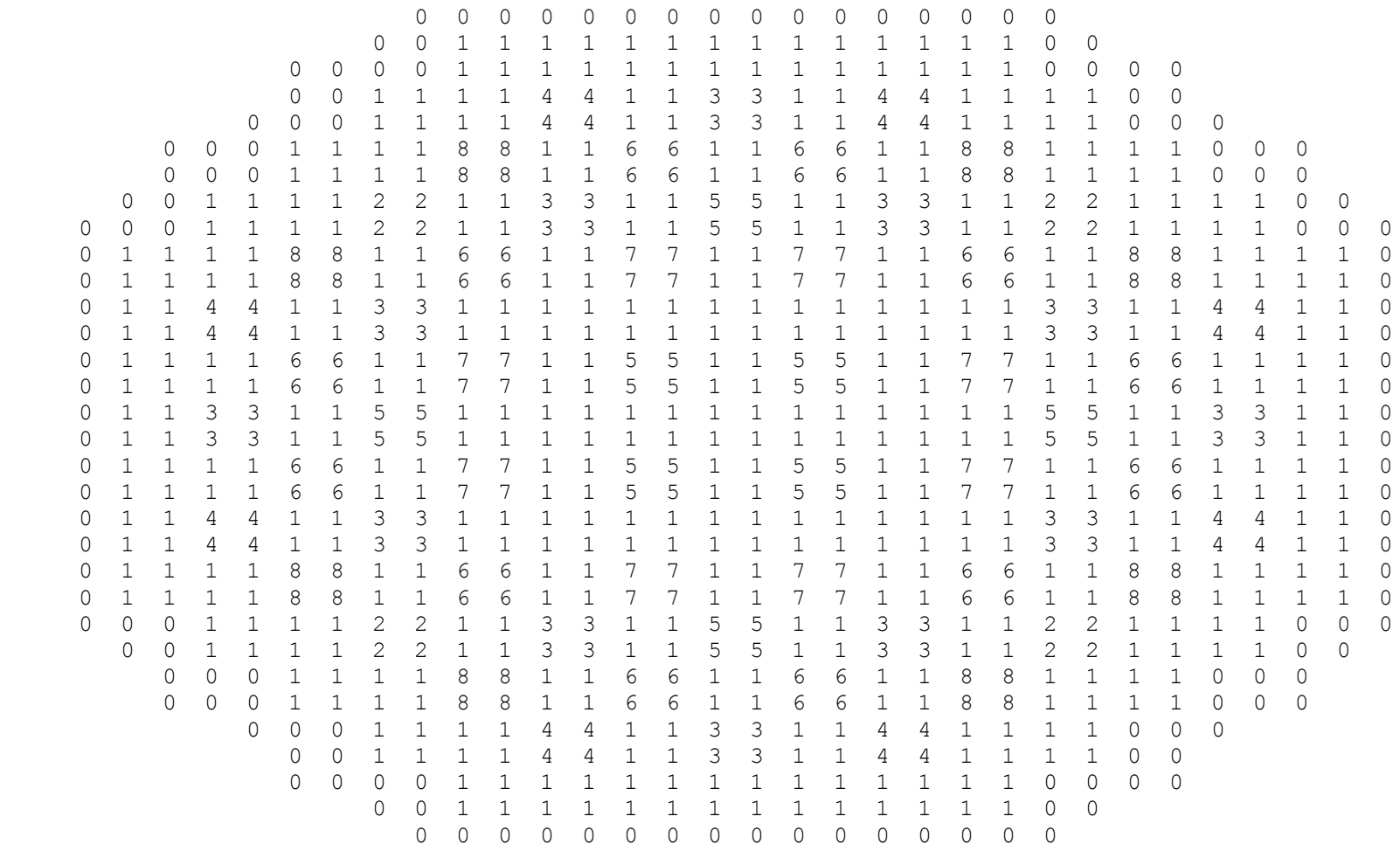

Figure **2-7**: PSU Control Rod Grouping

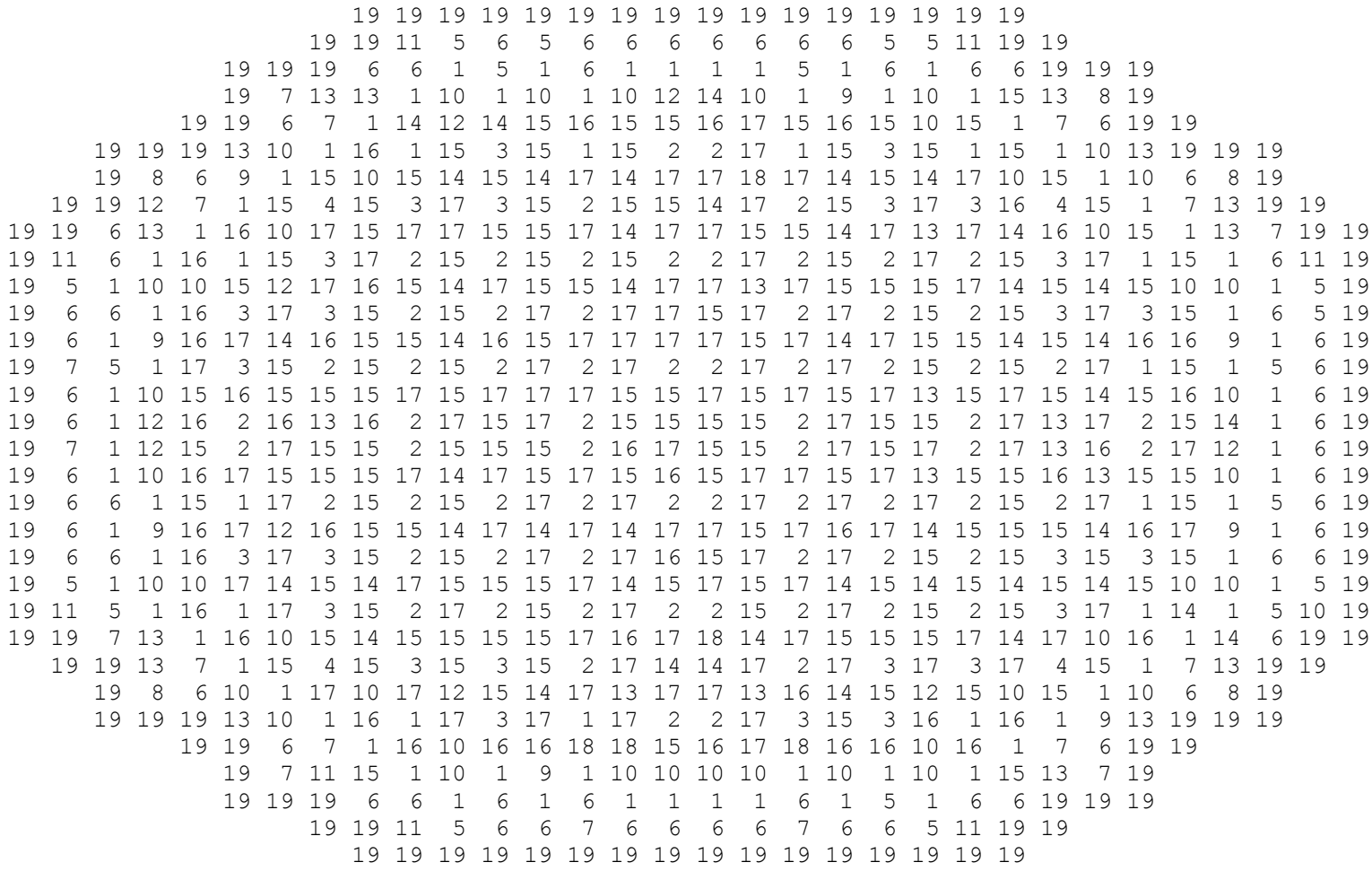

Figure **2-8**: Radial Distribution of Assembly Types

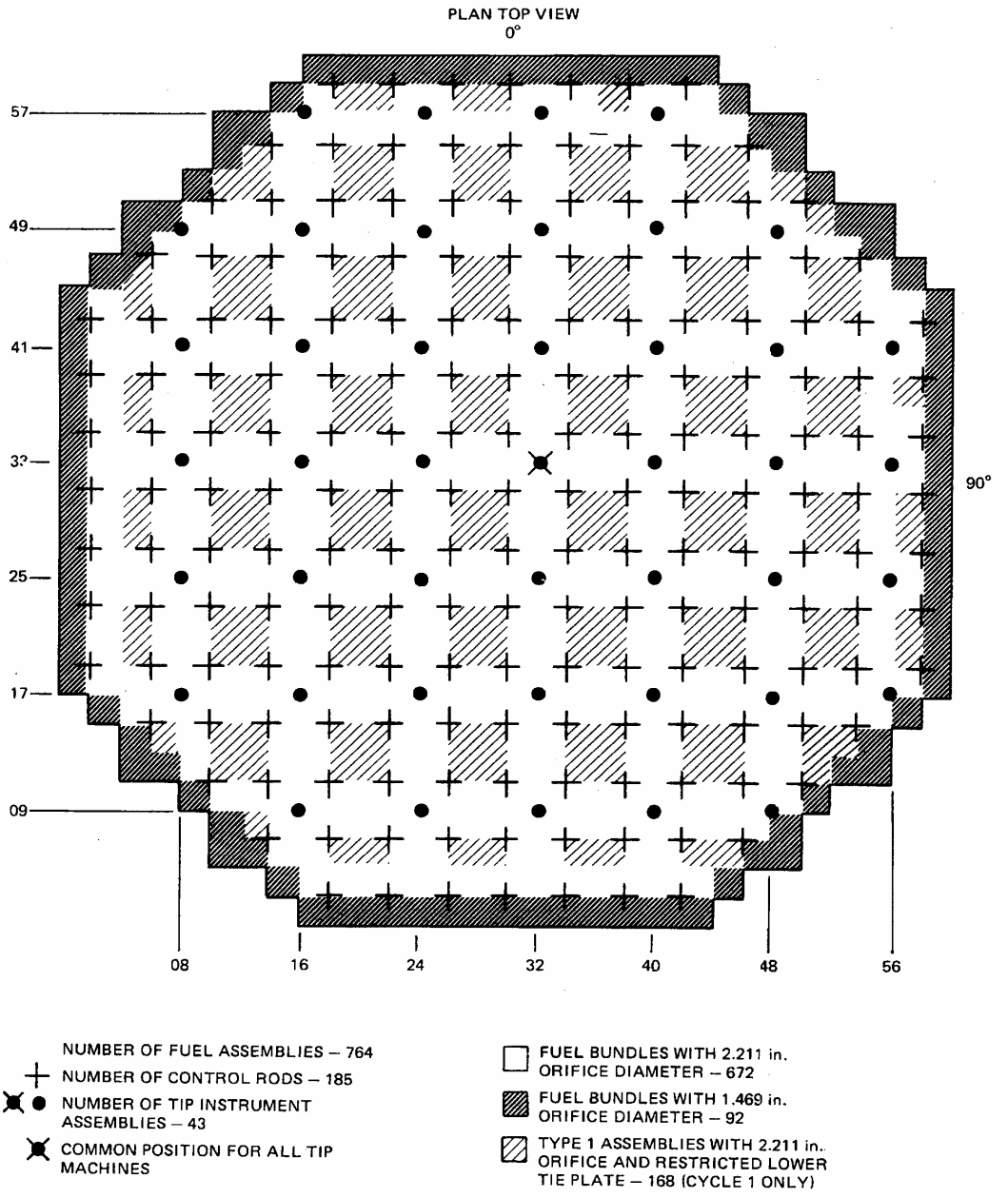

Figure **2-9**: Core Orificing and TIP System Arrangement

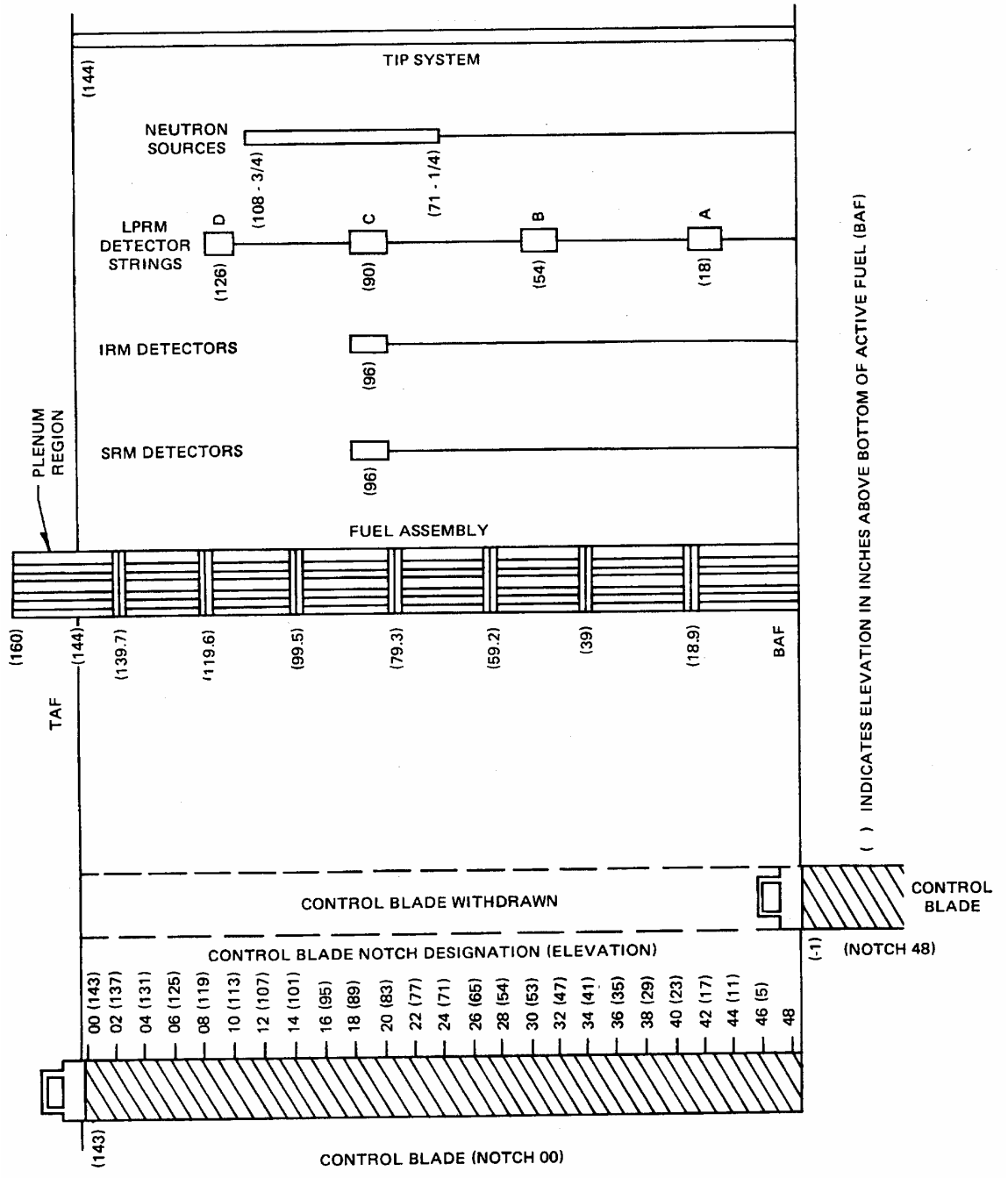

Figure **2-11**: Elevation of Core Components

2.1.2 Thermal Hydraulic Data

PB2 is a GE designed BWR/4 with a rated thermal power of 3, 293 MW, a rated core flow of 12, 915 kg/s (102.5 x10^6 lb/hr), a rated steam flow of 1,685 kg/s (13.37x10^6 lb/hr) and a turbine inlet pressure of 6.65 MPa (965 psia). The nuclear steam supply system (NSSS) has turbine driven feed pumps and a two-loop M-G driven recirculation system feeding a total of 20 jet-pumps. There are totally four steam lines and each has a flow-limiting nozzle, main steam isolation valves (MSIVs), safety relieve valves (SRVs), and a turbine stop valve (TSV). The steam by-pass system consists of nine by-pass valves (BPVs) mounted on a common header, which is connected to each of the four steam lines.

Figure 2-12 shows PSU thermal-hydraulic radial mapping scheme utilized to represent the PB2 reactor core. The feedback, or coupling between neutronics and thermal-hydraulics can be characterized by choosing user supplied mapping schemes (spatial mesh overlays) in the radial and axial core planes. Some of the inlet perturbations (inlet disturbances of both temperature and flow rate) are specified as a fraction of the position across the core inlet. This requires either a 3-D modeling of the vessel, or some type of a multi-channel model. For this thesis the developed core multi-channel model consists of 33 channels to represent the 764 fuel assemblies of the PB2 reactor core. The core thermal-hydraulic model was built according to different criteria. First, the fuel assemblies are ranked according to the inlet orifice characteristics. A second criterion is the fuel assembly type (e.g. 7x7 or 8x8). Finally, the thermal-hydraulic conditions are also considered (e.g. fuel assembly power, mass flow, etc)

It is recommended that an assembly flow are a of 15.535 in^2 (1.0023E^{-02} m^2) for fuel assemblies with 7x7 fuel rod arrays, and 15.5277 in^2 (1.0017E^{-02} m^2) for fuel assemblies with 8x8 fuel rod arrays be used in the core thermal-hydraulic multi-channel models. There are 764 fuel

assemblies in the PB2 reactor core. At EOC2, there are 576 fuel assemblies of 7x7 type, and 188 of the 8x8 type. The radial distribution of assembly type is shown in Figure 2-8 in which the assembly types from 1 to 4 identify a fuel assembly with 8x8 fuel arrays and the assembly types from 5 to 18 identify a fuel assembly with a 7x7 fuel rod arrays. The core hydraulic characteristics (e.g. core pressure drop) can be found in Ref [3]

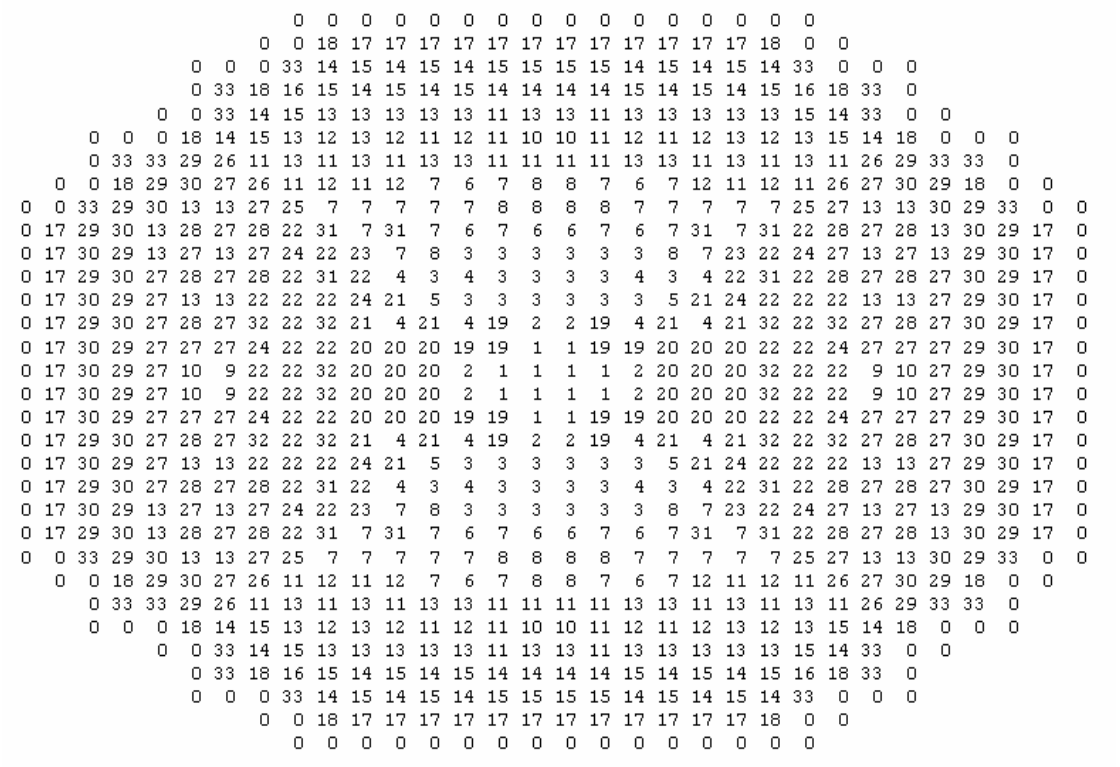

Figure **2-12**: Reactor Core Thermal-hydraulic Channel Radial Map

2.1.3 Initial Steady State Conditions

Table 2.22 provides the reactor initial conditions for performing steady state calculations while Figure 2-13 shows the PB2 TT2 initial control rod pattern. TT2 was initiated from steady-state conditions after obtaining P1 edits from the process computer for nuclear and thermal-hydraulic conditions of the core. PB2 was chosen for the turbine trip tests because it is a large BWR/4 with relatively small turbine by-pass capacity. During the test, the initial thermal power level was 61.6% rated 2030 NW; core flow was 80.9% rated 10, 445 kg/s (82.9 x 10^6 lb/hr); and average range power monitor (APRM) scram setting was 95% of nominal power. For the TT2 test, the dynamic measurements were taken with a high-speed digital data acquisition system capable of sampling over 150 signals every 6 milliseconds and the core power distribution measurements were taken from the plant's local in-core flux detectors. Special fast response pressure and differential pressure transducers were installed in parallel with the existing plant instruments in the nuclear steam supply system.

Table **2-1**: PB2 TT2 Initial Conditions from Process Computer P1 Edit

Core Thermal Power, MWt	2,030
Initial Power Level, % of rated	61.6
Gross Power Output, MWe	625.1
Feedwater Flow, kg/s	980.26
Reactor Pressure, Pa	6,798,470.0
Total Core Flow, kg/s	10,445.0
Core Inlet Subcooling, J/kg	48,005.291
Feedwater Temperature, K	442.31
Core Pressure Drop, Pa	113,560.7
Jet-pump Driving Flow, kg/s	2,871.24*
Core Average Exit Quality, fraction	0.097
Core Average Void Fraction, fraction	0.304
Core Average Power Density, kW/l	31.28

(48 – full withdrawn, 0 – full insertion)

	02	06	10	14	18	22	26	30	34	38	42	46	50	54	58
59					48	48	48	48	48	48	48				
55				48	48	34	48	36	48	34	48	48			
51			48	48	0	48	26	48	26	48	0	48	48		
47		48	48	40	48	36	48	32	48	36	48	40	48	48	
43	48	48	0	48	26	48	4	48	4	48	26	48	0	48	48
39	48	34	48	36	48	48	48	48	48	48	48	36	48	34	48
35	48	48	26	48	4	48	32	48	32	48	4	48	26	48	48
31	48	36	48	32	48	48	48	48	48	48	48	32	48	36	48
27	48	48	26	48	4	48	32	48	32	48	4	48	26	48	48
23	48	34	48	36	48	48	48	48	48	48	48	36	48	34	48
19	48	48	0	48	26	48	4	48	4	48	26	48	0	48	48
15		48	48	40	48	36	48	32	48	36	48	40	48	48	
11			48	48	0	48	26	48	26	48	0	48	48		
07				48	48	34	48	36	48	34	48	48			
03					48	48	48	48	48	48	48				

Figure **2-13**: PB2 HP Control Rod Pattern

The initial water level above vessel zero (AVZ) is equal to 14.1478 m (557 in). This measured level is the actual level inside the steam dryer shroud. The initial level AVZ is equal to 14.3256 m (564 in) for the narrow range measurement outside steam dryer shroud. AVZ is the lowest interior elevation of the vessel (bottom of lower plenum). Table 2-23 and Figure 2-14 provide the process computer P1 edit for the initial core axial relative power distribution.

Table **2-2**: PB2 TT2 Initial Core Axial Relative Power From P1 Edit

Axial Node Number	Axial Location (cm)	Relative Power
1	7.62	0.308051
2	22.86	0.616103
3	38.10	0.707754
4	53.34	0.773947
5	68.58	0.814681
6	83.82	0.880874
7	99.06	0.972526
8	114.30	1.066723
9	129.54	1.163467
10	144.78	1.260210
11	160.02	1.356953
12	175.26	1.407871
13	190.50	1.412963
14	205.74	1.402779
15	220.98	1.377320
16	236.22	1.328949
17	251.46	1.257664
18	266.70	1.188925
19	281.94	1.122733
20	297.18	1.031081
21	312.42	0.913971
22	327.66	0.763764
23	342.90	0.580460
24	358.14	0.290230

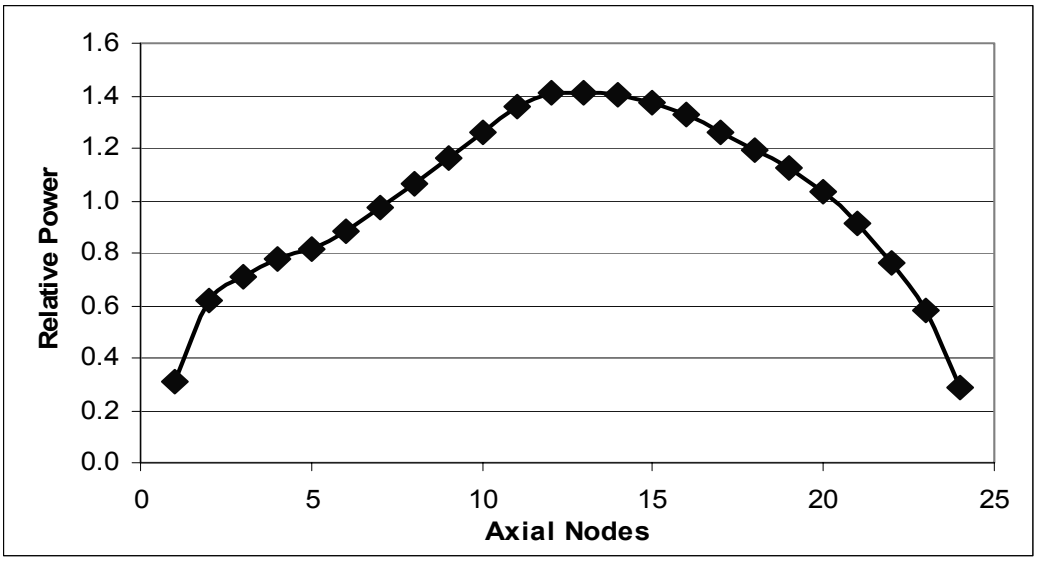

Figure **2-14**: PB2 TT2 Initial Core Axial Relative Power From P1 Edit

2.1.4 Transient Calculations

During the TT2 test, most of the important phenomena occur in the first five seconds of the transient. Therefore, the test is simulated for a five-second time period. This approach simplifies the number of components required for performing the analysis of TT2. Basically, the transient begins with the closure of the TSV. At some point in time, the turbine BPV begins to open. The only boundary conditions imposed in the analysis should be limited to the opening and closure of the above valves. Table 2-24 shows the event timing during the transient. Table 2-25 shows the scram initiation time and the delay time while Table 2-26 shows the average control rod density (CRD) position during the reactor scram. An average velocity can be obtained from Table 2-26 for the scram modelling in the 3-D kinetics case. An approximate value obtained from this table is 2.34 ft/s (0.713 m/s) for the first 0.04 seconds and 4.67 ft/s (1.423 m/s) thereafter. Also it should be noted that during the Exercise 3 Best Estimate Case, the set points of the SRVs are never reached. Table 2-27 summarises the safety relief valve reference design information to be utilized in Extreme Scenario 2.

Table **2-3**: PB2 TT2 Event Timing (Time in ms)

TSV begins to close		0 00
TSV closed		096
Begin bypass opening	0	60
Bypass full-open		846
Turbine pressure initial response		
Steam line A		102
Steam line D		126
Steam line pressure initial response		
Steam line A		348
Steam line D		378
Vessel pressure initial response		432
Core exit pressure initial response		486

Table **2-4**: PB2 TT2 Scram Characteristics

APRM high flux scram set-point, % rated	95 (3128.35 MWt)
Time delay prior to rod motion, msec	120
Time of scram initiation, sec	0.63
Initiates CR insertion, sec	0.75

Table **2-5**: CRD Position After Scram vs. Time

Time (sec)	Position (ft)
0.000	0.0000
0.120	0.0000
0.160	0.0935
0.247	0.5000
0.354	1.0000
0.457	1.5000
2.500	10.200
3.080	12.000
5.000	12.000

Table **2-6**: Nuclear System Safety and Relief Valves

	Number of valves	Set pressure (psig/Pa)	Capacity at 103% of set pressure (each), (lb/h)/(kg/s)
Relief valves	4	1 105/7.720E06	819 000/103.19
	4	1 115/7.789E06	827 000/104.20
	3	1 125/7.858E06	834 000/105.08
Total*	11 (5)		
Safety valves	2	1 230/8.582E06	939 858/118.40

* The number in parentheses indicates the number of relief valves which serve in the automatic depressurisation capacity.

2.2 Other PB2 TT Tests

The OECD/NRC BWR TT benchmark (based on PB2 TT2) was used in this study to develop and validate the TRACE/PARCS models. The information given in the current section and in section 2.3 was collected with an attempt to develop TRACE/PARCS models for PB2 turbine trip tests TT1 and TT3 as well as the three LFS tests. However the reference data collected so far were not sufficient to complete an input data file. Initial conditions of those test scenarios are given here and it could be used for future references.

The turbine tests TT1 and TT3 tests have the same core and fuel assembly geometries as TT2.

The TT1 test was conducted 6 days prior to the low flow stability test series and TT3 test was conducted 13 days after the stability testing. The steady state conditions are given in Table 2-28 and were found in [3], [4] and [5]. The TT1 and TT3 axial power profiles as well as the initial control rod patterns are shown in Figure 2-15 through Figure 2-18.

Table **2-7**: PB2 TT1 and TT3 Steady State Initial Conditions

	TT1	TT3
Core Thermal Power, MWt	1562	2275
Initial power level, % of rated	47.4	69.1
Gross power output, MWe	465.9	719.8
Feedwater flow, kg/s	742.92	1120.4
Reactor Pressure, MPa	6.853	6.8465
Total Core flow rate, (kg/s)	12763.586	12839.117
Core inlet subcooling kJ/kg	1129	2309.7
Feedwater temperature (^{o}C)	412.8722	447.8167
Core pressure drop (measured), MPa	0.15168	0.15996

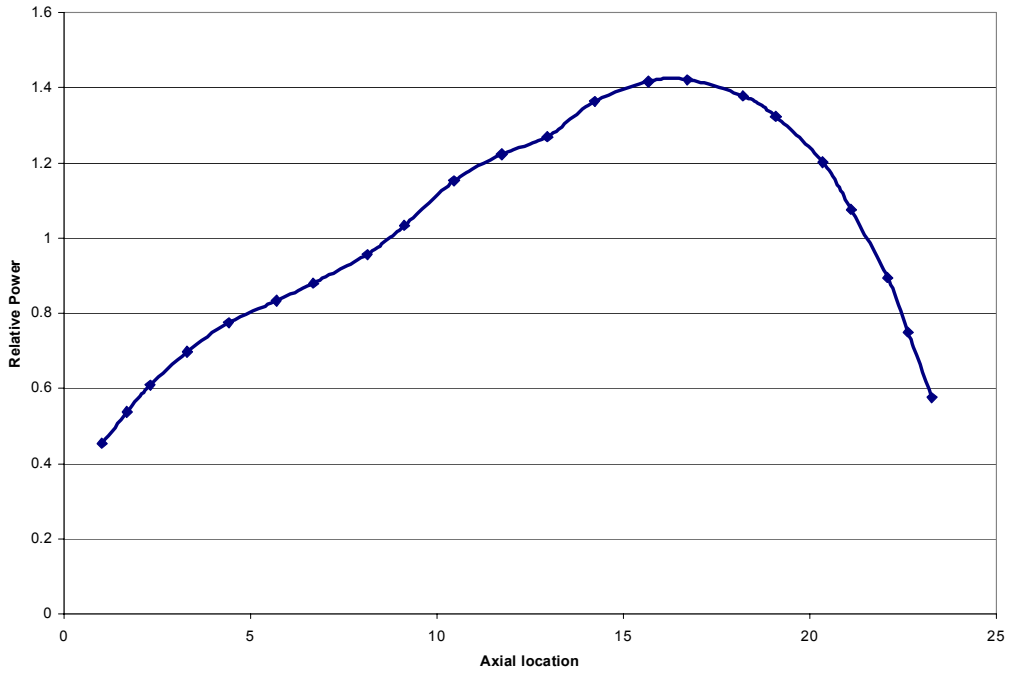

Figure **2-15**: PB2 TT1 Initial Core Axial Relative Power From P1 Edit

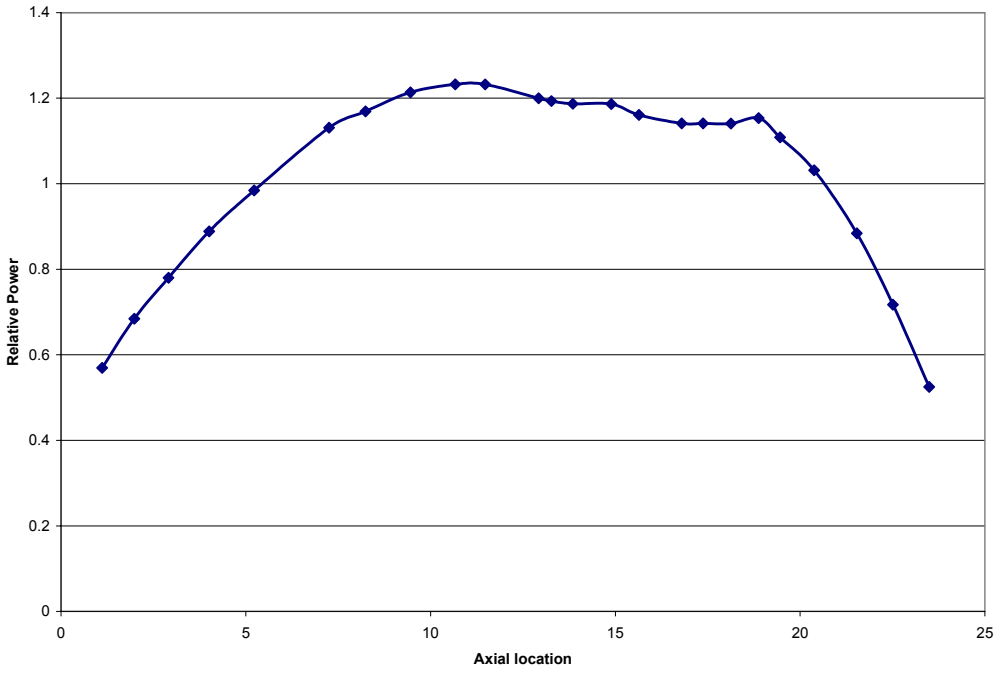

Figure **2-16**: PB2 TT3 Initial Core Axial Relative Power From P1 Edit

			48	48	48	48	48	48	48					
		48	48	38	48	28	48	38	48	48				
	48	48	0	48	0	48	0	48	0	48	48			
	48	48	40	48	20	48	10	48	20	48	40	48	48	
48	48	0	48	0	48	0	48	0	48	0	48	0	48	48
48	38	48	20	48	40	48	48	48	40	48	20	48	38	48
48	48	0	48	0	48	0	48	0	48	0	48	0	48	48
48	48	0	48	0	48	0	48	0	48	0	48	0	48	48
48	38	48	20	48	40	48	48	48	40	48	20	48	38	48
48	48	0	48	0	48	0	48	0	48	0	48	0	48	48
	48	48	40	48	20	48	10	48	20	48	40	48	48	
		48	48	0	48	0	48	0	48	0	48	48		
			48	48	38	48	28	48	38	48	48			
				48	48	48	48	48	48	48				

Figure **2-17**: PB2 TT1 HP Control Rod Pattern

				48	48	48	48	48	48	48				
			48	48	38	48	36	48	38	48	48			
		48	48	34	48	8	48	10	48	34	48	48		
	48	48	40	48	40	48	40	48	40	48	40	48	48	
48	48	34	48	12	48	0	48	0	48	12	48	34	48	48
48	38	48	40	48	48	48	48	48	48	48	40	48	38	48
48	48	10	48	0	48	32	48	32	48	0	48	8	48	48
48	48	10	48	0	48	32	48	32	48	0	48	8	48	48
48	38	48	40	48	48	48	48	48	48	48	40	48	38	48
48	48	34	48	12	48	0	48	0	48	12	48	34	48	48
	48	48	40	48	40	48	40	48	40	48	40	48	48	
		48	48	34	48	8	48	10	48	34	48	48		
			48	48	38	48	36	48	38	48	48	48		
				48	48	48	48	48	48	48				

Figure **2-18**: PB2 TT3 HP Control Rod Pattern

The transient begins with the closure of the TSV. The time of initiation of TSV closure for TT1 and TT3 is the same as for TT2. The turbine BPV begins to open at 0.312s for TT1 and

0.09 sec for TT3. The rate of BPV opening for TT1 and TT3 is not specified in the [3], [4] and [5] and further information is needed. Table 2-29 shows the scram initiation time and the delay time.

Table **2-8**: PB2 TT1 and TT3 Scram Characteristics

	TT1	TT3
APRM high flux scram set point, % rated	85(2 799.05 MWt)	77 (2535.6 MWt)
Time delay prior to rod motion, msec	120	120
Time of SCRAM initiation	0.68	0.56

2.3 PB Low Flow Stability Tests

Multiple LFS tests were performed at PB2 BWR during the first quarter of 1977. The tests were performed at the end of Cycle 2 with an accumulated average core exposure of 12.7 GWd/t.

The dynamic measurements were taken with a high speed digital data acquisition system capable of sampling over 15 signals every 6 milliseconds and the core contribution measurements were taken from the plants local in-core flux detectors. Special fast response pressure and differential pressure transducers were installed in parallel with existing plant instruments to measure the response of important variables in the nuclear steam supply system.

The stability tests were conducted along the low flow end of the rated power flow line, and along the power-flow line corresponding to minimum recirculation pump speed. The reactor core stability margin was determined from an empirical model fitted to the experimentally derived transfer function measurement between core pressure and the APRM, average neutron flux signals.

The LFS tests were intended to measure the reactor core stability margins at the limiting conditions used in design and safety analysis, providing a one-to-one comparison to design calculations.

2.3.1 Planning of Experiments

Four test conditions were planned to be as close as possible to one of the following reactor operating conditions:

- points along the rated power-flow control line (PT1 and PT2)
- points along the natural circulation power – flow control line (PT2, PT3 and PT4)
- extrapolated rod-block natural circulation power-flow control line (test point PT3)

The planned test conditions are shown in Figure 2.19

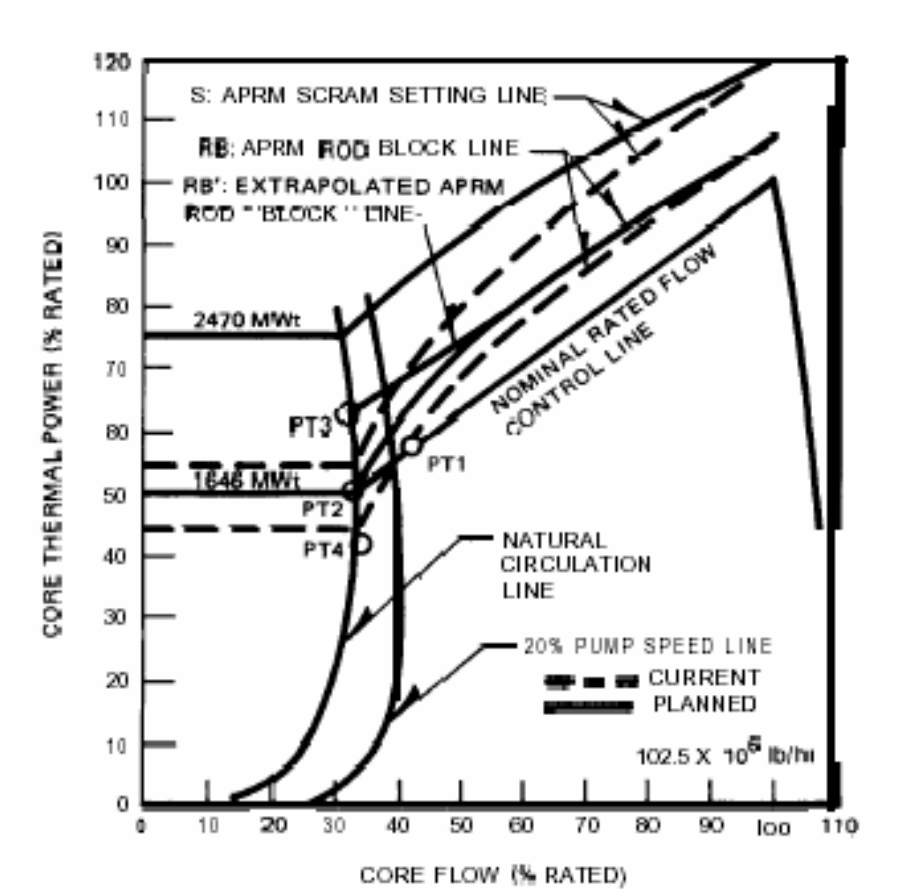

Figure **2-19**: PB2 Power-flow Diagram

In order to conduct reactor core stability tests at the LFS test conditions, interim changes in the plant Technical Specification o the APRM Rod Block and Scram Lines were requested from the NRC. The changes proposed for the duration of the low flow testing are given in Table 2-30

Table **2-30**: Interim Technical Specification Rod Block and APRM SCRAM Lines

INTERIM TECHNICAL SPECIFICATION ROD BLOCK AND APRM LINES	
Current	Planned
APRM Flux Scram Line	
S=(0.66xW+54)x(A/MTPF)	S=(0.45xW+75)x(A/MTPF)
APRM Rod Block Line	
S=(0.66xW+42)x(A/MTPF)	S=(0.58xW+50)x(A/MTPF)

Where:

- S= setting in % of rated thermal power (3293 MWt)
- W= loop recirculating flow rate in % of rated (rated loop recirculation flow equals 34.2 x 106 lb/hr)
- A= design value of the total core peaking power (2.63 for 7x7 and 2.44 for 8x8
- MTPF= operating maximum total peaking factor if greater than A: if less than or equal to A, MTPF=A

An operation time line was developed or the test program in order to minimize the impact of the testing on the Peach Bottom 2 power production. The planned test sequence is shown in Figure 2-20

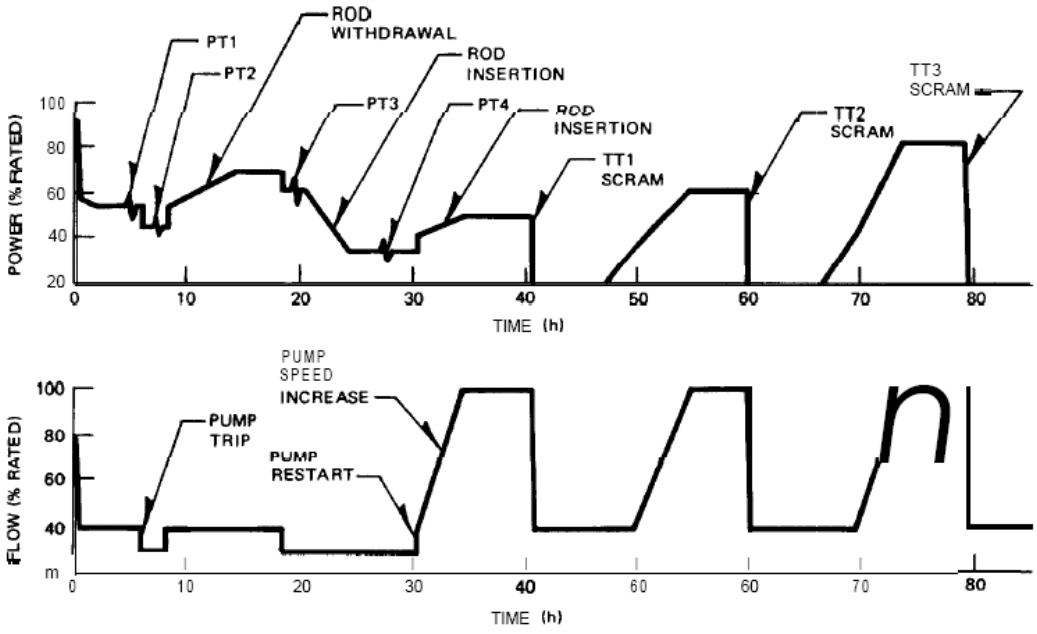

Figure **2-20**: PB2 EOC 2 Tests - Operational Time Line

The reactor was maneuvered by setting the desired fixed control rod pattern and by using flow control. The strategy was to conduct the tests on a tightly controlled time schedule which allowed for the xenon transient effects. By testing the maxima or minima xenon concentration, the waiting time for stable power level and flux distribution in the core could be reduced from 24 to 5 hours prior to each test.

During the Peach Bottom 2 testing, unforeseen changes in plant operation and utility load demand dictated some modifications of the planned test sequence shown in Figure 2-19.

2.3.2 Actual Test Conditions

The actual reactor operating conditions at which the low-flow core stability testing was conducted is listed in Table 2-31.

Table **2-31**: Actual Low-Flow Stability Test Conditions

	PT1	PT2	PT3	PT4
Core Thermal Power, MWt	1995.00	1702.00	1948.00	1434.00
Initial Power Level,% of rated	60.6	51.7	59.2	43.5
Total Core Flow, kg/s	6753.60	5657.40	5216.40	5203.8
Total reactor flow, % of rated	51.3	42.0	38.0	38.0
Reactor Steam Dome Pressure, Pa	6860286	6814781	6904413	6863044
Core exit pressure, Pa	7063682	7008689	7098052	7056808
Core Inlet Enthalpy, kJ/kg	1183.610	1187.78	1184.610	1183.83
Core Inlet Subcooling, kJ/kg	75.160	79.648	77.442	76.075
Core Inlet Temperature, ^{o}C	270.11	270.73	270.09	269.96
Feed Water Mass Flow, kg/s	963.90	808.92	941.22	671.58

The strong effect of the xenon transient occurring during the stability testing can be determined from a plot of the test conditions on a power flow map in Figure 2-19. The skewing of the rated rod line between test conditions PT1 and PT2 from the equilibrium xenon calculated

line gives an indication of the effect of the xenon transient. The average axial power distribution in the core was found to be stable following the xenon soak (Hourly tests of the average axial power distribution indicated local power changes of less than 0.5 % taking place).

The control rod patterns and axial power distributions obtained from the four PB2 EOC 2 low flow stability tests PT1, PT2, PT3 and PT4 are shown in Figure 2-21 through 2-28.

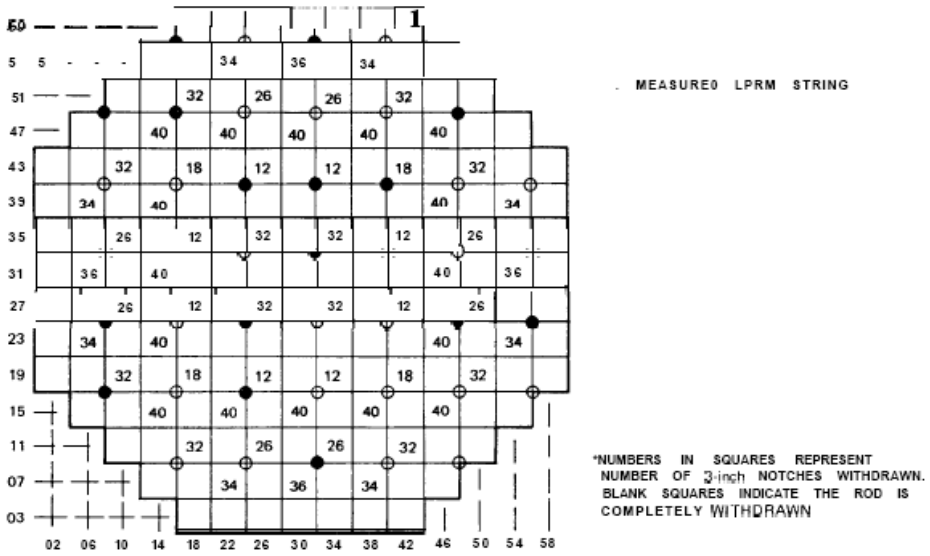

Figure **2-21**: PB2 EOC 2 PT1 Test – Control Rod Pattern

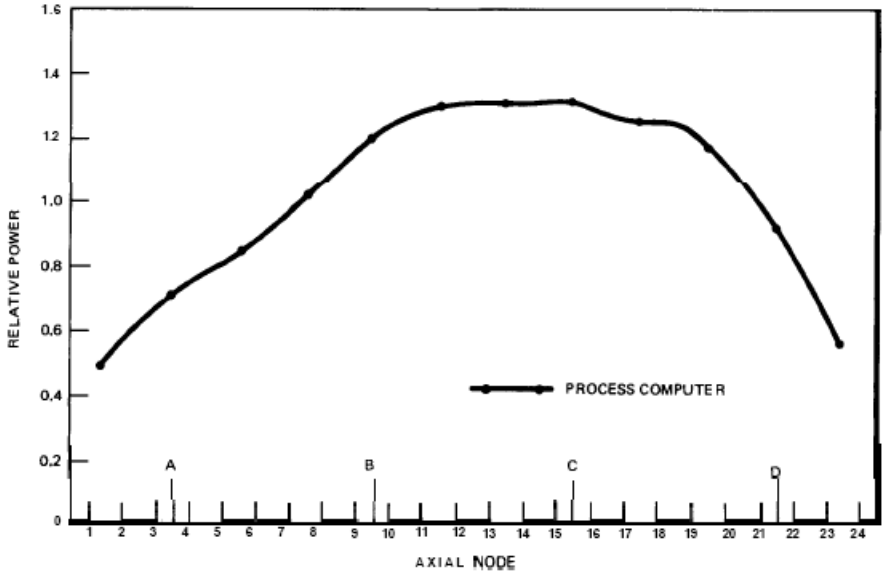

Figure **2-22**: PB2 EOC 2 PT1 Test - Average Axial Power Distribution

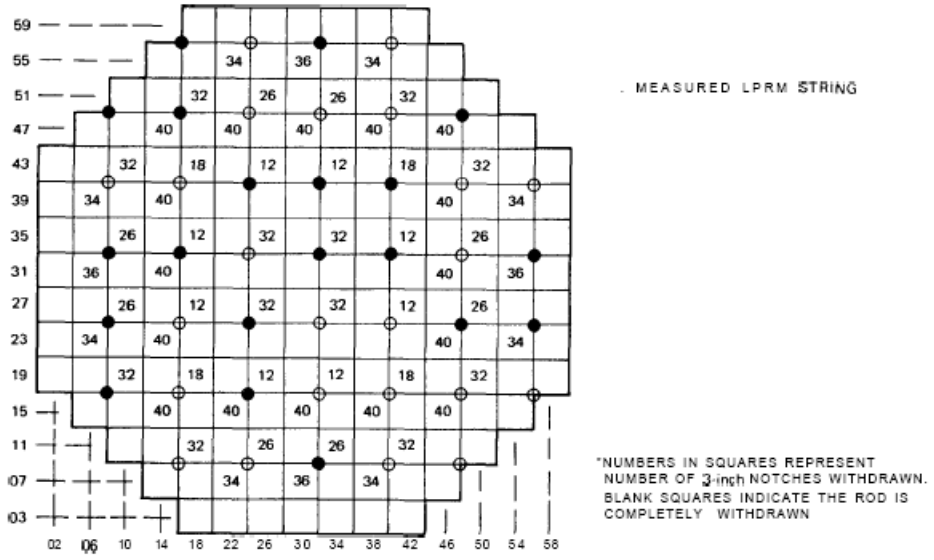

Figure **2-23**: PB2 EOC 2 PT2 Test – Control Rod Pattern

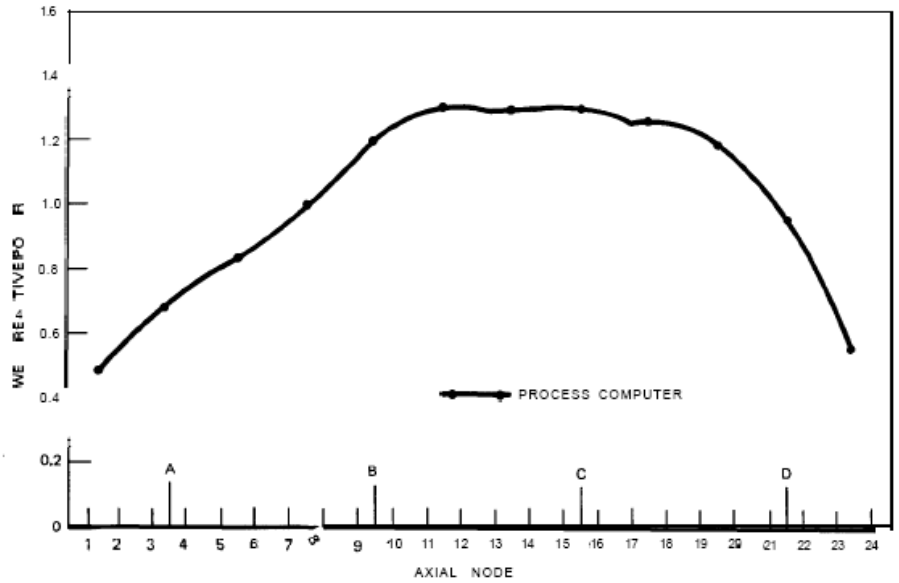

Figure **2-24**: PB2 EOC 2 PT2 Test - Average Axial Power Distribution

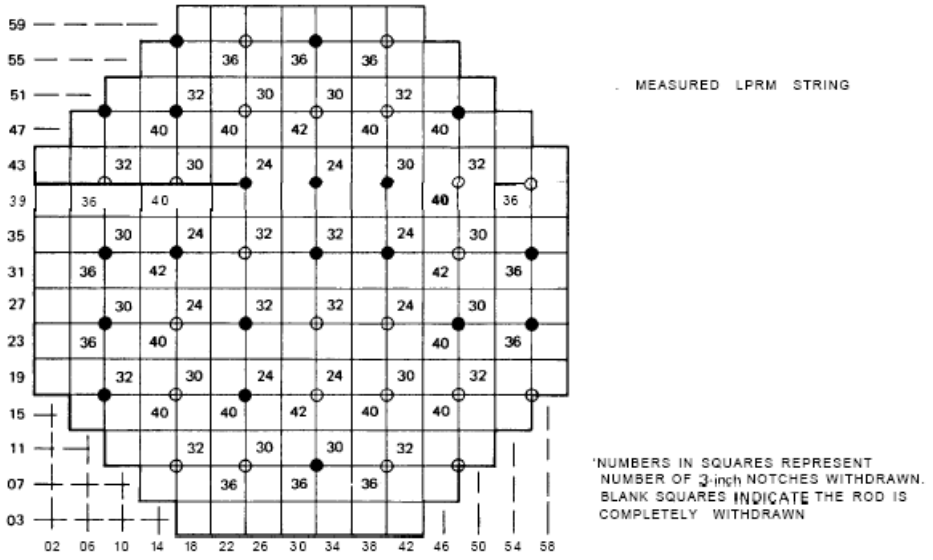

Figure **2-25**: PB2 EOC 2 PT3 Test – Control Rod Pattern

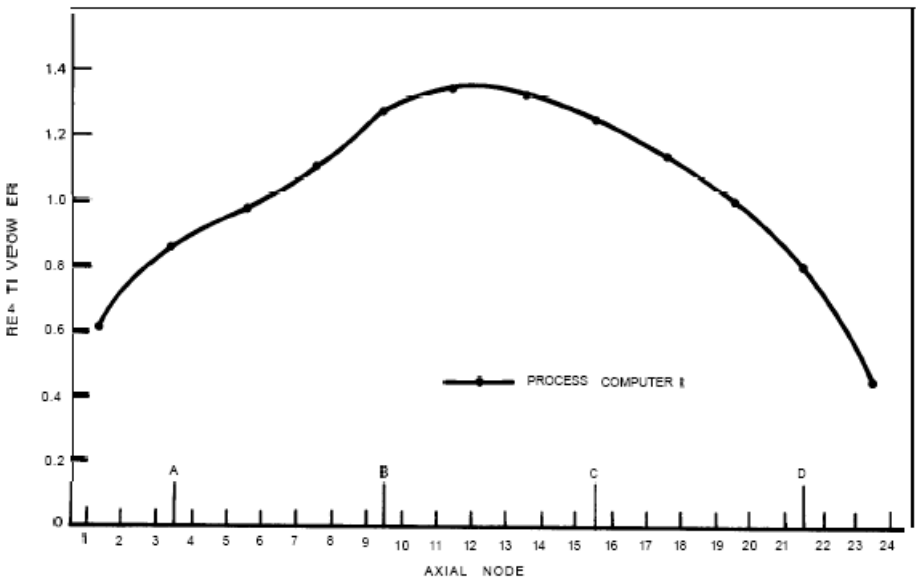

Figure **2-26**: PB2 EOC 2 PT3 Test - Average Axial Power Distribution

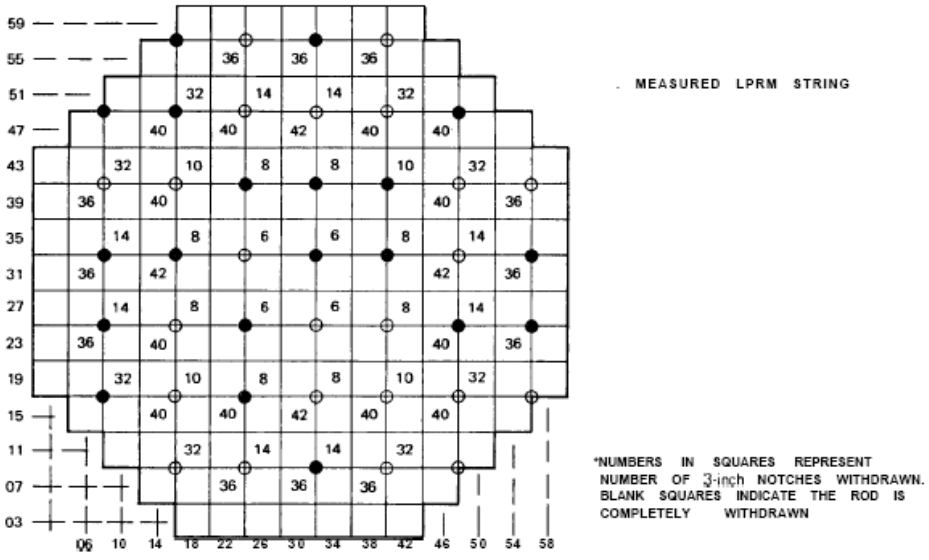

Figure **2-27**: PB2 EOC 2 PT4 Test – Control Rod Pattern

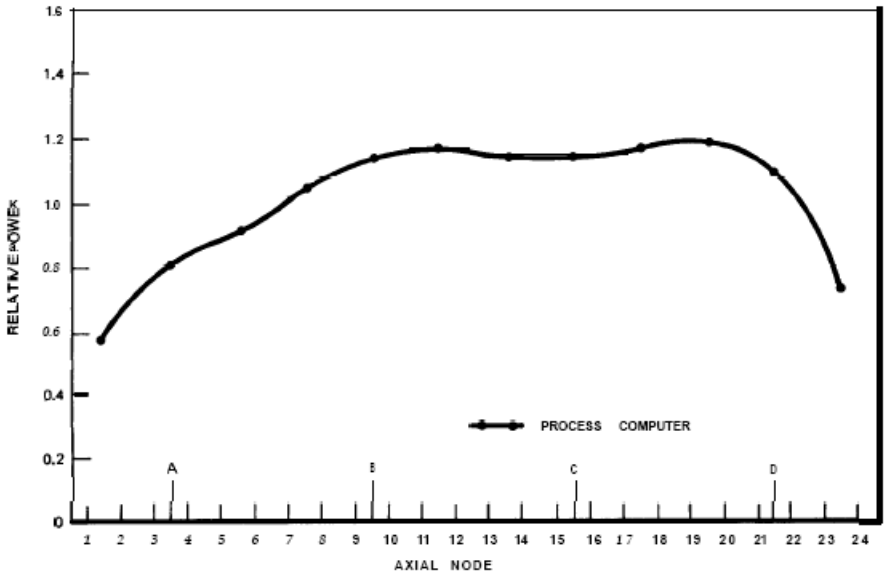

Figure **2-28**: PB2 EOC 2 PT4 Test - Average Axial Power Distribution

2.3.3 Test Procedures

The reactor was maneuvered to the test conditions by setting the desired fixed control rod pattern and by using flow control. Small power changes (±5%) during the pre-test xenon soaks were generally made by flow control. When the xenon concentration had reached a local maximum or minimum (about 4-6 hours after initial maneuvering), the test data were collected.

The test consisted of two sequences

1) noise recording
2) pseudorandom pressure step recording

For the noise data, three reels of recording of ten or more minutes each were taken. Process computer edits OD1 (LPRM Calibration and Base Data) and PI (periodic log with heat balance data, calibrated LPRM readings, control rod positions and failed LPRM and sensor list) were obtained.

Two TIPs were then set at symmetric locations in the core, the first at $\sim 117[cm]$ and the second at $\sim 178[cm]$ above the bottom.

The pseudorandom pressure step recording was preceded by preliminary trial pressure steps. First, a single pressure step was run. The signal-to-noise level was examined and, if not adequate, the step size was increased in small increments of about 0.17 bars until the signal-to-noise level was satisfactory. Usually a 0.55 bars step was adequate. Then, with the reactor operator concurrence, a pseudorandom stepping sequence (down, then up) was run with a sampling interval of 1 second. Three reels of 10 to 20 minutes of data were taken.

The perturbation data were evaluated to verify that the following criteria had been met:

1) maximum APRM response for pressure set point steps was less than 220 % of rated (checked prior to start of stepping sequence);
2) the decay ratio was less than 1.0 for each process variable that exhibits oscillatory response to pressure set points;
3) the daily off gas increase did not exceed 50% of the unit release rate prior to beginning testing (release rate 1 hour after test had to be less than 150% of release rate prior to start of test)

2.3.4 Adopted Transient Analyses

Two types of transient perturbation have been investigated with the objective to study the reactor behavior within the stability region of the Power/Flow Map. These are Control Rod (CR) perturbation and pressure perturbation. All the analyses performed reproduce cases than can normally occur in a BWR reactor, more specifically, the disturbances applied in the several tests are similar to the perturbations used in the reference tests.

The various analyses have also been intended to demonstrate the reliability of using small pressure perturbation tests to determine the stability margin of a large BWR code.

The CR perturbation is actuated by changing the PARCS input deck related to the Control Rod position at the beginning of the transient, i.e. end of coupled steady state calculation. As a consequence the cross sections provide variations of their compositions which of course cause a reactivity variation and power oscillations.

The pressure perturbation is actuated by the Turbine Control Valve. The applied perturbation was a triangular variation of the TCV flow area in 0.2 sec and magnitude of 0.055 MPa.

Chapter 3

TRACE/PARCS Code Description and Model Development

The calculation analyses described in this thesis involve the applications of simulation tools such as thermal hydraulics system code TRACE and 3-D neutron kinetics code PARCS and the coupling between the two. This chapter is focused on their description as well as the approximations made during the analysis and their justification. The description begins with detailed information in regards to TRACE [8], followed by a description of PARCS [9]. The low flow stability tests require the utilization of a special tool DRARMAX [10]. DRARMAX is a post-processing code, which was developed at Purdue University and is applied to evaluate the decay ratio (DR) and natural frequency (NF) from the time series output of the TRACE/PARCS calculation.

3.1 Thermal-hydraulics System Code TRACE

TRACE (TRAC RELAP5 Advanced Computational Engine) code is a US NRC reactor system analysis code [8]. It is designed to perform best-estimate analysis of loss-of-coolant accidents (LOCAs), operational transients, and other accident scenarios in Pressurized Water Reactors (PWR) and Boiling Water Reactors (BWRs). Experimental facilities and fluid phenomena occurring in them are also within the range of simulation abilities of the code. Models applied in the code include multidimensional two-phase flow, non-equilibrium thermo-dynamics, generalized heat transfer, reflood, level tracking, and reactor kinetics. The code also provides automatic steady-state and dump/restart capabilities.

3.1.1 TRACE Field Equations

TRACE uses two-fluid, two-phase field equation set based on single phase Navier-Stokes equations for each phase, and jump conditions between the phases. It consists of separate mass, energy, and momentum conservations for the liquid and gas fields which defines six partial differential equations (PDEs). The components of non-condensable gas in the system and its mixture with steam are assumed to move at the same velocity and temperature. As a result a single momentum equation and a single energy equation are used for the gas mixture. Relative concentrations of steam and non-condensables are determined by using separate equations for each component of the gas field. For example, TRACE permits users to treat nitrogen and air as two separate components of gas field (two additional mass equations), and allows requests for more non-condensable equations if needed (e.g. hydrogen). The set of field equations can be further extended if a user chooses to follow the boron concentration in the system.

Time and volume averaging is applied to this combination of equations, to obtain a useful set of two-fluid, two phase conservation equations. TRACE uses this flow model in both one and three dimensions. Detailed description of the TRACE field equations are given in [8]

The TRACE code invokes a quasi-steady approach to the heat-transfer coupling between the wall and the fluid as the closure relations for interfacial and wall-to-fluid heat transfer and drag. This approach assumes detailed knowledge of the local fluid parameters and ignores time dependencies so that the time rate of change in the closure relationships becomes infinite and the time constants are zero. It has the advantages of being reasonably simple (and, therefore generally applicable to a wide range of problems) and not requiring previous knowledge of a given transient. Where appropriate, the quasi-steady methodology presented in this chapter is somewhat limited. Detailed description of the quasi-steady approach is given in [8].

The partial differential equations are solved using finite volume numerical method. The heat transfer equations are evaluated using a semi-implicit time-differencing technique. The fluid-dynamics equations in the spatial one-dimensional (1D), and three-dimensional (3D) components use, by default, a multi-step time-differencing procedure that allows the material Courant-limit condition to be exceeded. A more straightforward semi-implicit time-differencing method is also available. The finite difference equations for hydrodynamic phenomena form a system of coupled, nonlinear equations that are solved by the Newton-Raphson iteration method. The resulting linearized equations are solved by direct matrix inversion. For the 1D network matrix, this is done by a direct full-matrix solver; for the multiple-vessel matrix, this is done by the capacitance-matrix method using a direct banded-matrix solver.

TRACE takes a component-based approach to modeling a reactor system. Each physical piece of equipment in a flow loop can be represented as some type of component, and each component can be further nodalized into some number of physical volumes (also called cells) over which fluid, conduction and kinetics equations are averaged. The number of reactor components in the problem and the manner in which they are coupled is arbitrary. There is no built-in limit for the number of components or volumes that can be modeled; the size of a problem is theoretically only limited by the available computer memory. Reactor hydraulic components in TRACE include PIPEs, PLENUMs, PRIZERs (pressurizers), CHANs (BWR fuel channels), PUMPs, JETPs (jet pumps), SEPD (separators), TEEs, TURBs (turbines), HEATRs (feedwater heaters), CONTANs (containment), VALVEs, and VESSELs (with associated internals). HTSTR (heat structure) and REPEAT-HTSTR components modeling fuel elements or heated walls in the reactor system are available to compute two-dimensional conduction and surface-convection heat transfer in Cartesian or cylindrical geometries. POWER components are available as a means for delivering energy to the fluid via the HTSTR or hydraulic component walls. FLPOWER (fluid power) components are capable of delivering energy directly to the fluid

(such as might happen in was transmutation facilities). RADENC (radiation enclosures) components may be used to simulate radiation heat transfer between multiple arbitrary surfaces. Fill and BREAK components are used to apply the desired coolant-flow and pressure boundary conditions, respectively, in the reactor system to perform steady-state and transient calculations. EXTERIOR components are available to facilitate the development of input models designed to exploit TRACE's parallel execution features.

3.2 Neutron Kinetics Code PARCS

PARCS is a three-dimensional (3D) reactor core simulator which solves the steady-state and time-dependent, multigroup neutron diffusion and SP3 transport equations in orthogonal and non-orthogonal geometries. PARCS is coupled directly to the thermal-hydraulic system code TRACE which provides the temperature and flow field information to PARCS during the transient calculations via the few group cross sections. A separate code module, GENPMAXS, is used to process the cross sections generated by a lattice physics code into the PMAXS format that can be read by PARCS.

Since the initial release of the NRC version of PARCS (v1.01) in November 1998, there have been numerous functional improvements and code feature extensions [11, 12]. The major calculation features in PARCS include the ability to perform eigenvalue calculations, transient (kinetics) calculations, Xenon transient calculations, decay heat calculations, pin power calculations, and adjoint calculations for commercial Light Water Reactors. The primary use of PARCS involves a 3D calculation model for the realistic representation of the physical reactor. However various one dimensional (1D) modeling features are available in PARCS to support faster simulations for a group of transients in which the dominant variation of the flux is in the axial direction, as for example in several BWR applications.

A card name based input system is employed in PARCS such that the use of default input parameters is maximized and the amount of the input data is minimized. A restart feature is available to continue the transient calculation from the point where the restart file was written. Various edit options are available in PARCS to show many different aspects of the calculation results. The online graphics features of PARCS provide a quick and versatile visualization of the various physical phenomena occurring during the transient calculation.

Numerous sophisticated spatial kinetics calculation methods have been incorporated into PARCS in order to accomplish the various tasks with high accuracy and efficiency. For example, the Coarse Mesh Finite Difference (CMFD) formulation provides a means of performing a fast transient calculation by avoiding expensive nodal calculations at times in the transient when there is no strong variation in the neutron flux spatial distribution. The temporal discretization is performed using the theta method with an exponential transformation of the group fluxes. A transient fixed source problem is formed and solved at each time point in the transient. For special discretization, a variety of solution kernels are also available to include the most popular LWR two group nodal methods, Analytical Nodal Method (ANM) and Nodal Expansion Method (NEM).

Advanced numerical solution methods are used in PARCS in order to minimize the computational burden. The solution of the CMFD linear system is obtained using a Krylov subspace method which utilizes a BILU3D preconditioner. The eigenvalue calculation to establish the initial steady-state is performed using the Wielandt eigenvalue shift method. When using the two group nodal methods, a pin power reconstruction method is available in which predefined heterogeneous powers from functions are combined with a homogenous intranodal distribution.

PARCS is also capable of performing core depletion analysis. Burnup dependent macroscopic sections are read from the PMAXS file prepared by the code GENPMAS and the PARCS node-wise power is used to calculate the region-wise burnup increment for time advancing the macroscopic cross sections. Details of the PMAXS file and the GENPMAXS code are provided in the GENPMAXS manual.

PARCS was written in FORTRAN 90 and its portability has been tested on various platforms and operating systems, to include SUN Solaris UNIX, DEC ALPHA UNIX, HP UNIX, LINUX, and various Windows OS (i.e. 95, 98, NT and 2000). Because of its various functional features, PARCS can be run in numerous execution modes. The following section will first provide a brief overview of the important PARCS user features.

3.2.1 Calculation Features

PARCS is equipped with various calculation modules needed to predict the global and local response of the reactor in steady-state and transient conditions. The various features of PARCS are described in this section along with the corresponding modules.

Eigenvalue Calculation

In order to establish the initial steady state, it is necessary to perform an eigenvalue calculation. PARCS performs the eigenvalue calculation using the Wielandt eigenvalue shift method. The eigenvalue obtained is used to adjust the nu (ν) values in the subsequent transient calculation in order to make the initial reactor state critical. In addition to the standard k-eff calculation for a given reactor configuration, the critical boron concentration (CBC) search function is available. The type of search is defined in the SEARCH card of the CNTL block input.

Transient (Kinetics) Calculation

This is primary function of PARCS that solves the time-dependent neutron diffusion equation involving both delayed and prompt neutrons. . The transient calculation option is turned

on and off by the TRANSIENT card in the CNTL block. The temporal differencing based on the exponential transform and the theta method yields a transient fixed source problem at each time step. The fixed source problem is solved using the Coarse Mesh Finite Difference (CMFD) method in which a conditional nodal update scheme is employed. The temporal discretization schemes can be specified by the THETA and EXPO_OPT cards in the TRAN input block. Exponential extrapolation can be sued to obtain an initial flux guess at each new time step by activating this option in the expo_opt card. The conditional nodal update scheme activates the higher order nodal update only when there are substantial local cross section changes. The conditional nodal update is controlled by the EPS_XSEC card in the TRAN block.

Xenon Transient Calculation

For slow reactor transients, it is essential to provide a Xenon transient capability. In PARCS, the conventional quasi-static treatment of xenon transients is used that employs the eigenvalue problem solver instead of the transient fixed source problem. The number densities of Xenon and Samarium are updated by solving the respective balance equations using the fluxes resulting from the eigenvalue calculation. The Xenon option is controlled in the XE_SM card in the CNTL block by choosing one of the following options: 1)No Xenon, 2) Equilibrium Xenon, or 3) Transient Xenon.

Decay Heat Calculation

A simplified decay heat model involving six groups of decay heat precursor groups is employed in PARCS. The 6 group decay heat precursor equation is treated in the same way as the delayed neutron precursor equation. The solution of the precursor equation is thus node wise and provides at each time step the decay heat to sum with the fission power in order to determine the total power produced in each node. Default values of the precursor fractions and decay constants of the 6 groups are provided for UO2 fueled cores which are operated for a sufficiently long period of time. The option exists for the user to specify alternate values for the precursor fractions

and decay constants. The decay heat option is specified in the DECAY_HEAT card in the CNTL block and the input parameters are specified in the DHP_BETA and DHP_LAMBDA cards in the XSEC block.

Pin Power Calculation

The primary dependent variables in PARCS are the node average fluxes and interface currents. In order to obtain local pin power distributions, it is thus necessary to "reconstruct" pin powers. This is performed in PARCS by multiplying the heterogeneous power form functions with the homogeneous intra-nodal flux distribution. The homogeneous intra-nodal flux is calculated by performing an analytical solution of a 2D fixed source problem in which the surface average currents are specified at the four boundaries. The surface average currents are obtained from the converged node average flux distribution at a given state. Pin power reconstruction is performed for both the steady-state and transient condition. The pin power calculation option is activated by the PIN_POWER card in the CNTL block and the heterogeneous power form functions are supplied via the PFF block. Corner discontinuity factors can be used to enhance the accuracy of the pin power distribution and can be specified in the CDF card in the XSEC block. In order to save computing time for the pin power calculation in the PINCAL_LOC card of the GEOM block. The transient pin power calculation needs not to be performed at every time step since the pin-to-box factor does not change appreciably unless there is a substantial change in the core configuration. The transient pin power calculation frequency is activated by the PIN_FREQ card in the TRAN block.

Modeling Features

One of the essential neutronics problems for a reactor core is to represent the physical system with an accurate numerical model. Among the various fundamental modeling issues in the reactor kinetics calculation are the geometric representation, the cross section representation, and the thermal-hydraulic (T-H) feedback modeling. PARCS provides a 3 D geometric representation

of the core that can be reduced to 2D, 1D, or 0D by the choice of the appropriate boundary conditions. However, a special 1D kinetics capability is also available for more accurate and versatile 1D modeling. Various geometric representation features will be described in the first and fourth subsections below. The basic cross section representation scheme in PARCS is to functionalize the macroscopic cross sections with linear or quadratic dependence on the T-H state variables. The details of the PARCS cross section representation scheme are provided in the second subsection. Thermal-hydraulically, PARCS uses an external T-H solver which greatly extends its range of applicability. The original T-H solver of PARCS is intended primarily for code testing and not for practical applications, and therefore only the external T-H features are detailed in third subsection. The input description for the internal T-H solver is still provided since PARCS continues to process this block.

Geometric Representation

In PARCS, the reactor core is modeled by a group of homogeneous computational nodes. Radially, the computational node can be either rectangular or hexagonal. The size of the node is of the order of fuel assembly pitch, while axially the size is 10~30 cm. In the rectangular option, the core geometry is specified in the GEOM block, whereas the block name is changed to GEOMH for the hexagonal option. The core radial configuration is specified using the unity of a fuel assembly by the RAD_CONF card in GEOM block. The radial node size is then specified by the number of subdivisions of the assembly node by the NEUTMESH_X and NEUTMESH_Y cards. So the number of nodes per assembly can be freely chosen as nsubx*nsuby. Normally, one or four nodes per assembly are used for practical calculations. However, it is possible to perform a fine mesh calculation using the geometry input structure. Also by taking the assembly-wise configuration as the pin-wise configuration, a pin-by-pin heterogeneous core representation is also possible. The refined geometry feature is, however limited to the rectangular case only. In

the hexagonal case, a hexagon is always represented with one node although internally it is divided into 6 triangular nodes within the TPEN kernel.

Cross section Functionalization

PARCS uses macroscopic cross sections which can be input in either the two group of multi-group form using the same input cards. The macroscopic nodal cross sections are functionalized in terms of boron concentration (B, in ppm), square root of fuel temperature, moderator temperature and densities, void fraction and the effective rodded fractions. Only the linear dependence of cross sections is considered on these state variables except for the moderator density and void fractions for which the quadratic variation is provided. Symbolically, the cross sections are functionalized as

$$\begin{aligned}&\Sigma\left(B, T_f, T_m, D_m, \alpha, \xi\right) = \\ &\Sigma_0 + a_1\left(B - B_0\right) + a_2\sqrt{T_f} - \sqrt{T_{f0}} + a_3\left(T_m - T_{m0}\right) + \\ &+a_4\left(D_m - D_{m0}\right) + a_5\left(D_m - D_{m0}\right)^2 + a_6\alpha + a_7\alpha^2 + \xi\Delta\Sigma_{CR}\end{aligned} \tag{3.1}$$

Here the effective rodded fraction is defined as the product of the volumetric rodded fraction and the flux depression factor that is computed by the de-cusping routine for the partially rodded node. For Xenon calculations, the Xenon and Samarium microscopic cross sections are represented in the same form.

Currently, a few special benchmark cross section representation types are available: e.g. for the OECD PWR MSLB (Main Steam Line Break) problem, for the OECD BWR PBTT (Peach Bottom Turbine Trip) problem, and for the OECD VVER 1000 Coolant Transient CT-1 problem.

Thermal-Hydraulics Feedback

PARCS is coupled with the thermal-hydraulics code TRACE by the EXT_TH card in the CNTL block. The coupling between PARCS and the TRACE code is achieved by the inter-

process protocol, PVM. The two processes are loaded in parallel and the PARCS process transfers the nodal power data to the T-H process. The T-H process then sends back the temperature (fuel and coolant) and density data back to the PARCS process. Originally, it was necessary to execute a third intermediate process, General Interface (GI), which manages the data transfer between the two processes. But this process has been integrated into PARCS so that only two processes are to be run in parallel. Currently TRACE uses PARCS as a library of subroutines, eliminating the need for parallel communications links.

In general the neutronics spatial mesh/node structure is different from the T-H spatial mesh/node structure. The difference is to be mitigated by a proper mapping scheme (spatial mesh overlays). This mapping used to be explicit in that the fractions of different T-H nodes belonging to a neutronic node had to be specified in a file called MAPTAB for all the neutronic nodes. In order to reduce the user effort to prepare the MAPTAP file, automatic mapping scheme were developed for the coupled TRACE/PARCS code that take data from both PARCS and TRACE input files to generate mapping information internally.

The time step used in system T-H calculations is often small because of stability consideration. Some times it is so small that no significant changes occur in the core T-H condition and performing a neutronic calculation with such a small change would be wasteful since the neutronics solution does not change much either. In order to circumvent this inefficiency, a skip factor can be used in the coupled calculation such that the T-H code calls PARCS based on this user defined frequency. Different skip factors can be specified for the steady state and transient calculation in the EXT_TH card.

Core Depletion Analysis

PARCS performs macroscopic core depletion analysis by time advancing burnup dependent macroscopic cross sections. The PARCS node-wise power is used to calculate the region-wise burnup increment which is then used to update the macroscopic cross sections using

the PMAXS cross section file. The assembly-wise history effects (e.g. moderator density history, control rod history) are also treated using the local burnup dependence.

The depletion capability was added to the PARCS code in version 2.5. A macroscopic depletion module adds the following functions to PARCS:

1) Ability to read in the macroscopic cross sections from PMAXS, the XS file prepared by the interface code GENPXS.
2) Ability to calculate region wise macroscopic cross sections as a function of the history state, such as burnup, moderate density history, control rod history.
3) Ability to calculate region wise burnup increment at each step based on the region wise fluxes

The depletion module was implemented in PARCS by inserting several entry points in the code. The depletion module is activated in PARCS using the input block DEPL which is described in the user input. Utilization of the depletion option also requires the use of the two cards in the CNRL block and four cards in the T_H block

3.3 TRACE/PARCS Coupled Methodology

When T_H conditions for PARCS are provided by an external system code (e.g. TRACE), the temperature/fluid condition required at each neutronics node for the feedback calculation consists of the coolant density/temperature and the effective fuel temperature. The nodal power information determined by PARCS is then transferred back to the system code. During the course of data transfer, the difference in the neutronic and T-H nodalizations are reconciled by the mapping scheme described below.

In general, coarser node sizes are used in the core T-H calculation than in the PARCS neutronics calculation. Therefore, a T-H node usually consists of several neutronics nodes.

However, it is possible that a neutronics node can belong to multiple T-H nodes. Because of this possibility, the PARCS T-H variable is obtained as the weighted average of the T-H variables of several T-H nodes as:

$$T_i^P = \sum_{k=1}^{N_i^P} \alpha^P{}_{i,j(i,k)} T^T{}_{j(i,k)} \tag{3.2}$$

where the superscript P and T stands for PARCS and T-H codes, and $j(i,k)$ is the $k-th$ T-H node number out of the N_i^P T-H nodes belonging to the $i-th$ PARCS node. $\alpha^P{}_{i,j}$ is the volume fraction of the $j-th$ T-H node in the $i-th$ PARCS node, which must sum to unity. On the other hand, the nodal power of the $j-th$ T-H node is obtained as follows:

$$\sum_{k=1}^{N^P} \alpha^T{}_{j,i} = 1 ; \sum_{k=1}^{N^P} \alpha^T{}_{j,i(j,k)} > 1 \tag{3-3}$$

where $i(j,k)$ is the $k-th$ PARCS node number out of the N_j^T PARCS nodes belonging to the $j-th$ T-H node. $\alpha^T{}_{i,j}$ is the volume fraction of the $i-th$ PARCS nodes in the $j-th$ T-H node and satisfies the following conditions:

$$\sum_{k=1}^{N^T} \alpha^T{}_{j,i} = 1 ; \sum_{k=1}^{N^T} \alpha^T{}_{j,i(j,k)} > 1 \tag{3-4}$$

where N^T is the number of all the T-H nodes. The second relation above implies that the T-H node is lager than the PARCS nodes.

3.3.1 T-H/Neutronic Mapping and the MAPTAB File

The GI code, which is the central interface unit between TRACE and PARCS, is included in the PARCS spatial kinetics code as a separate module. In this configuration the PVM

communication between PARCS and the GI has been replaced with direct data copy logic, and the GI continues to manage all PVM communication with TRACE. Thus, two processes (TRACE and PARCS) need to be executed. In addition to this merging of the GI into PARCS, an automatic mapping kernel for the GI has been designed and implemented. This kernel is currently able to manage the following mapping configurations:

(1) Cylindrical T-H volumes from the TRACE vessel component to Cartesian neutronics nodes, where no mapping information is specified. The weighting factors are computed based strictly on geometric union of the cylindrical T/H grid and the Cartesian neutronic grid.

(2) Cylindrical T-H volumes from the TRACE vessel component to Cartesian neutronics nodes, where a radial map is used to explicitly specify which radial T-H cell should be coupled to which neutronic node. Specifying this radial map allows the user to bypass the mapping logic which computes weighting fractions based on strictly on the geometric union of the T/H and Neutronic grids.

(3) Multiple BWR CHAN components to a 3 D neutronic core. This functionality requires that the user input a radial map which specifies the CHAN(s) to be coupled to each neutronic node and with what weighting factor. It is the responsibility of the user to ensure that the geometric volume of each T-H CHAN is consistent with the number of neutronic nodes to which it is coupled.

(4) BWR CHAN component(s) to a 1D neutronic core. This scenario arises from calculations performed with either a TRAC-BF1 input deck (where PARCS processes the 1D kinetics data from the TRAC-BF1 deck and thus does not need a separate PARCS input deck or "MAPTAB" file), or a TRACE deck (where PARCS must process the 1D kinetics data from its own input deck and a "MAPTAB" file is required).

The auto-mapping kernel works for calculations involving both old and new TRACE heat structure formats, and no changes to the PARCS input deck or the "MAPTAB" file are required.

The radial mapping for volumes and heat structures is performed based on one of the mapping configurations listed above, and the axial mapping is performed without user intervention. For the axial mapping, a linear interpolation scheme is used for both the hydraulics cells and the heat structures, which provides a fluid/fuel temperature distribution in the channel which is more accurate than without interpolation. For the mapping of axial hydraulic cells, it is assumed that the fluid conditions exist at the exit of the cell.

The tabular weighting factors required in previous "MAPTAB" files are now no longer necessary. If this data is not input, or if only a radial map is specified, the code will assume that automatic mapping is to be performed. However, if this tabular data is present in the "MAPTAB" file, the auto-mapping logic will be deactivated, and the input weighting factors will be used.

Most 1D routines were written in FORTRAN 90 to take advantage of dynamic memory allocation and derived data types. The 1D module thus has different memory addresses even through the same variable names are used as in the 3D routines. Due to the use of dynamic memory allocation, no 1D memory will be allocated during the normal 3D runs so that the addition of the 1D routine will not harm the execution of the 3D module.

The input/output (I/O) formats of the 1D module were made consistent with the 3D module in order to minimize newly defined input cards and also to provide convenient user accessibility. When the 1D module is invoked, the input data necessary for the 1D module is transferred from 3D common blocks to 1D common blocks. After that the 1D module is independently executed in the normal calculation mode without triggering any 3D routines.

3.4 DRARMAX

The post processing code, DRARMAX, which was developed at Purdue University, is selected to evaluate the DR and NF from the time series output of the TRACE/PARCS

calculation. DRARMAX evaluates the decay ratio and the natural frequency for signals obtained from transients initiated by short perturbations as well as those obtained from noise simulation during stationary operation. DRAMAX is able to calculate the DR and NF taking into consideration also the signal constituting the perturbation given to the system. DRARMAX also determines DRs and NFs for three types of functions: the output signal, its autocorrelation function (ACF) and the impulse response function (IRF). For each of the three types of functions

DRARMAX fits the function with a damped sinusoidal form:

$$x(t) = c_0 + ce^{-\alpha t}\cos(\omega t + \varphi) \tag{3-5}$$

The first xx seconds of the calculated time trace are not used for the fit because they have contamination from higher order modes and the particular shape of the perturbation used. If least square fitting is successful, the DR and the NF are given as:

$$DR_f = e^{-2\pi\alpha/\omega} \tag{3-6}$$

$$Fr_f = \omega/(2\pi) \tag{3-7}$$

The definition of DR and NF is appropriate for transients with short perturbation, such as control rod and pressure perturbations.

For the measured or simulated noise signals, DRARMAX code will first extract the impulse response function (IRF) by an autoregressive and moving average (ARMA) process [14].

$$x(i) = -\sum_{k=1}^{p} a_k x(i-k) + \sum_{m=0}^{q} b_m u(i-m) \tag{3-8}$$

where u, x are input and output noise signals, p, q are orders of the ARMA process, and coefficients a_k, b_m are obtained by the prediction-error identification method (PEM). An index referred to as Final Prediction Error (FPE) is defined to estimate the quality of the ARMA model:

$$FPE = \frac{N+q+1}{N-2p-q-1}\| x - \hat{x} \| \tag{3-9}$$

where N is the number of sampled data points and $\hat{x}$ is approximation of the output signal by ARMA.

The Lyapunov DR and NF are used for noise signals:

$$DR_L = e^{-2\pi \mathrm{Re}(\gamma)/\mathrm{Im}(\gamma)} \tag{3-10}$$

$$Fr_L = \mathrm{Im}(\gamma)/(2\pi\Delta t) \tag{3-11}$$

where Δt is the time interval of input and output time series, and $\gamma = \ln(\beta_m)$ and β_m is the dominant rood of $1+\sum_{k=1}^{p} a_k \beta^k$ [15].

Chapter 4

TRACE/PARCS Peach Bottom Modeling Scheme and Turbine Trip Results

Chapter 4 begins with a description of the nodalization schemes developed for TRACE and PARCS utilized to simulate PB2 NPP. The coupling scheme applied between the thermal-hydraulics and neutronics nodalizations is provided as well.

Thermal Hydraulic Model and Nodalization Scheme

TRACE uses an input-data file in which the components of the Peach Bottom Nuclear Power Plant Unit 2 are modeled in appropriate manner. The description below does not include all possible modeling features of the TRACE code. However it embodies the major parts for primary-side and control procedure. The TRACE input-data file in the current studies is named as tracin file and it includes control system description and an overview of the components.

Control system

The control system in the current input-data file consists of the four basic building blocks:

- **Signal variables** – model system parameters with real values that the user selects as signals for application in the TRACE control procedure. They are equivalent to the signals that an operator receives from the various detectors throughout a plant. Based on the one used in the input data file those are: problem time, jet pump mass flow rate, steam dome pressure, downcomer collapsed level, steam line mass flow rate, feed water mass flow rate, core inlet temperature and channels average void fraction.

- **Control blocks** – are function operators which take as input either signal variables or the output from the other control blocks and manipulate them in some way to produce a single output such as: core mass flow rate, steam dome pressure, downcomer water level, core inlet temperature, total core mass flow rate. The control blocks used in the input-data file have similar structure. They act like a proportional integral (PI) controller. The set point is provided in each control block. The gain and the constant sets in the control blocks are defined through series of sensitivity studies following the guidelines in [16]
- **Trips** – is an ON/OFF logical switch that can be used to decide when to evaluate a component hardware action, to define a ± 1.0 or 0.0 (ON or OFF) factor for application within the control-procedure logic. In the current input deck are used: turbine stop valve and bypass valves closing time trips;
- **Component action tables** - provides a means for modeling the adjustable hardware action of a component. They are essentially just a lookup tables from which the response of some key component parameter may be determined as a function of an independent variable.

Reactor power

The reactor power during steady state and transient stand alone calculations (without the application of PARCS neutron kinetics code) is defined by POWER component card. Within this card the total reactor core power, connected to the heat structure elements provides heat to 33 channel components. During steady state and transient stand alone calculations the reactor-power is manipulated via trip-initiated table lookup. In the power component cards are also defined the fraction of prompt and decay heat applied directly to the moderator, the prompt neutron lifetime and the fraction of the moderator heating that appears in the bypass. The 1D-axial power shape table is provided here. It is fixed during steady state standalone calculations. The Peach Bottom power data information is specified in [17].

Reactor vessel

In TRACE the reactor vessel component and its internals are modeled utilizing a VESSEL component card. The VESSEL component in the current input-data file is 3D cylindrical geometry. The internals of the PB BWR vessel include the down-comer section, fuel-assembly reactor core, upper and lower plenums. It contains the jet pumps which are modeled through a separate JETP component card. The reactor VESSEL component card consists of 4 radial rings and 14 axial levels and 4 azimuthal sections.

Reactor re-circulation system

The two re-circulation loops are modeled separately. Each re-circulation loop is modeled with four fluid volumes: suction pipe represented by PIPE component 60 and 64, recirculation pump represented by PUMP components 61 and 65, and discharge side represented by TEE components 62 and 66 and PIPE components 67 and 70. Each loop drives ten jet pumps lumped as one. Actual pump data is used to input pump performance parameters in the normal operating quadrants based on built-in curves for a pump specific speed. Rated values for pump flows, head and torque are based on actual pump data, as is the pump moment of inertia. The included jet pump model corresponds to the TRACE JETP component model. The geometry data of the recirculation loop together with the pump information was provided by the benchmark specifications [17].

Core region

33 channel components are used to model the active (fuelled) region of the core. They represent the 764 fuel assemblies of the PB2 reactor core. The core thermal hydraulic model was built according to different criteria. The fuel assemblies are ranked according to the inlet orifice

characteristics, fuel assembly type (e.g. 7x7 or 8x8) and thermal-hydraulic conditions (e.g. fuel assembly power, mass flow, etc). Each channel is modeled as CHAN component. It has 27 axial nodes, 24 of which are considered as active region. 2 nodes and 1 node are used to represent the core lower tie plate and core upper plate regions respectively. The CHAN components are connected to the vessel between levels 3 and 6. A leak path flow area from the first cell of the channel to the vessel has been modeled within the CHAN component card. This leak simulates the flow rate contribution to the core bypass flow rate coming from the core channels.

Steam lines

The PB Unit 2 has in total four steam lines and each consists of a flow-limiting nozzle, main steam isolation valve (MSIV), safety relief valves (SRVs) and a turbine stop valve (TSV). The steam bypass system consists of nine-by-pass valves (BPVs) mounted on a common header, which is connected to each of the four steam lines.

In the TRACE input-data file the four steam lines are lumped into one line which is represented by TEE components 52 and 54. The SRVs, MSIVs, TSVs and BPVs are represented by VALVE components 59, 53, 55 and 96, respectively. The bypass line is modeled by PIPE component 94. The condensers, the turbines and the safety relief tanks are modeled via BREAK components 91, 90 and 93 respectively. The BREAK component is utilized to set the pressure boundary condition.

Feedwater lines

The main feedwater line is modeled as FILL component 50 while the secondary feedwater line is modeled as FILL component 83. TEE component 88 is part of the feedwater supply line. The fill provides a boundary condition mass flow rate, which is controlled by the control system. It acts as a control on FW temperature based on the core inlet temperature. It also

controls feed water flow rate based upon the water level in the downcomer. The difference between the steam line and feed water flow rate gives the amount of flow rate for the control rod guide tubes. This flow rate is not considered, since it is just 2% of the feedwater flow rate, and the steam line flow rate is assumed equal to the feedwater flow rate.

Separator

The separator in TRACE input-data file is modeled as mechanistic separator. It contains 3 stage separator dryers and in the input–data file is represented as SEPD components 71, 72 and 73. The user needs to supply geometric parameters that describe the physical separator. The coding that supports this option was written by General Electric Company (GE), and it assumes a design similar to that used in a GE BWR steam/water separator.

A summary of the input-data file components is given in Table 4-1.

Table **4-1**: Input-data File Component Description

Component Number	Component Type
1-33	Core channels
50	Main feedwater fill component
52	Main steam line tee component
53	Main steam line isolation valve
54	Main steam line tee component
55	Turbine stop valve
57	Fill for guide tubes
58	Fill for guide tubes
59	Safety and relief valve
60	Pipe component
61	Recirculation pump
62	Tee component for recirculation loop
63,68	Jetpump
64	Pipe component which connects RPV and recirculation pump (Pump 65)
66	Tee component for recirculation loop
67	Pipe component which connects jet pump 63 and recirculation loop
69	Manifold isolation valve which separates/connects two recirculation loops
70	Pipe component which connects jet pump 68 and recirculation loop
71, 72, 73	Steam separator and dryer components
76	Fill for guide tubes
80, 81, 82	Pipe components for guide tubes
83	Secondary fill for feedwater line
88	Tee component
90	Break for turbine stop valve
91	Break for safety and relief valve
93	Break for bypass valve
94	Pipe component which connects bypass valve (Valve 96) to Break 93
95	3-D Vessel Reactor Pressure Vessel (RPV)
96	Main steam bypass valve

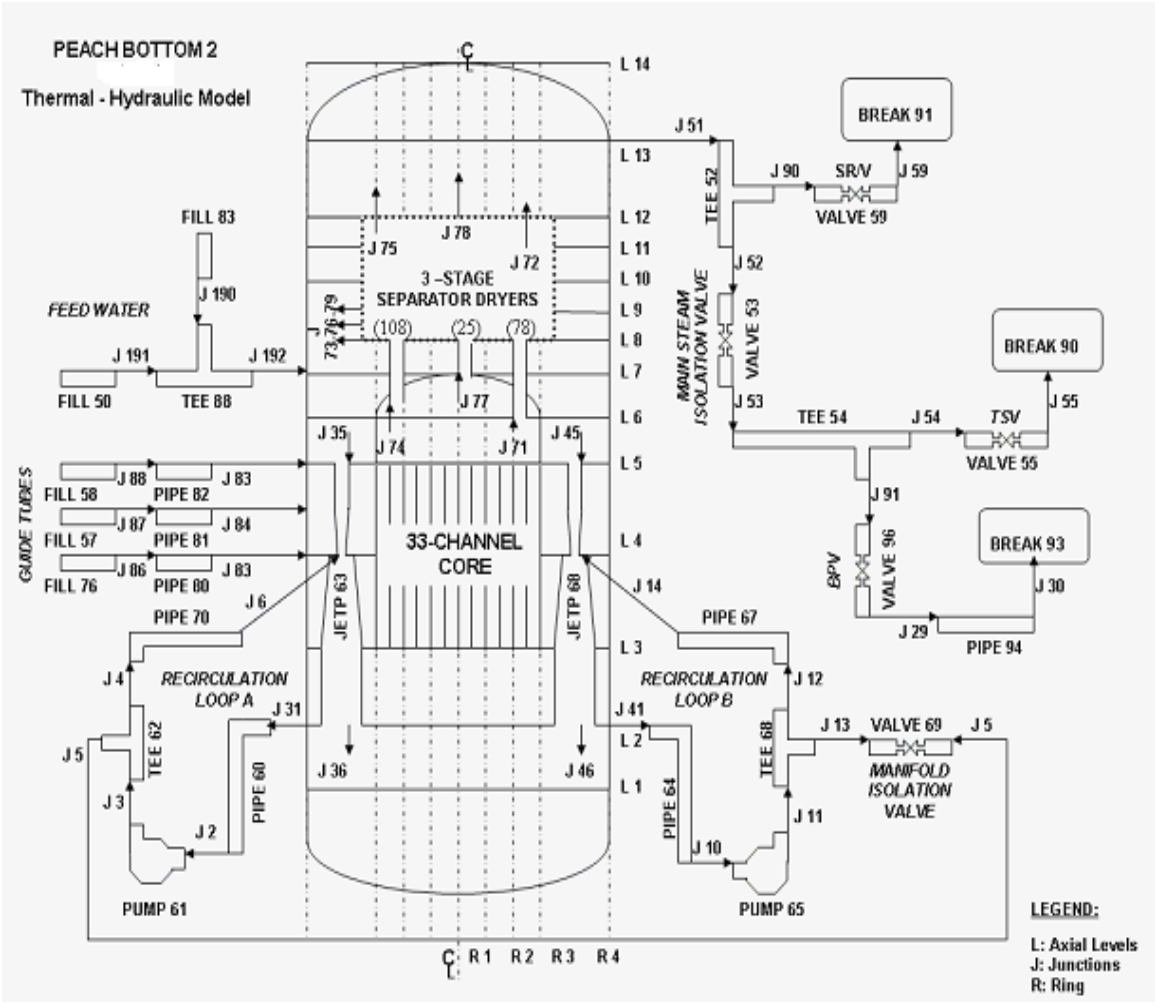

Figure **4-1**: PB2 Input-data File Nodalization Scheme

4.2 PARCS Neutronics Model

A PARCS neutronics model was developed for PB2 based on the end-of cycle state core conditions. The core is a BWR/4 consisting of 764 fuel assemblies and 185 control rods and at the time of the TT2 test there were 576 7x7 and 188 8x8 fuel assembly type. The PARCS model represents each of the 764 fuel assemblies as a single neutronics node. The active core height of PB2 is 365 cm and is modeled in PARCS with 24 axial layers. At the top and bottom of the active core the PARCS model uses additional 15.24 cm thick axial reflector regions. As noted previously, asymmetries in the radial burnup distribution result in an asymmetric which requires the use of full core model.

The benchmark specifications [17] provide a cross-section library with 432 sets of cross sections in the fuel region and 3 sets for the reflector region (bottom, top, and radial reflector). The group constants for each set consists of two types of macroscopic cross section data, one for rodded and one for unrodded fuel assemblies. The Peach Bottom Unit 2 core is equipped with LPRMs and forty-three detector strings are provided for the in-core instrumentation with each string containing four LPRM located at four axial elevations in the core. In the cross section library, the microscopic fission cross sections are provided for fissile material of the fission chambers, as well as the assembly detector factors which are the ratio between the flux in the detector location and the average flux in the neutronic cell. An LPRM model was developed and implemented in PARCS in order to compare the calculations with the measured in-core detector signals.

4.3 Coupled TRACE/PARCS Model (Exercise 3)

Within the framework of this thesis and as part of the PB2 benchmark, the PARCS neutronics nodes were mapped into 33 thermal-hydraulic (T-H) channels as shown in Figure 4-2

	1	2	3	4	5	6	7	8	9	10	11	12	13	14	15	16	17	18	19	20	21	22	23	24	25	26	27	28	29	30	31	32
1								0	0	0	0	0	0	0	0	0	0	0	0	0	0	0	0	0	0							
2							0	0	0	18	17	17	17	17	17	17	17	17	17	17	17	17	18	0	0	0						
3						0	0	0	33	14	15	14	15	14	15	15	15	15	14	15	14	15	14	33	0	0	0					
4					0	0	33	18	16	15	14	15	14	15	14	14	14	14	15	14	15	14	15	16	18	33	0	0				
5				0	0	0	33	14	15	13	13	13	13	13	11	13	13	11	13	13	13	13	13	15	14	33	0	0	0			
6			0	0	0	18	14	15	13	12	13	12	11	12	11	10	10	11	12	11	12	13	12	13	15	14	18	0	0	0		
7		0	0	33	33	29	26	11	13	11	13	11	13	13	11	11	11	11	13	13	11	13	11	13	11	26	29	33	33	0	0	
8	0	0	0	18	29	30	27	26	11	12	11	12	7	6	7	8	8	7	6	7	12	11	12	11	26	27	30	29	18	0	0	0
9	0	0	33	29	30	13	13	27	25	7	7	7	7	7	8	8	8	8	7	7	7	7	7	25	27	13	13	30	29	33	0	0
10	0	17	29	30	13	28	27	28	22	31	7	31	7	6	7	6	6	7	6	7	31	7	31	22	28	27	28	13	30	29	17	0
11	0	17	30	29	13	27	13	27	24	22	23	7	8	3	3	3	3	3	3	8	7	23	22	24	27	13	27	13	29	30	17	0
12	0	17	29	30	27	28	27	28	22	31	22	4	3	4	3	3	3	3	4	3	4	22	31	22	28	27	28	27	30	29	17	0
13	0	17	30	29	27	13	13	22	22	22	24	21	5	3	3	3	3	3	3	5	21	24	22	22	22	13	13	27	29	30	17	0
14	0	17	29	30	27	28	27	32	22	32	21	4	21	4	19	2	2	19	4	21	4	21	32	22	32	27	28	27	30	29	17	0
15	0	17	30	29	27	27	27	24	22	22	20	20	20	19	19	1	1	19	19	20	20	20	22	22	24	27	27	27	29	30	17	0
16	0	17	30	29	27	10	9	22	22	32	20	20	20	2	1	1	1	1	2	20	20	20	32	22	22	9	10	27	29	30	17	0
17	0	17	30	29	27	10	9	22	22	32	20	20	20	2	1	1	1	1	2	20	20	20	32	22	22	9	10	27	29	30	17	0
18	0	17	30	29	27	27	27	24	22	22	20	20	20	19	19	1	1	19	19	20	20	20	22	22	24	27	27	27	29	30	17	0
19	0	17	29	30	27	28	27	32	22	32	21	4	21	4	19	2	2	19	4	21	4	21	32	22	32	27	28	27	30	29	17	0
20	0	17	30	29	27	13	13	22	22	22	24	21	5	3	3	3	3	3	3	5	21	24	22	22	22	13	13	27	29	30	17	0
21	0	17	29	30	27	28	27	28	22	31	22	4	3	4	3	3	3	3	4	3	4	22	31	22	28	27	28	27	30	29	17	0
22	0	17	30	29	13	27	13	27	24	22	23	7	8	3	3	3	3	3	3	8	7	23	22	24	27	13	27	13	29	30	17	0
23	0	17	29	30	13	28	27	28	22	31	7	31	7	6	7	6	6	7	6	7	31	7	31	22	28	27	28	13	30	29	17	0
24	0	0	33	29	30	13	13	27	25	7	7	7	7	7	8	8	8	8	7	7	7	7	7	25	27	13	13	30	29	33	0	0
25	0	0	0	18	29	30	27	26	11	12	11	12	7	6	7	8	8	7	6	7	12	11	12	11	26	27	30	29	18	0	0	0
26		0	0	33	33	29	26	11	13	11	13	11	13	13	11	11	11	11	13	13	11	13	11	13	11	26	29	33	33	0	0	
27			0	0	0	18	14	15	13	12	13	12	11	12	11	10	10	11	12	11	12	13	12	13	15	14	18	0	0	0		
28				0	0	0	33	14	15	13	13	13	13	13	11	13	13	11	13	13	13	13	13	15	14	33	0	0	0			
29					0	0	33	18	16	15	14	15	14	15	14	14	14	14	15	14	15	14	15	16	18	33	0	0				
30						0	0	0	33	14	15	14	15	14	15	15	15	15	14	15	14	15	14	33	0	0	0					
31							0	0	0	18	17	17	17	17	17	17	17	17	17	17	17	17	18	0	0	0						
32								0	0	0	0	0	0	0	0	0	0	0	0	0	0	0	0	0	0							

Figure **4-2**: Thermal Hydraulic Channel Mapping for PB2 TT2

The numbers in Figure 4-2 indicate the channel assignments of the fuel assemblies and 0 corresponds to the reflector region. A thermal-hydraulic channel was not assigned to the reflector so that fixed reflector properties were used as provided in the benchmark specifications [17].

4.4 PB2 TT2 Steady State Results

Correct modeling of the initial steady state is important. The TT2 test has been initiated from the steady state conditions of the EOC2.

4.4.1 Steady State Stand Alone Results (Exercise 1)

A comparison of the TRACE predictions for Exercise 1 with the plant data is shown in Table 4-3. In Figure 4.3 the core average axial void fraction predicted by TRACE is compared with the code used by Exelon for core analysis, RETRAN. As indicated, the TRACE results are in excellent agreement with the steady state parameters. The maximum deviation for the core inlet sub-cooling is less than 0.7%. The inlet sub-cooling usually depends on the amount of steam carry-under from the separator. The transient response of the system is very sensitive to separator modeling because this affects the initial location of the bulk boiling in core channels. The accuracy of the core pressure drop is affected mostly by the loss coefficients in the vessel and channels. The loss coefficients are defined through series of sensitivity studies.

The most challenging part of the steady state analysis is the prediction of the void fraction distribution. This prediction depends on the modeling of core channels, vessel levels, steam dryers/separators, jet pumps and recirculation loops and also depends on the features of the TRACE code such as heat transfer models and sub-cooled boiling model.

The transient response of the system is very sensitive to the separator modeling because this affects the initial location of the bulk boiling in the core channels and the accuracy of the void distribution in the core. As indicated in Figure 4.2 there is less than 1% difference in the core average void distribution and excellent agreement in the prediction of the axial void distribution to the RETRAN code.

Table **4-2**: Comparison of Stand Alone TRACE Steady State Results with Measured Plant Data

Parameter	Measurement	TRACE
Total Core Flow (kg/s)	10445.5	10445.12
Core Inchannel Flow Rate (kg/s)	9603.6	9603.456
Core Bypass Flow Rate (kg/s)	841.9	841.554
Core Inlet Pressure (MPa)	6.972	6.940
Core Outlet Pressure (MPa)	6.834	6.841
Core Steam Dome Pressure (MPa)	6.799	6.799
Core Inlet Sub-cooling (K)	11.72	10.87
Feedwater Flow Rate/Steam Line Flow Rate (kg/s)	984.75	986.3
Power (MW)	2.030e+09	2.030e+09

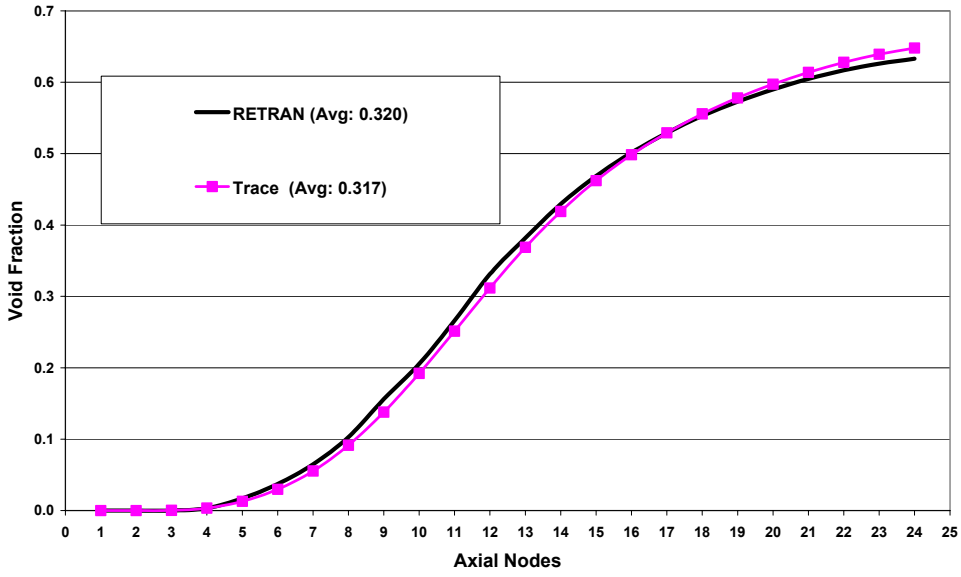

Figure **4-3**: Steady State Core Average Void Fraction Distribution

4.4.2 Steady State Coupled TRACE/PARCS Results (Exercise 3)

The k-effective predicted by the coupled code TRACE/PARCS is 1.005375 which is slightly greater than critical, but in good agreement when compared with other participants in the PB2 TT2 benchmark. A comparison of the steady-state results predicted by TRACE/PARCS with measured plant data is shown in Table 4-3. As indicated, the predicted and measured results are generally in very good agreement. Figures 4-4 and 4-5 show the average axial void distribution and axial power distribution, respectively as predicted by the coupled TRACE/PARCS codes. TRACE/PARCS tends to under-predict the axial power profile at the core bottom, and slightly over-predict it at the core center and core top. This small discrepancy is supported by the core axial void distribution in Figure 4-4. A possible reason could be the application of the particular heat transfer model used in the TRACE code version.

In summary, steady state simulation of a large system such as PB Unit 2 is very difficult and requires extensive work on each component's model. In addition, correct simulation is necessary of the control phenomena in input models, such as water level control, recirculation pump speed, jet pump flows, feed-water flow and steam line pressure.

Table **4-3**: Comparison of Coupled TRACE/PARCS Steady State Results with Measured Plant Data

Parameter	Measurement	TRACE
Total Core Flow (kg/s)	10445.5	10445.087
Core Inchannel Flow Rate (kg/s)	9603.6	9601.5319
Core Bypass Flow Rate (kg/s)	841.9	843.555
Core Inlet Pressure (MPa)	6.972	6.937
Core Outlet Pressure (MPa)	6.834	6.842
Core Steam Dome Pressure (MPa)	6.799	6.799
Core Inlet Sub-cooling (K)	11.72	10.84
Feedwater Flow Rate/Steam Line Flow Rate (kg/s)	984.75	985.235
Power (MW)	2.030e+09	2.030e+09

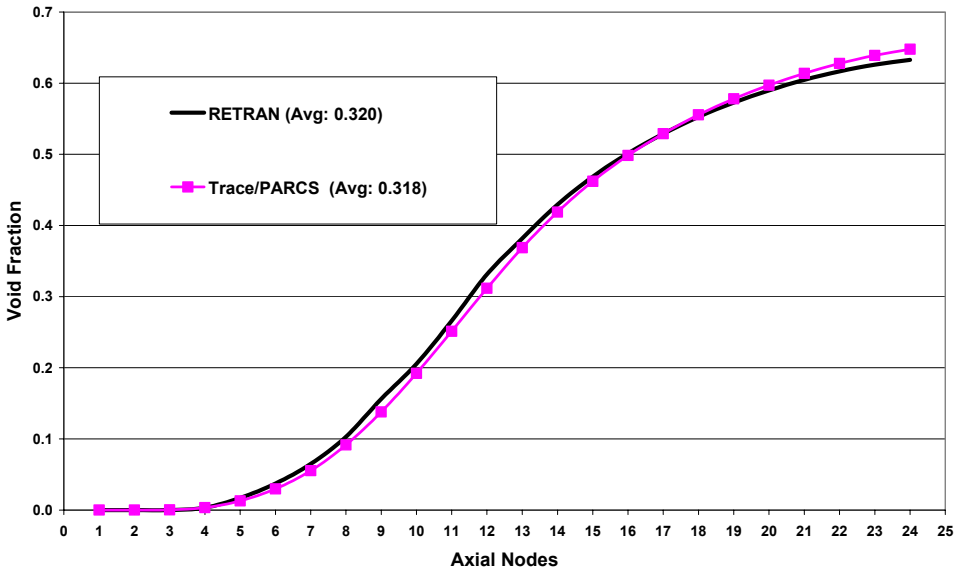

Figure **4-4**: Steady State Coupled TRACE/PARCS Core Average Void Fraction Distribution

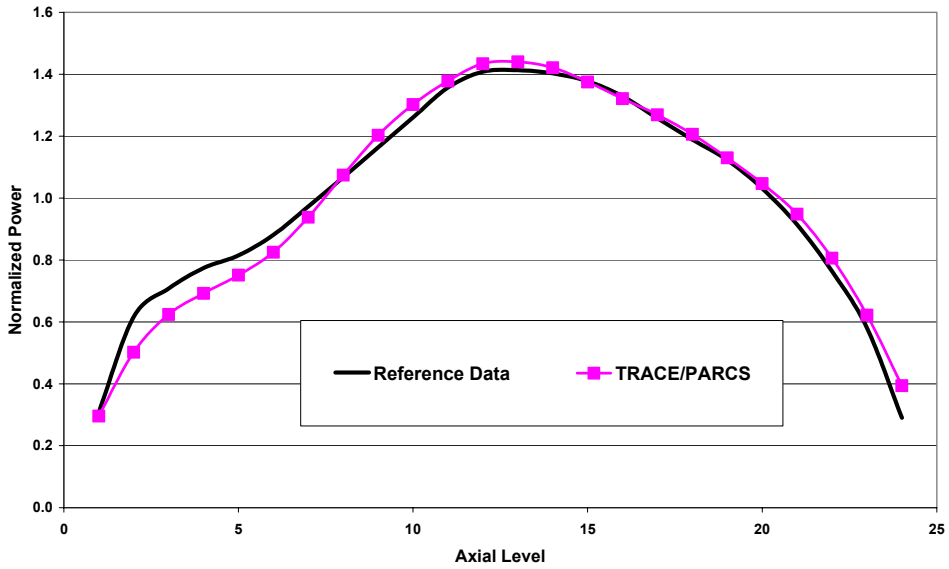

Figure **4-5**: Steady State Coupled TRACE/PARCS Axial Power Profile

4.5 PB2 TT2 Transient Results

The calculated transient results and the comparisons presented in this chapter not only provide an opportunity to understand the phenomena behind the turbine transient tests but also to engage in comprehensive testing and examination of the capability of TRACE/PARCS to simulate such transient.

4.5.1 TRACE Stand Alone Transient Results (Exercise 1)

During the transient analyses of PB2 TT2 it was observed that a major impact on the pressure response is associated with the steam bypass line together with the main steam line via the relative position of the TSV and BPV. It was seen that the acoustical pressure wave (oscillation) can exist in the reactor main steam piping due to the combined compressibility and momentum effects in the steam line. The fundamental mode of the acoustical pressure oscillation is strongly excited as a result of the turbine trip, which causes a sharp initial pressure rise in the reactor as the first pressure wave enters the reactor vessel. In addition, the fundamental acoustical mode propagates in the main steam piping, entering the reactor vessel and passing through the steam separators into the reactor core with relatively little attenuation. These physical facts can be seen in Figures 4-5 and 4-6, where the time histories for the total core mass flow rate and steam dome pressure are shown respectively.

The time of the maximum peaks at major locations is compared to the measured plant data in Table 4-4

Table **4-4**: Comparison of Predicted and Measured Time of Transient Events

Events	TRACE	Measured
Turbine Stop Valve	0.096	0.096
Bypass Valve Beginning to Open	0.060	0.060
Bypass Valve Full Open	0.846	0.846
Dome Initial Response	0.430	0.432
Core Exit Initial Response	0.490	0.486

In general there is good agreement between the TRACE results and plant data and TRACE appears to accurately model the detailed progression of the pressure response in the core. In particular, the good agreement in the times of occurrence of the initial pressure rise indicates that the time effects such as delays and frequencies in the core are modeled well. In addition, the amplitudes of the pressure are commonly in good agreement. As indicated in the Figure 4-6, there are some differences in the TRACE prediction from plant data during the later phases of the transient. These differences can be attributed to inaccurate modeling of some of the depressurization rate mechanisms such as critical flow and steam formation.

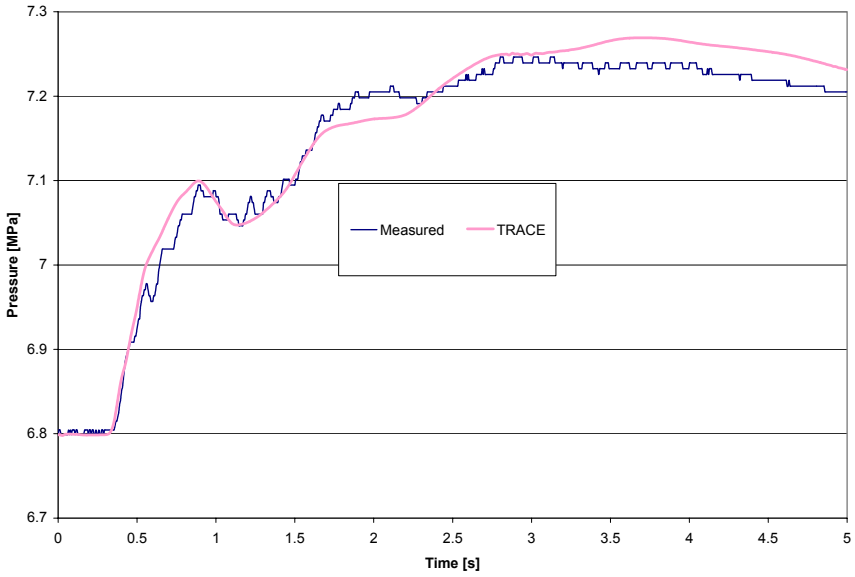

Figure **4-6**: Transient Stand Alone Steam Dome Pressure

4.5.2 TRACE/PARCS Coupled Transient Results (Exercise 3)

The timing of transient events predicted by TRACE/PARCS for exercise 3 is compared to the reported timing of the events in Table 4.5. In general the predictions are in very good agreement with the time of measured responses.

Table **4-5**: Comparison of Predicted and Measured Time of Transient Events

Events	TRACE/PARCS	Measured
Turbine Stop Valve	0.090	0.096
Bypass Valve Beginning to Open	0.060	0.060
Bypass Valve Full Open	0.846	0.846
Dome Initial Response	0.444	0.432
Core Exit Initial Response	0.490	0.486

The time history of the steam dome pressure predicted by TRACE/PARCS during the transient is compared to the measured data in Table 4-5. After a slight delay the pressure wave reaches the core and results in a decrease in the core average void fraction from 32% to 29 % as shown in Figure 4-7. The void collapse in the core leads to an axial redistribution of the power as shown in Figure 4-8, and positive reactivity insertion as demonstrated in Figure 4-9. Upon opening of the bypass relief valve the void fraction in the core increases again as the core pressure is reduced. The core power excursion is terminated by a combination of the negative void and negative Doppler reactivity resulting from the initial power increase. The control rods are inserted into the core at about 0.8 seconds. The core power response predicted by TRACE/PARCS during the transient is compared to the measured power in Figure 4-10. As

indicated, the predicted power response is slightly lower and slightly delayed (22ms) compared to the measured values.

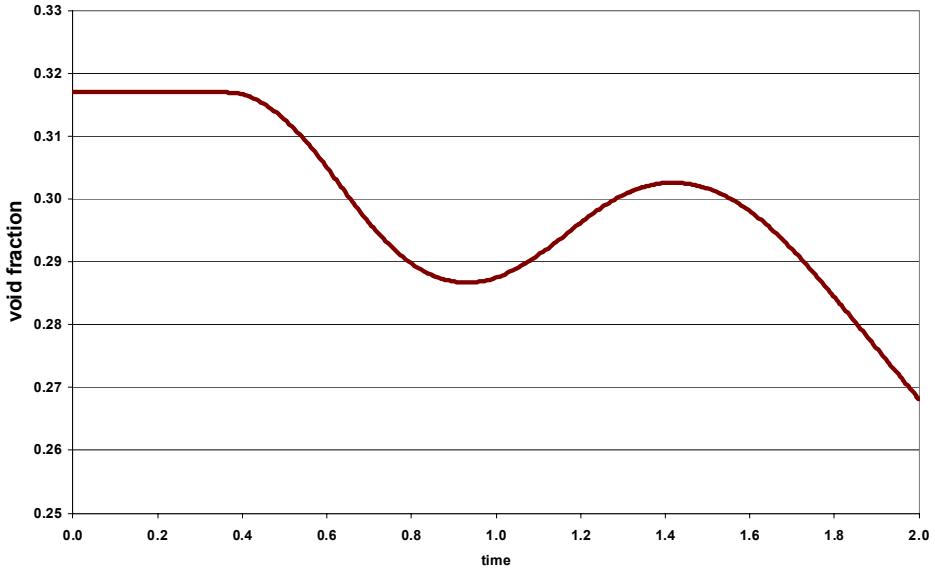

Figure **4-7**: TRACE/PARCS Core Average Void Fraction

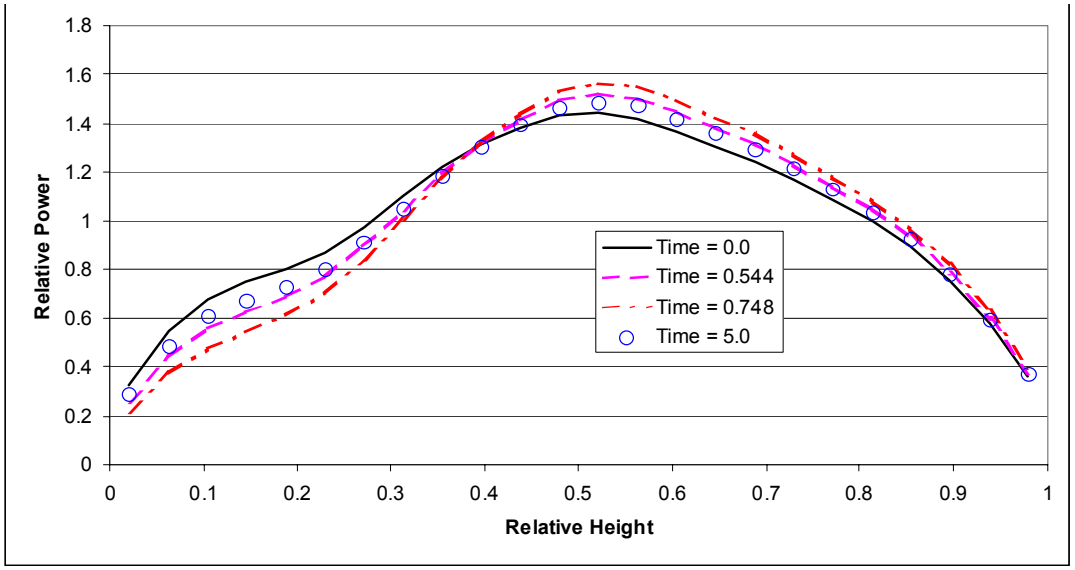

Figure **4-8**: TRACE/PARCS Core Average Axial Power

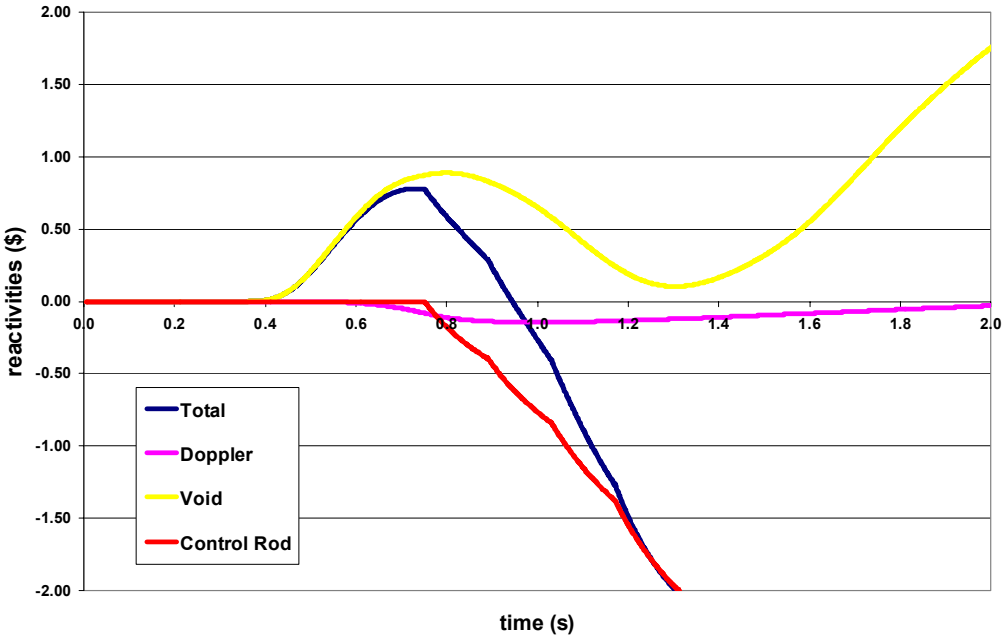

Figure **4-9**: TRACE/PARCS Component of Core Reactivity

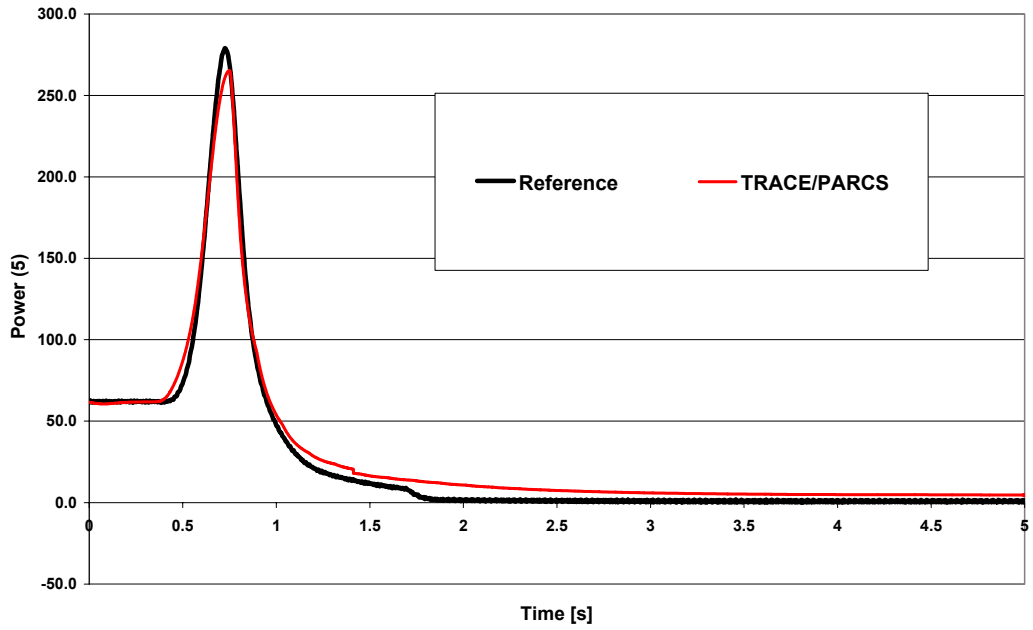

Figure **4-10**: Transient Power with SCRAM

Chapter 5

TRACE/PARCS PB Low Flow Stability Results

Chapter 5 focuses on the LFS simulation results and their discussion. At first the steady state results are shown and compared with available measured data. This is important in order to demonstrate that a steady state consistent with the actual plant data was achieved. Follows the transient results where stability parameters from time series generated in the transient calculations are presented and discussed. The PB2 TRACE/PARCS model used here was the same as used previously for the PB2 TT2 analyses. The stability simulation calculation begins with a stand-alone TRACE initialization of the thermal-hydraulics field using a fixed power distribution. Upon convergence a steady state calculation is then performed with the coupled TRACE/PARCS code to achieve a converged coupled thermal-hydraulic/neutron flux solution. Only coupled simulation results are shown here.

5.1 PB2 Low Flow Stability Tests Steady State Results

The list of parameters chosen for comparison covers reactor power, core mass flow rate, steam dome pressure, core inlet temperature, core inlet sub-cooling, core average axial power distribution and feed-water mass flow rate. The steady state results for points PT1, PT2 and PT3 are each point are shown in Tables 5-1, 5-2 and 5-3, respectively. It should be noted that there is a good agreement among all the parameters when compared to the reference data. The feed-water mass flow rate for each test point is slightly higher which suggest that the controller for inlet sub-cooling needs further investigation. In order to confirm that coupled steady state was reached the

axial power distribution was plotted as well. PT1, PT2 and PT3 steady state axial power profiles are shown in Figures 5-1, 5-2 and 5-3, respectively. A slight shift is observed in the simulated axial power distribution of TRACE/PARCS, a probable source for this discrepancy could be the heat transfer models in TRACE. However the difference is within acceptable range.

Table **5-1**: PT1 Comparison of TRACE/PARCS Steady State Results with Measured Plant Data

Parameter	Measurement	TRACE/PARCS
Total Core Flow (kg/s)	6753.6	6753.46
Core Inlet Pressure (MPa)	NA	6.95744
Core Outlet Pressure (MPa)	NA	6.8897
Steam Dome Pressure (MPa)	6.860286	6.8603
Core Inlet Enthalpy	1184.61	1190.82
Core Inlet Subcooling (KJ/kg)	75.160	73.87
Core Inlet Temperature (K)	543.26	544.35
Feedwater Flow Rate/Steam Line Flow Rate (kg/s)	963.22	1005.2
Power (MW)	1.995e+09	1.995e+09

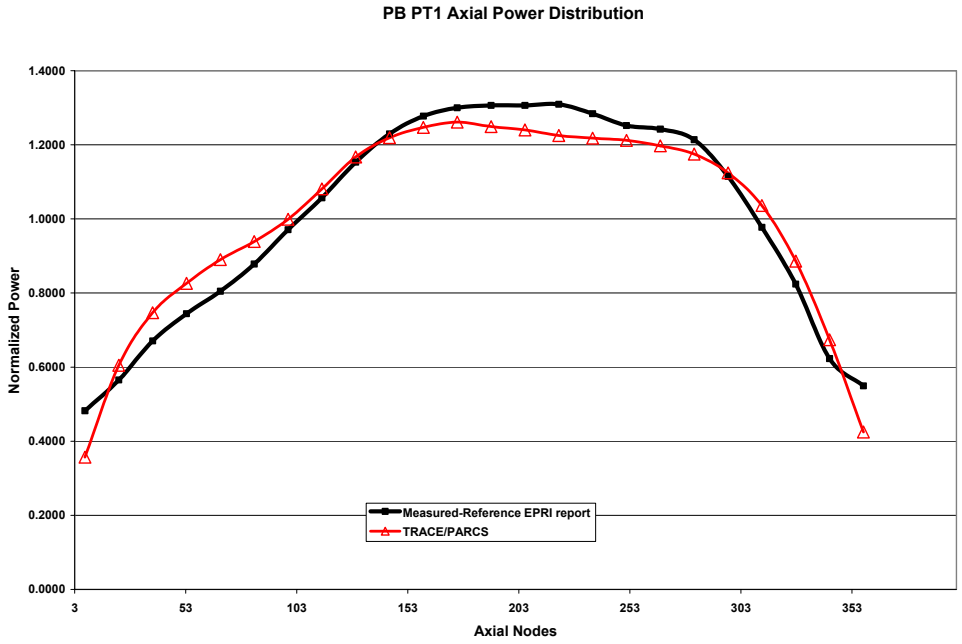

Figure **5-1**: PT 1 Steady State TRACE/PARCS Axial Power Profile

Table **5-2**: PT2 Comparison of TRACE/PARCS Steady State Results with Measured Plant Data

Parameter	Measurement	TRACE
Total Core Flow (kg/s)	5657.40	5656.7
Core Inlet Pressure (MPa)	NA	6.896
Core Outlet Pressure (MPa)	NA	6.842
Steam Dome Pressure (MPa)	6.814781	6.814
Core Inlet Enthalpy	1187.78	1182.95
Core Inlet Subcooling (KJ/kg)	79.648	78.52
Core Inlet Temperature (K)	543.24	542.86
Feedwater Flow Rate/Steam Line Flow Rate (kg/s)	808.92	865.27
Power (MW)	1.702e+09	1.702e+09

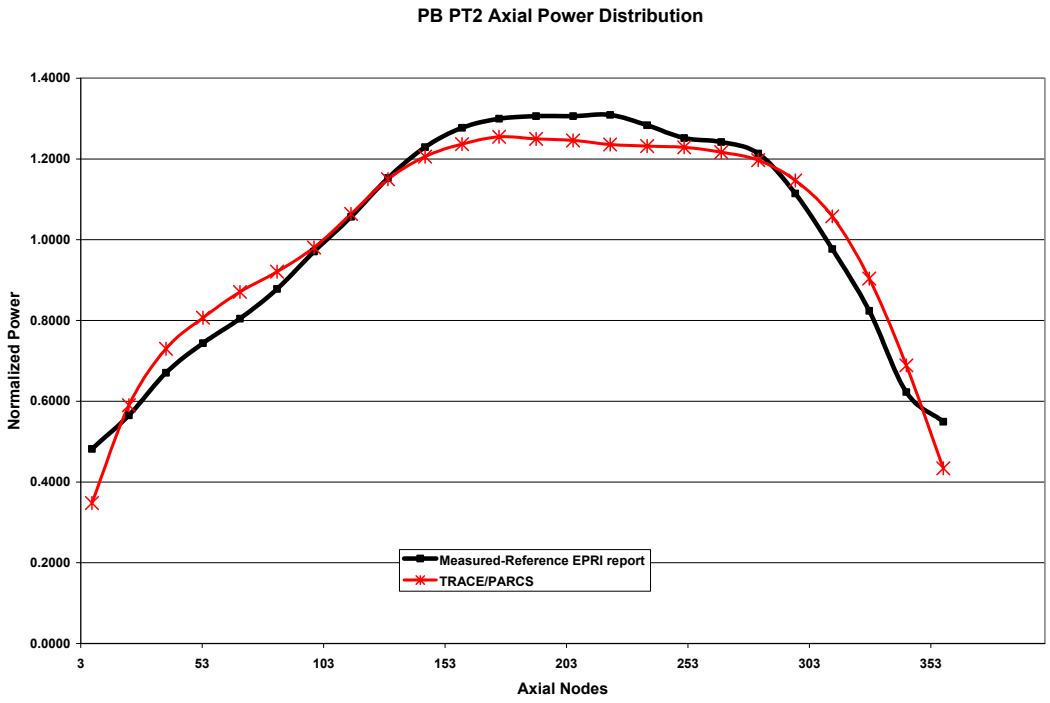

Figure **5-2**: PT 2 Steady State TRACE/PARCS Axial Power Profile

Table **5-3**: PT3 Comparison of TRACE/PARCS Steady State Results with Measured Plant Data

Parameter	Measurement	TRACE
Total Core Flow (kg/s)	5216.40	5216.40
Core Inlet Pressure (MPa)	NA	6.981
Core Outlet Pressure (MPa)	NA	6.929
Steam Dome Pressure (MPa)	6.904413	6.9044
Core Inlet Enthalpy	1184.61	1190.31
Core Inlet Subcooling (KJ/kg)	77.442	74.69
Core Inlet Temperature (K)	543.24	544.2
Feedwater Flow Rate/Steam Line Flow Rate (kg/s)	941.22	1021.77
Power (MW)	1.948e+09	1.948e+09

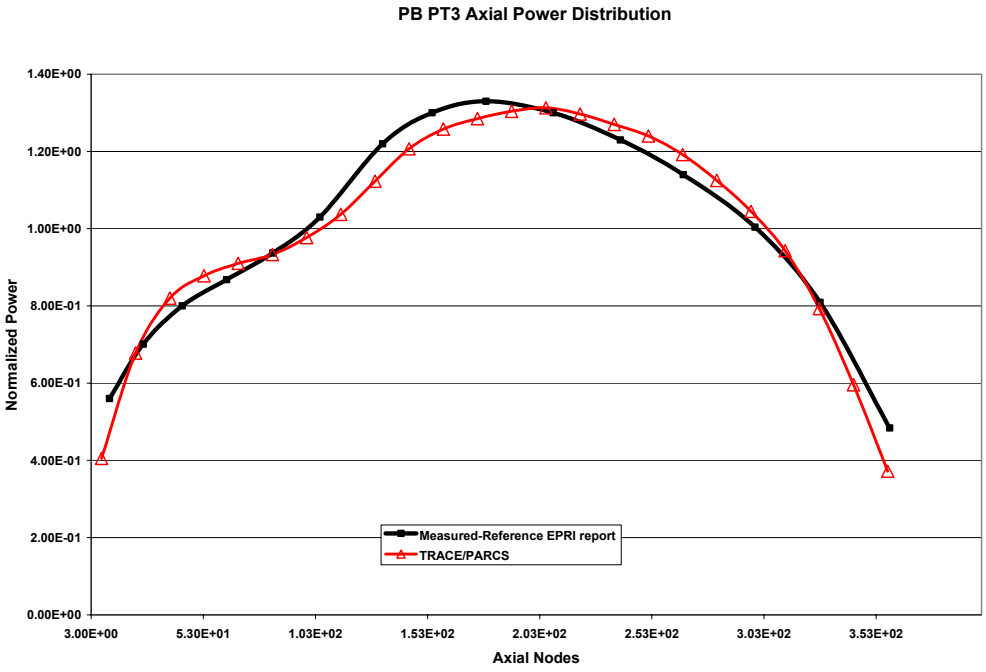

Figure **5-3**: PT 3 Steady State TRACE/PARCS Axial Power Profile

5.2 PB2 Low Flow Stability Tests Transient Results

The stability simulation is performed using the semi-implicit method in TRACE by introducing one of the two excitations to the core to initiate the transient.

1) Control Rod (CR) neutronics perturbation: one or more control rods are temporarily moved in and then replaced to its original position in PARCS model.
2) Pressure (thermal-hydraulic) perturbation (PP) where a single peak perturbation is applied to the steam line of the TRACE model

The DRARMAX program, described in Chapter 3, was used to calculate the Decay Ratio (DR) and Natural Frequency (NF) of the power responses caused by control rod and pressure perturbations. Figures 5-4, 5-5 and 5-6 show the power response of the control rod perturbation while Figures 5-7, 5-8 and 5-9 demonstrate the power response of the pressure perturbations. Tables 5-4 and 5-5 contain the evaluation of DR and NF, respectively. From the tables, it becomes clear that the DR and NF results are within uncertainty range when compared to the experimental data.

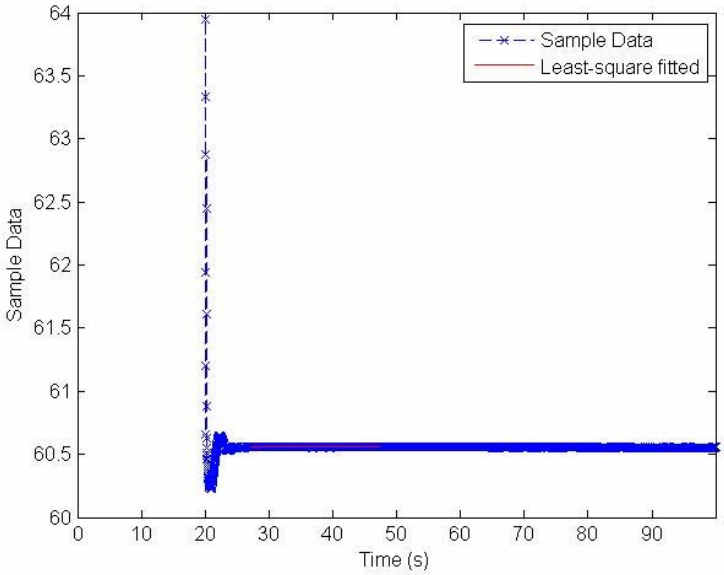

Figure **5-4**: PT1 Control Rod Perturbation Power Response

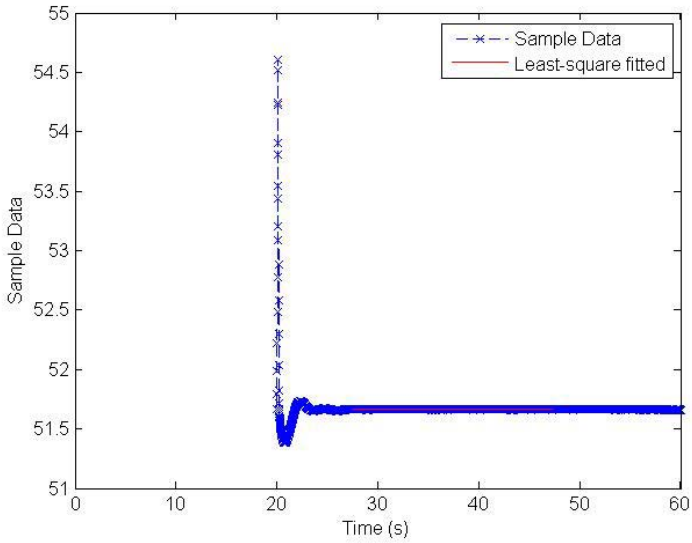

Figure **5-5**: PT2 Control Rod Perturbation Power Response

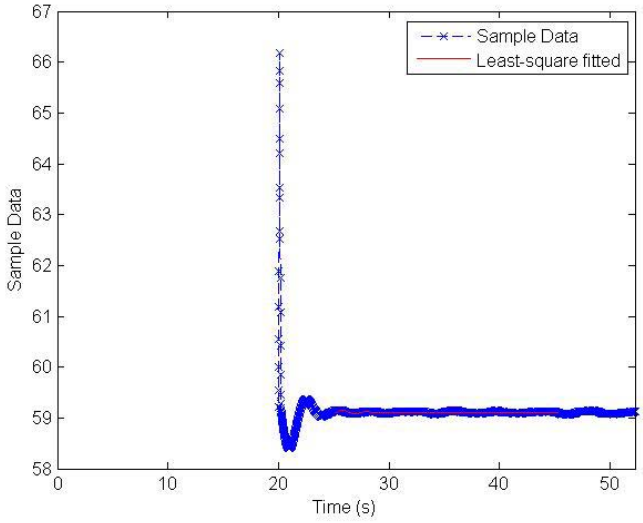

Figure **5-6**: PT3 Control Rod Perturbation Power Response

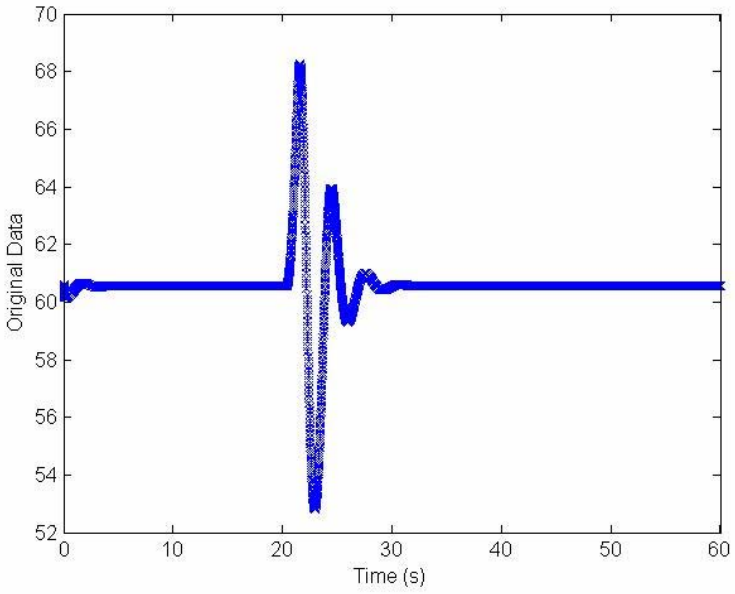

Figure **5-7**: PT1 Pressure Perturbation Power Response

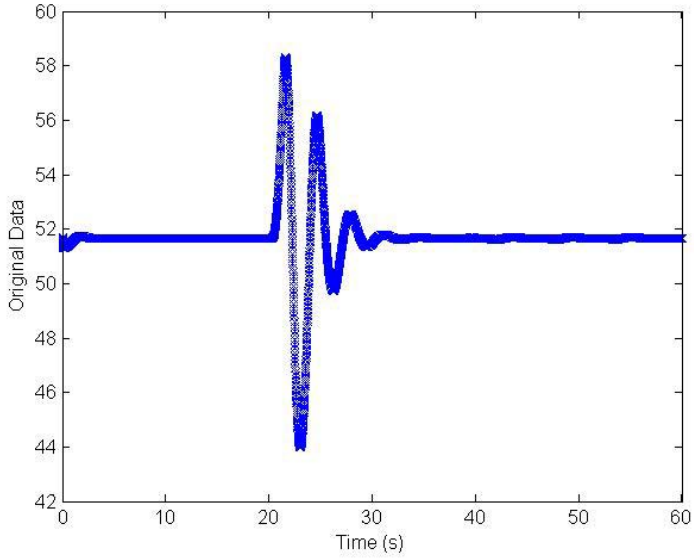

Figure **5-8**: PT2 Pressure Perturbation Power Response

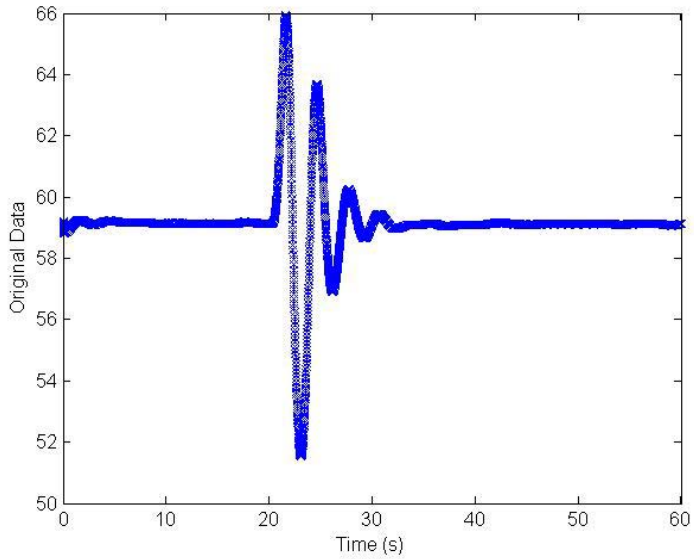

Figure **5-9**: PT3 Pressure Perturbation Power Response

Table **5-4**: DRARMAX Calculation of DR

Cycle 2 Comparisons with DRARMAX Method			
	Reference	Calculated DR (Global)	
PT	DR (Global)	CR	PP
1	0.26	0.353	0.353
2	0.30	0.32	0.26
3	0.33	0.29	0.301

Table **5-5**: DRARMAX Calculation of NF

Cycle 2 Comparisons with DRARMAX Method			
	Reference	Calculated NF (Global)	
PT	FR (Global)	CR	PP
1	0.45	0.86	0.30
2	0.45	0.36	0.32
3	0.43	0.46	0.34

In the analyzed control rod and pressure perturbation some characteristics peculiar for in-phase instability are recognized. For instance, frequencies in all oscillations obtained in analyses varied from 0.3 to 0.5 Hz, which is a typical frequency range of this kind of instability events.

The control rod movement perturbations produce highly localized power spikes around perturbed control rods. This leads to undesirable higher modal components included in the response. Therefore the first few peaks need to be skipped in the time series response with the expectation that these higher modes decay more quickly than the fundamental or the first azimuthal mode. However the skipped peaks may also result in a loss of measureable signals and generate poor decay ratio values. A selection of the control rods depends on the operating

condition and its influence on the excited higher modes cannot be easily quantified. Therefore it is difficult to ensure high accuracy for DR values calculating with such perturbation

Chapter 6

Conclusions

Based on an existing TRACE input data file for BWR NPP of Peach Bottom Cycle 2, an input deck was developed to perform turbine trip and low flow stability transients. The modified input data file was coupled with the PARCS code in order to perform analyses with a three dimensional neutron kinetics (3-D kinetics) code.

The performed analyses demonstrated that the coupled TRACE/PARCS Peach Bottom nodalization is able to predict steady state and transient conditions and agrees well with experimental data from the actual Peach Bottom Plant operation. The steady state PB TT2 TRACE/PARCS results demonstrated that the maximum deviation for the core inlet sub-cooling is less than 0.7%. The sensitivity analyses performed showed that the transient response of the system is very sensitive to separator modeling because it affects the initial location of the bulk boiling in core channels. The accuracy of the core pressure drop is affected mostly by the loss coefficients in the vessel and channels.

The most challenging part of the steady state analysis is the prediction of the void fraction distribution. This prediction depends on the modeling of core channels, vessel levels, steam dryers/separators, jet pumps and recirculation loops and also depends on the features of the TRACE code such as heat transfer models and sub-cooled boiling model. It was suggested that the small discrepancy in the core axial void distribution is a result of the application of the heat transfer model used in the TRACE code version.

In addition, correct simulation is necessary of the control phenomena in input models, such as water level control, recirculation pump speed, jet pump flows, feed-water flow and steam line pressure.

During the transient analyses of PB2 TT2 it was observed that a major impact on the pressure response has the steam bypass line together with the main steam line via the relative position of the TSV and BPV. It was seen that the acoustical pressure wave (oscillation) can exist in the reactor main steam piping due to the combined compressibility and momentum effects in the steam line. TRACE appears to accurately model the detailed progression of the pressure response in the core. There are some differences in the TRACE prediction from plant data during the later phases of the transient. These differences can be attributed to inaccurate modeling of some of the depressurization rate mechanisms such as critical flow and steam formation
Other transients, Low Flow Stability Tests, were simulated as well. The stability simulation calculation begins again with steady state stand-alone and coupled calculations. During steady state calculations, there is very good agreement among all the parameters when compared to the reference data. A possible source of the feed-water mass flow rate discrepancies between measured data and simulated results could be the control block which controls the inlet sub-cooling. Another slight discrepancy was observed in the axial power distribution of TRACE/PARCS which depends on the heat transfer models in TRACE.

After steady state validation with measured plant data, pressure and control rod perturbation transients were performed. During transient tests it was observed that the pressure perturbation produces better results especially in terms of natural frequency (NF), than the control rod perturbation. This could be explained with control rod movement perturbations which produce highly localized power spikes around perturbed control rods. This result in undesirable higher modal components included in the response. When calculating the decay ratio (DR) and NF the first few peaks of the power response need to be skipped with the expectation that these

higher modes decay more quickly than the fundamental or the first azimuthal mode. However, the skipped peaks may also result in a loss of measureable signals and generate poor DR and NF values and it is difficult to ensure high accuracy when simulating such perturbation.

REFERENCES

[1] T. Kozlowski, T. Downar, et al. Analysis of the OECD/NEA PWR Main Steam Line Break Benchmark with TRAC-M/PACS, Nuclear Technology, September, 2004.

[2] “Transient and Stability Tests at Peach Bottom Atomic Power Station Unit 2 at End of Cycle 2”, General Electric Company/Nuclear Energy Engineering Division, NP-564, Research Project 1020-I, Topical Report, June 1978

[3] L. Carmichael, and R. Niemi, “Transient and Stability Tests at Peach Bottom Atomic Power Station Unit 2 at End of Cycle 2”, EPRI NP-564, June 1978.

[4] N. Larsen, “Core Design and Operating Data for Cycles 1 and 2 of Peach Bottom 2”, EPRI NP-563, June 1978.

[5] K. Hornyik, and J. Naser, “RETRAN Analysis of the Turbine Trip Tests at Peach Bottom Atomic Power Station Unit 2 at the End of Cycle 2”, EPRI NP-1076-SR Special Report, April 1979.

[6] D. Lee, T. Ulses, et al., “Analysis of the OECD/NEA Peach Bottom Turbine Trip Benchmark with TRAC-M/PARCS,” Nuclear Science and Engineering, January, 2005.

[7] A. Olson, “Methods for Performing BWR System Transient Analysis”, Philadelphia Electric Company, Topical Report PECo-FMS-0004-A (1988).

[8] TRACE v5.0 Theory Manual - Field Equations, Solution Methods, and Physical Models, 15 August 2007

[9] PARCS Volume 2: User Manual for the PARCS Kinetics Core Simulator Module, Purdue University, 15 November 2004

[10] Y. Xu 2005, DRARMAX - Users manual, 6 December 2005

[11] H. Joo, D. Barber, G. Jiang and T. Downar, “PARCS :- A Multi-Dimensional Two Group Reactor Kinetics Code Based on the Nonlinear Analytical Nodal Method,” (1998)

[12] N. M. Schnurr et al. 1992, TRAC-PF1/MOD2 Theory manual, Los Alamos National Laboratory Report LA 2031-M, US Nuclear Regulatory Commission Report NUREG/CR 5673.

[13] PARCS Volume 2: User Manual for the PARCS Kinetics Core Simulator Module, Purdue University, 15 November 2004.

[14] S. L. Marple, 1987, “Digital Spectral Analysis with Applications”, Prentice Hall, Englewood Cliffs, Chapter 8.

[15] J. L. Munoz, G. Verdù, C. Pereira, 1992, “Dynamic Reconstruction and Lyapunov Exponents from Time Series Data in Boiling Water Reactor Application to BWR Stability Analysis”, Ann. Nucl. Energy, 19, 223.

[16] F. Odar, C. Murray, R. Shumway, M. Bolander, D. Barber, J. Mahaffy - TRACE Users Manual, 2003

[17] J. Solis, K. Ivanov, B. Sarikaya, A. Olson, and K. Hunt, “BWR TT Benchmark. Volume I: Final Specifications”, NEA/NSC/DOC(2001)1